Applications of SIFT-MS to the Environment and Petroleum Exploration

A thesis presented for the degree

Of

Master of Science in

Chemistry

By

Majed Mohammed Alghamdi

2008-2009

Chapter 4: **Further SIFT-MS petroleum applications**

Chapter 5: **TD-SIFT-MS potential for air monitoring**

Chapter 6: Conclusion and suggestions for future work

Acknowledgements

I would like to express my sincere appreciation to my research supervisor, Prof. Murray McEwan, for his advice, support and guidance throughout this work. Many thanks are also due to the science staff at Syft Company: Dr. Vaughan Langford, Dr. Brett Davis, Dr. Barry Prince, Dr. Daniel Milligan, and John Gray for helping me to finish this study. Lastly, very special thanks are delivered to my sponsor King Khalid University in Saudi Arabia.

Abstract

In this project, "selected ion flow tube mass spectrometry" (SIFT-MS), a sensitive analytical technique, reveals potential for the development of applications in the environment and petroleum areas. Many prior applications have shown their potential for analyzing samples in widely disparate areas. Its fast analysis process and high sensitivity gives it a significant advantage over more conventional methods. This project is directed at expanding this technology to more applications in the petroleum and air quality areas.

The application to the petroleum industry has shown that SIFT-MS can quantify H_2S and CH_3SH in natural gas to 11.8 and 1.2 ppbv, respectively. The SIFT-MS results showed a good linear response with increasing sulfide concentrations by using the H_3O^+ reagent ion to quantify H_2S, CH_3SH, and the total combined concentration of DMS and C_2H_5SH. The ability to use the SIFT-MS instrument to trace chemical tracers, such as bromobenzene and chlorobenzene in hydrocarbon mediums, was also investigated. SIFT-MS showed also the capacity to trace these compounds in natural gas and LPG. The limits of detection (LOD) were also obtained. This study furthermore, found the utility of the NO^+ reagent ion to analyse qualitatively some of the large hydrocarbons. Unfortunately, however, the SIFT-MS reactions could not distinguish between the structural isomers of these aromatic and aliphatic hydrocarbons and there was probable conflict between the fragmentation product ions with smaller hydrocarbons.

From the air quality perspective, the SIFT-MS also proved its potential for use in air monitoring, using passive techniques and particularly for BTEX (benzene, toluene, ethyl benzene, and xylene) compounds. The study illustrated SIFT-MS's ability to deal with thermal desorption and passive methodology in general. Ecan (Environmental Canterbury) routinely examines environmental pollutants in Christchurch air by passive sampling methodologies. In this study, we compared and achieved agreement by comparing the result of thermal desorption-SIFT-MS (TD-SIFT-MS) of Christchurch air with the more conventional methodologies of TD-GC-MS and the Ecan agency measurements.

List of Figures

List of Tables

Chapter 1

Introduction to SIFT-MS methodology

1. Introduction

In this chapter, by way of introduction, I will summarise the most important developments in the area of ion-molecule reactions with an emphasis on the experimental observations. This summary will be followed by some details of the Selected Ion Flow Tube Mass Spectrometer (SIFT-MS).

1.1 Ion-molecule reactions

Ion-molecule reactions have been noted, as early as the1913s. After the confirmation of the existence of gas phase ion-molecule reactions was reported by Dempster in 1916, many studies have been made in order to understand these charged gas phase neutral interactions. Ion-molecule reactions in the gas phase have been frequently found to proceed very quickly (on almost every collision) and with high efficiency. In addition, in the 1966s, Munson and Field realized the promise of these types of reactions as an alternative softer mean of ion generation. These two features, of rate and efficiency, have enabled ion-molecule reaction methodology to be applied to analytical applications.

Moreover, the rapid growth of the application was due, in part, to the precision of mass spectrometric identification of molecular weight information. Understanding these reactions has opened the door for them to be used in many applications. Further, the use of ion-molecule reactions provides a diverse frontier for extending the boundary of mass spectrometry. [1]

Several instruments have been used to study the ion-molecule reactions from a wide range of perceptions. Flowing afterglow, ion beam and pulsed electron high-pressure mass

spectrometry techniques, all have important roles in understanding these reactions. Ion beam methods, for example, are being employed for the study of ion-molecule reaction dynamics including the elucidation of the energy dependencies of these reactions and the measurement of their reaction cross-section. [1] Flowing afterglow and selected ion flow tube are primarily used for measurement of rate constants of ion-molecule reactions and the identification of product ions. Ion-molecule equilibria enable the determination of thermo chemical information. Other kinetic aspects can be typically obtained from pulsed electron high-pressure mass spectrometers. Fourier Transform Ion Cyclotron Resonance Mass spectrometry (FTICR-MS) can also be used to study ion-molecule reactions with very high mass resolution mode, allowing the determination of molecular formulae of product ions.

1.2 Application of ion-molecule reactions

Ion-molecule reactions have introduced numerous and novel applications mainly in the analytical field. Ion-molecule reaction product distributions provide key diagnostic information for structure identification. Using the soft ionisation method, proton transfer reactions in particular, have solved complex structural spectrum problems. Because they are so efficient, proton transfer reactions have also been used in a variety of analytical applications where only small quantities of reagents are needed. In another application, ion-molecule reactions have been used for the determination of the sites of protonation in multicharged proteins, as new ways are developed to characterize the structures of drugs [2] and to solve stereo chemical problems. However, the application of most relevance to this research, is the utilisation of the SIFT technique for analysis, which will be discussed next.

1.3 SIFT-MS

1.3.1 Overview

Selected ion flow tube mass spectrometry (SIFT-MS) can be considered as a sensitive analytical method. It is used for monitoring volatile compounds both organic and inorganic, based on the chemical ionisation principle to a very low concentration, parts per billion (ppb) by volume.

The technique evolved out of flow tubes used in physical chemical investigations of ion neutral kinetics before it was used in analytical chemistry. At Canterbury University, one of the areas of interest in the ion chemistry groups was understanding the astrochemical reactions that occur in the interstellar medium. The applications of flow tubes to ion molecule chemistry were begun by Ferguson and co-workers in 1969. [2] They applied the flowing afterglow technique to understand the ionospheric process occurring in the atmosphere. This technique then became a standard method for the study of the ion-molecules reaction at thermal energies. [3]

The flowing afterglow method is a fast flow tube ion swarm method for the study of the reactions of positive and negative ions with atoms and molecules. It has been extensively used to study ion molecular reaction kinetics and has had numerous applications to atmospheric and interstellar ion chemistry over a 20 year period. In this period many polyatomic and diatomic cations have been found to exist in the interstellar medium by the use of radio astronomy methods.

The flowing afterglow method for following kinetics has been used since 1963. It was developed almost 60 years ago. [4] Originally, a glass flow tube was used in order to neutralise molecule kinetics using optical spectroscopy techniques.[5] One problem with the

flowing afterglow technique, when applied to ion-neutral chemistry, was the combination of all positive ions, negative ions and electrons together in the flow tube, making identification of the production difficult. This problem was addressed by Smith and Adams [6] who introduced a second quadrupole mass spectrometer to select the ion whose reactions were to be studied. This modification became known as Selected Ion Flow Tube, SIFT.

Recently, the SIFT technique underwent a further development as a sensitive analytical technique for the quantification of the trace gases in air and human breath, down to the pptv level in real time, using chemical ionisation. [7] This new development in analytical chemistry is known as SIFT-MS. The initial larger SIFT instrument, in the Department of Chemistry of the University Canterbury, was modified for use as a SIFT-MS instrument in the late 1990s. Then, a purpose built smaller SIFT-MS instrument was constructed. This became the property of Syft Technologies Ltd on its formation in 2002. Early in 2004, Syft Technologies Ltd commissioned a new SIFT-MS specifically designed for the analyses of trace volatile organic compounds (VOCs). Subsequently, the Voice 100, first generation of SIFT-MS, was released to the commercial market in November 2004 followed by Voice 200 in late 2007.

1.3.2 SIFT-MS Instrument

The SIFT-MS instrument can be separated into three regions: ion source region, reaction region, and the detection region. Figure 1.1 shows the main parts of this instrument and further information of these regions will be discussed individually.

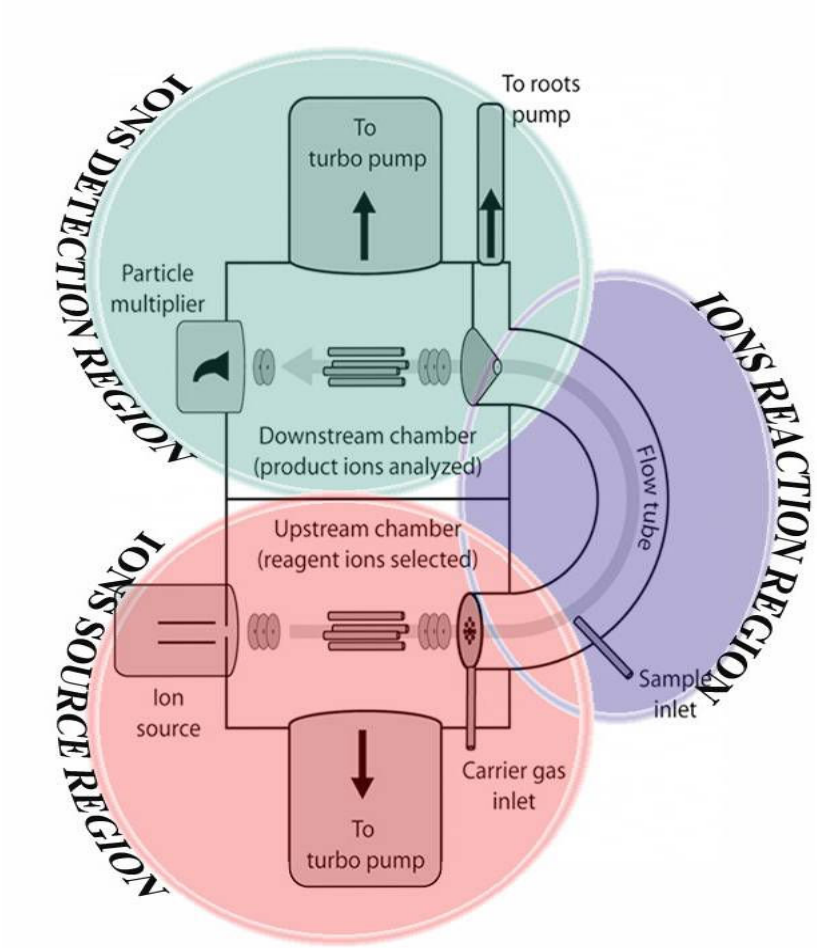

Figure 1.1 The main parts of SIFT-MS Voice 100 instrument.

1.3.2.1 Ion source region

The ion source region is where the ions are created before they are transmitted to the reaction region. This region can be divided further into two sub-regions, the ion creation region and the ion selection region. In the ion creation region, ions are generated under 0.3 Torr pressure by using microwave discharge, operating on moist air. The air is made moist by adding water from the water reservoir that is held inside the machine. The ions generated from this source are H_3O^+, NO^+, and O_2^+ and are the most thermodynamically stable ions. Figure 1.2 shows the mechanism for generating these ions and their energy. Once formed, these ions are focused by electrostatic lenses into the quadrupole mass filter in the ion selection section. The quadrupole mass filter enables the selection of specific ion precursors for more analytical

advantages. That is, SIFT-MS allows each ion of interest to be selectively injected into the reaction region with a rapid switching time < 10 ms between the three ions. After the mass selection, the reagent ions are injected into the ion reaction region.

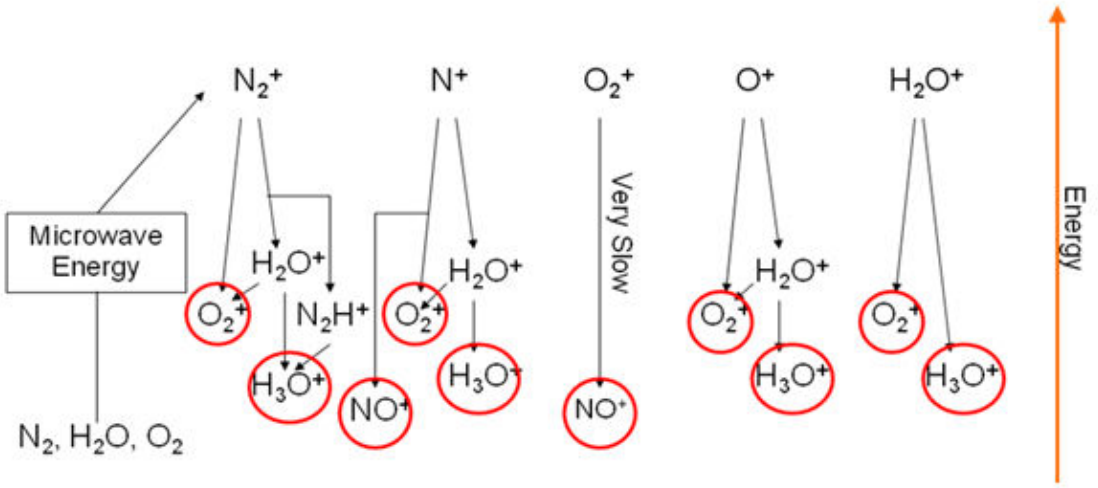

Figure 1.2 The mechanism of generating the main ion precursors using a microwave discharge and their energy. (Adapted from the Syft Technologies Ltd profile notes)

1.3.2.2 Ion reaction region

After generating the ions in the source region, they are transported to the flow tube, which is the reaction region where the ion molecule reactions take place. The flow tube operates at 0.5 Torr pressure. It is made of stainless steel with an internal diameter of 48 mm. The flow tube is located between two high vacuum chambers connected one at each end. The two chambers are the ion source and the ion detection chambers. The outer edge of the tube has an arc radius of 120 mm and it is bent in a half circle. This bent tube is a novel feature in the Voice 100 SIFT-MS instrument. A mixture of carrier gases helium and argon is introduced to the flow tube through the Venturi orifice. This is not a common practice in the conventional flow tube. These Venturi orifices also contain wire cut annular slits. The first carrier gas, which is helium, is introduced to the flow tube through the inner annulus. This annulus is 0.025 mm

wide and is 4.35 mm outside the ion aperture. The outer annulus is 0.4 mm wide at a radial distance of 37.1 mm from the ion aperture and is used to introduce the second carrier gas, argon. Helium is passed through the inner annulus at 15 Torr L s^{-1}, creating the Venturi effect that helps to inject the ions into the flow tube against the pressure gradient. The argon, on the other hand, is passed through the outer annulus slit at 25 Torr L s^{-1}.

Furthermore, the flow tube has five inlets connected to it for transmission of various gases and vapour mixtures. The tetradecane inlet, ambient air inlet, calibrant inlet, direct inlet and sample inlet are connected to the flow tube for different tasks. For example, a quadrupole mass calibration can be done by using the tetradecane inlet, which adjusts the mass peaks to the known tetradecane mass peaks.

Many parameters have to be taken into account in order to determine the analyte concentration. The carrier gas flow rate, ion velocity, sample flow rate, relative diffusions of the reagent ions and product ions and the flow dynamics of the gas inside the flow tube, all have to be known for reliable analytical measurement to be achieved.

1.3.2.3 Ion detection region

The reagent precursor ions that have not reacted and the product ions that are formed are conveyed to the detection region, which is a high vacuum chamber at about 1×10^{-5} Torr, through a 0.46 mm hole in a stainless disk. The detection region consists of the analysis quadrupole mass filter, an Einzel focus lens array and the electron multiplier. After passage through the orifice at the end of the flow tube, the ions are refocused by an Einzel lens array before they pass to the quadrupole mass filter. Once they have been transmitted through the quadrupole mass filter, they are collected by the electron multiplier and counted by a pulse amplifier. More details of these components are explained next.

1.3.2.4 Quadrupole mass filter

Quadrupole mass analyzers are currently used most frequently by chemists to obtain the molecular weight, particularly in chemical analysis. This device has significant advantages over other traditional mass analyzers, although it is not a high-resolution device. It is a relatively low cast device and couples readily with the detectors. It is also widely used with GC-MS and LC-MS instruments.

Resolving ions by this technique is based on the ion mass to charge ratio (m/z) rather than momentum or kinetic energy. [8] Another useful feature in the quadrupole mass device is the mechanical simplicity of the instrument. It does not rely on the use of a magnetic field in mass discrimination, avoiding the conventional magnetic field problems, such as the weight of the instrument, the cost and slow scan speeds. Moreover, the resolution of the quadrupole is set electronically rather than mechanically. Therefore, and in light of the previous advantages, it seems to be an ideal instrument for remote and fast analytical applications.

Physically, the quadrupole consists of four electrodes that are accurately positioned in a radial array making a circular cross section, as shown in Figure 1.3.

Figure 1.3 The quadrupole mass filter

DC and RF potentials are applied in these electrodes in order to control the ions' passage to the detector. Therefore, when the RF is positive in regard to the centre axis, a beam of positive ions will be accelerated and focused onto the center axis of the electrodes' structure. On the other hand, when negative RF is applied, the ions will be accelerated toward the negatively biased electrodes. The combination of both RF and DC potential will affect the trajectory of the collection of ions on the quadrupole. So, by controlling the RF and DC potential, a mass spectrum can be achieved. By appropriate controlling of the RF/DC ratio, ions will be filtered based on their mass to charge ratio. Consequently, mass resolution of the device is governed by the ratio of the RF to DC potential, applied to the electrodes.

Another effect that needs to be accounted for is related to ion mass. The heavier ions' count rate is enhanced by lower differential diffusion away from the flow tube axis and diminished through the discrimination effect in the quadrupole. In contrast, the light ions' count rate is diminished through diffusion away from the flow tube axis and enhanced through the quadrupole discrimination. These two phenomena therefore tend to cancel each other out, but they must be appraised for accurate analysis.

The DC-RF stability diagram provides a powerful method of visualizing the operation of the quadrupole mass filter at the different voltages. Moreover, it is used to set the scan line when the instrument mass scale is calibrated.

Mass stability of this quadrupole is very important. This stability is tested by monitoring a specific mass as a function of temperature and time. The normal situation for a particular mass feature is, that it should hold its position to better than ± 0.1 amu movement.

1.3.2.5 Einzel lenses

These electronic lens arrays are used for refocusing the ions before entering the quadrupole mass filter, in both the upstream and downstream chambers. An array of these lenses is set before and after the quadrupole, with an overall negative voltage gradient for adjusting and alignment purposes. This is in order to optimise the number of ions reaching the detector and hence to maximise the ion signals. These lenses are illustrated by Figure 1.4.

A high negative voltage is used in the first two lenses of the ion source region with the aim of: breaking the plasma sheath; pulling the positively charged ions out of the static plasma and also reducing the ion-electron recombination in the plasma, which is very fast.

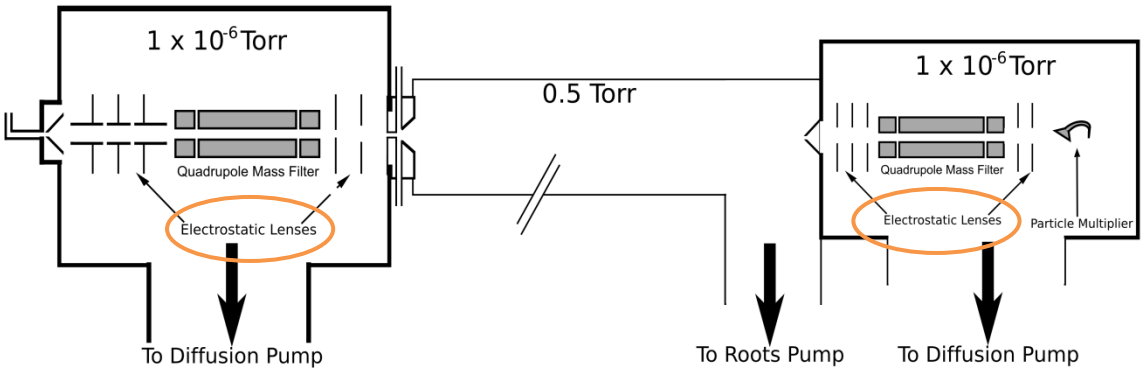

Figure 1.4 Schematic diagram of the SIFT-MS instrument – illustrating the Einzel lenses

1.3.2.6 Multiplier

An electron multiplier is used in the end of the downstream chamber, for detecting the ion signals. It converts single ions into a measurable electrical pulse. This type of electron multiplier has been used widely to detect charged particles either positive or negative, especially in analytical instruments, for more than 30 years. [9]

The multiplier is a vacuum tube-type structure that multiplies incident charges. This tube is often built as a funnel of glass coated inside with a thin film of a semi-conducting material.

For positive ion detection, a negative high voltage is applied at the wider input end. A small positive voltage near the ground potential is applied at the narrower output end, as shown in Figure 1.5. When the ion is bombarded on the funnel, electron emission is induced. Then, the large potential gradient on the surface accelerates the electron with the process being repeated many times over, creating an avalanche of secondary electrons. A typical gain of an electron multiplier is 5×10^7. The ion signal on the output is then counted by a pulse amplifier discriminator unit. [10] The particle multiplier used in the SIFT-MS Voice100 is a DeTech model 203. [11] One drawback, when very high ion count rates are experienced, is that successive pulse may not be able to be resolved. This however, is unlikely to occur at the count levels that are typical of a Voice 100 instrument.

Figure1.5 The particle multiplier.

1.3.2.7 Pumps

Specific conditions have to be maintained in the SIFT-MS instrument to make it operate and transmit ions. Pressure is one of the critical conditions for the operation of the mass spectrometer. The high voltages required for the detector, lead to internal discharges at low to moderate pressures. They must be operated below 10^{-4} Torr. Thus, different types of pumps are coupled to the instrument for getting the right pressure conditions that are needed. Each region in the instrument needs a particular pressure. The upstream and downstream chambers

require very low pressure in order to allow molecules to flow. For this reason, a high capacity pump is required to achieve the very low-pressure needed for maintaining a flow pressure and reducing the number of collisions. For both chambers, a turbo molecular pump has been chosen for this task. The turbo molecular pump has the capacity to go to very low pressures of 10^{-5}-10^{-8} Torr and at speeds of 150-2500 L/s. This pump has a series of vaned blades on a shaft, rotating at speeds up to 60,000 rmp between an alternate series of slotted stator places (Figure 1.6). Air, as described in McMaster's book [12], is grabbed by the blades, whipped through the stator slots and grabbed by the next blade. In this process, although only a small amount of air is moved each time, the number of blades and high rotary speed rapidly move more air from the chamber to the exhaust. In addition, the biggest advantage of using the turbo pump rather than the oil diffusion pump, which operates in a similar process regime, is that it contains no oil to contaminate the analyzer.

However, some conditions are required to make the turbo pump operate at the high rpm rates required. These high rotational speeds can only be achieved by providing the turbo pump, backed by another pump, with less capacity to lower the pressure at which it operates. This backing pump is a rotary vane vacuum pump (Figure 1.7) and has the capacity to take the pressure down to 10^{-3} Torr, which is required for the turbo to operate. This pump has the capacity of moving 50-150 L/min. A further pump is required to achieve the flow speeds necessary for the flow tube gas at 0.5 Torr. A Roots pump, backed by a rotary vane pump, is used for this purpose.

This variety of pumps used in the instrument are in fact important for keeping the system in the right and proper conditions that are required for the analysis goals. The flow tube pressure has to be 0.5 Torr, whereas the other two regions have to be 10^{-5} Torr. Figure 1.8 shows a detailed schematic diagram of a Voice 100 SIFT-MS.

Figure 1.6 Turbo pump cross-section

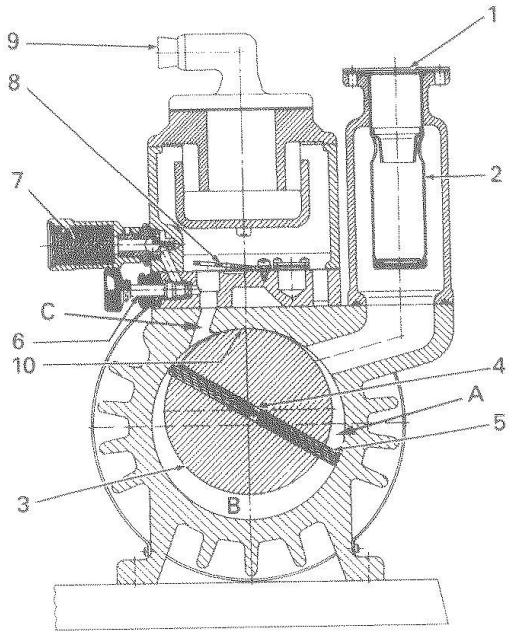

Figure 1.7 The rotary vane vacuum pump

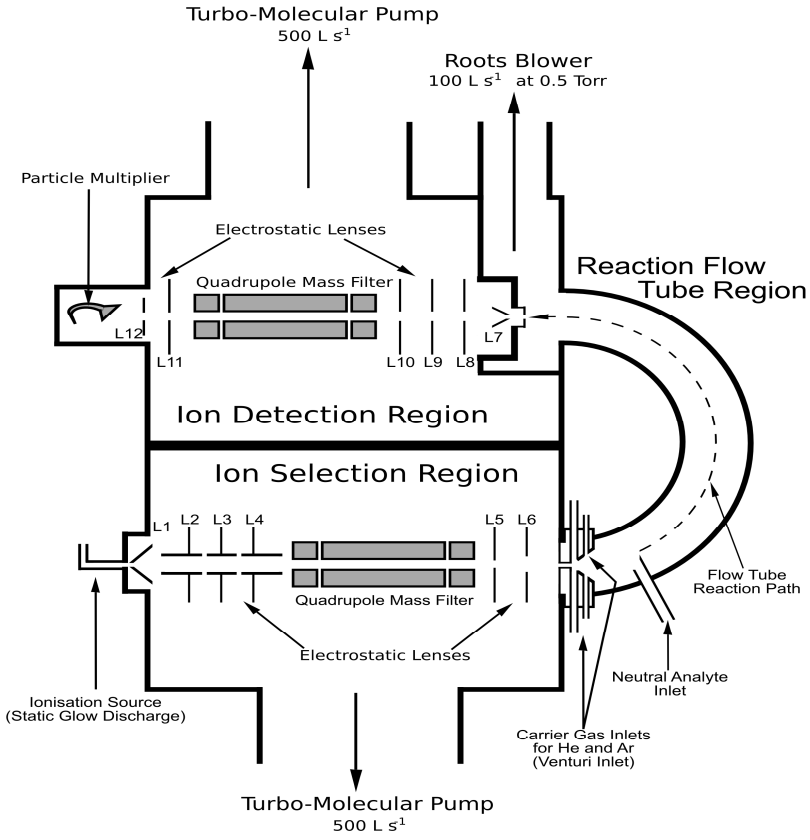

Figure 1.8 A detailed schematic diagram of the Voice 100 SIFT-MS.

1.3.3 How SIFT-MS works

After turning the instrument on and getting to the right operating conditions, ion precursors are generated to give the most stable positive ions: H_3O^+, NO^+ and O_2^+. These ions are focused by the lenses, into the quadrupole mass filter. At that stage, a specific ion of interest is selected by the quadrupole mass filter. The ion of interest is refocused again by the next lens array and injected into the flow tube in which the pressure is higher than the upstream source chamber pressure. These ions are passed to the flow tube taking advantage of the Venturi effect from the venture nozzle. After that, these ions undergo many collisions with the bath gas in the first few cm of the flow tube. In this thermalising process, the excess energy is removed from the excited ions, transferring most of them to the ground electronic state and thermal velocity distributions as illustrated in Figure 1.9. The presence of the excited ions can lead to different ion products and can affect the reproducibility of the system. Excited NO^+ has only been found in small quantities of about 2% in the flow tube. However, the thermalization process still seems to be very effective. Then, the ions are carried by both carrier gases, argon and helium, inside the tube, colliding with neutral compounds that are inserted from a heated capillary in the sample inlet. Argon is used in this instrument for its advantage of reducing the radial diffusion of ions in the tube. [13]

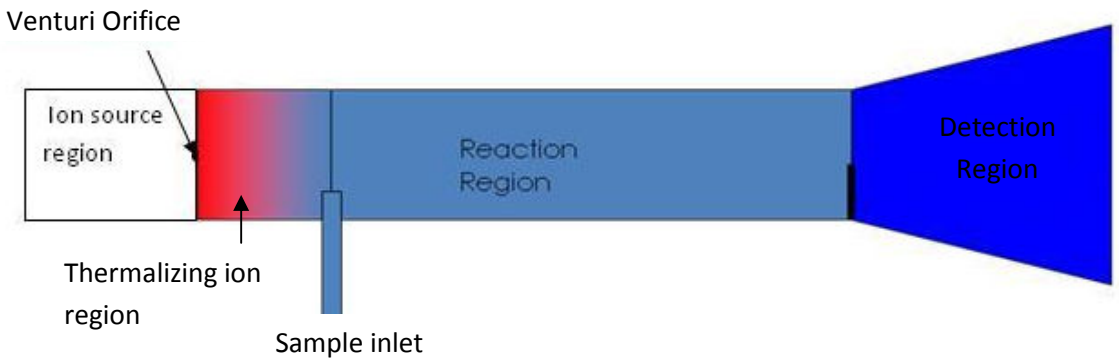

Figure 1.9 Sketch illustrates the thermalizing ions region

The sample to be analysed is inserted from the sample inlet, which contains a heated capillary (~ 100 °C). The flow rate of the sample through the capillary has been found to be crucial for the determination of the kinetic parameters. Each ion precursor reacts with an analyte producing characteristic ion products via ion-molecule reactions. These products and the rest of the ion precursors are then transported by the carrier gas to the detection region. However, not all ions pass through the flow tube and the detection region with equal efficiency. Some of these ions are found to be lost through diffusion, which is mass dependent. There is also, mass discrimination in the quadrupole and lens system. In the detection region, the pressure is very low, so the reaction stops. After entry into the detection chamber, the ions are refocused again before they are mass analysed by the quadrupole, according to their mass to charge ratio. After passage through the quadrupole, they are focussed into the particle multiplier and are detected. The measurements, obtained by collecting the results, appear as a reduction in the count rate of the main ion precursors and an introduction of product ions of their appropriate m/z ratios. Figure 1.10 shows the output data. Thus, by analysing all the peaks and assigning them to their appropriate ions, the analyte identification can be achieved. Consequently, and after an appropriate calculation on the computer of the ratio of product ion count to the reagent ion count, the concentration of analyte can be determined**.**

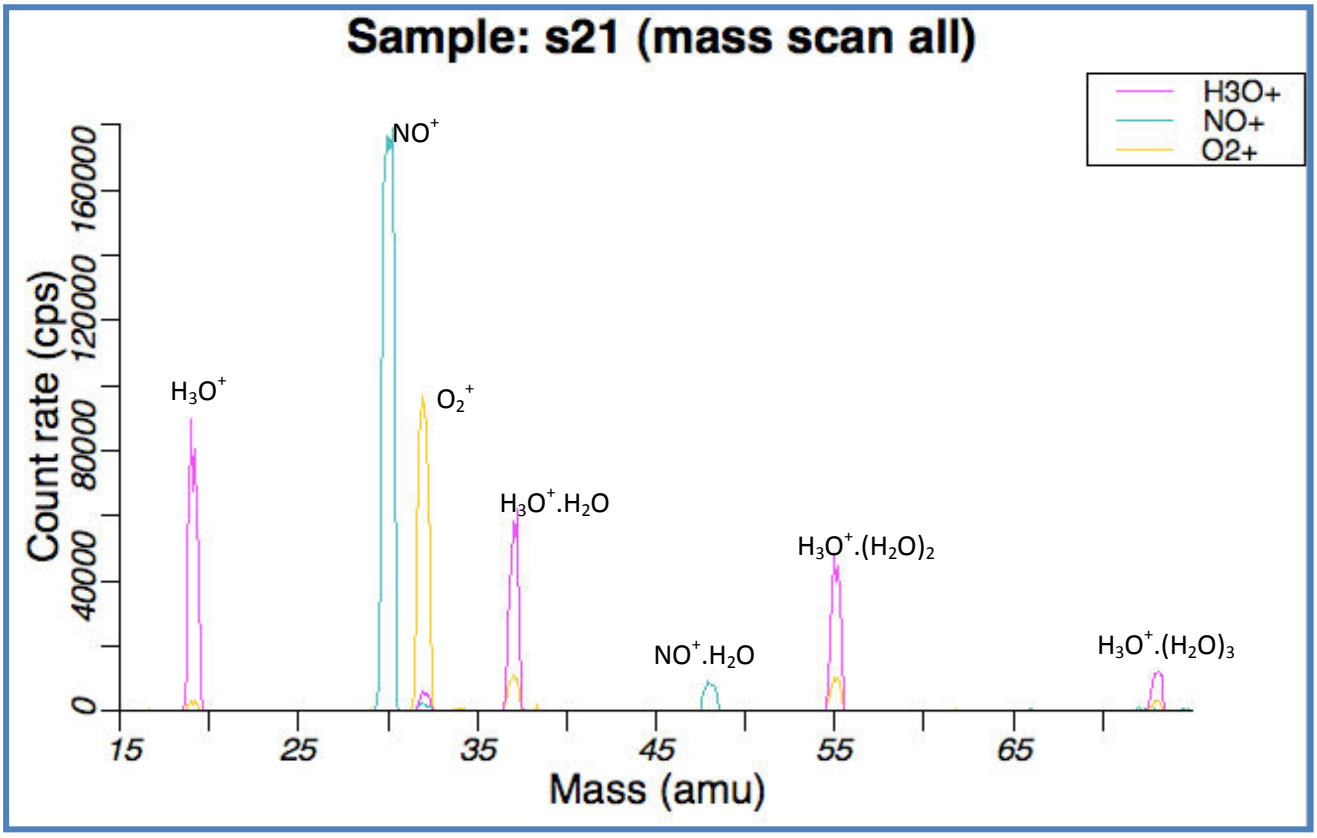

Figure 1.10 SIFT-MS outcome spectrum, indicating the main and secondary ion precursor peaks

1.3.4 Important Points that must be considered when using SIFT-MS

There are some important points that have to be considered when dealing with SIFT-MS in order to have accurate and precise measurements. Firstly, the applicable concentration range of the SIFT-MS for the quantization analysis of molecules has to result in a less than 15% reduction in the precursor ion signal as a consequence of the reaction with the analyte. Secondly, the uneven loss of ions according to mass through the instrument can lead to inaccurate measurements and has to be corrected. The diffusion phenomenon and mass discrimination variation of the quadrupole, perhaps, are the most contributing phenomena to the loss of the unit efficiency of this system. However, the radial diffusion losses, away from the flow tube axis, are reduced by using argon gas. [13] Therefore, a correction is essential for achieving good results considering these phenomena. Based on that, an instrument

calibration is usually done to correct the ion signals. Two different methods have been used to measure the instrument calibration factor (ICF), which will be discussed later. However, the SIFT-MS technique does not require a calibration to be carried out on a per-analyte basis.

Thirdly, downstream quadrupole stability has to be checked in order to hold the signal in a fixed position as a function of time and increasing temperature of the instrument. This can be checked by selecting a specific mass signal, monitoring the movement of the signal for a period of time and by increasing the instrument temperature, using 10 steps per a.m.u. scan.

Fourthly, the capillary and sample flow rate are also very important in terms of their effects on the analytical measurements. The sample flow rate has to be preset to reach the desired good results. In addition, there is another problem in introducing the sample to the capillary, which is the adsorption of the analyte compounds on the capillary walls. Heating the capillary has been found to reduce this phenomenon; it minimizes the loss of condensable trace gases by surface adsorption but does not completely dominate the problem for “sticky” molecules. A better solution is to use a passivated capillary and inlet system in order to reduce the adsorption and to produce a linear relationship between the concentration and the count rate.

Finally, the secondary chemistry reactions have also to be taken into account to produce a good measurement. A consequence of this is the $H_3O^+.(H_2O)_{1+2+3}$ cluster reactions with the analyte need to be studied kinetically as well. The quantitative understanding of secondary chemistry has to be included in the analysis.

1.3.5 Ion molecule reactions

The three most common ion-molecule reactions that have been noted with the SIFT-MS ion precursors, H_3O^+, NO^+, and O_2^+, are proton transfer, charge transfer and dissociative charge transfer, and ion precursor association reactions. H_3O^+, NO^+, and O_2^+ are considered the best ions of choice in most analysis cases because of their prominence in an air afterglow in the SIFT-MS ion source. These ion reagents are not highly reactive with the major components of air. Their use can allow some mass identification of VOCs, unlike the PTR-MS, which mainly uses H_3O^+. Further, a combination of these ion precursors facilitates the determination of many of the compounds of interest. At the same time, they resolve many of the interference problems and add some extra complementary information.

1.3.5.1 H_3O^+ reactions

H_3O^+ can be deemed the most common ion precursor for quantifying polar organic compounds. Generally, most reactions proceed mostly via exothermic proton transfer as exemplified in reaction 1. An important feature of this reaction is that it mostly proceeds with unit efficiency.

$$H_3O^+ + M \longrightarrow MH^+ + H_2O \quad (1)$$

Of the three precursors, this type of reaction occurs only with the H_3O^+ ion. Whether it occurs depends on the proton affinity (PA) of the analytes. The H_3O^+ proton affinity (PA) is 691kJmol^{-1}. Therefore, proton transfer reaction can only occur when the PA of the analyte is higher than 691kJmol^{-1}. However, in some cases, particularly with some alcohols, aldehydes, and carboxylic acids, dissociative proton transfer takes place. Its MH^+ dissociates and loses a H_2O molecule.[7] In contrast, when OH is bonded directly to the aromatic ring as in phenols, H_2O elimination does not occur and MH^+ is the only product formed. Both products can be

formed, in parallel, in some cases, so a careful search must be made to determine all the product ions. More complex product ions formation has been found with ether and ester reactions.

In addition, the formation of water clusters, as indicated by equation 2, can provide secondary reactions that need to be included in the analyte quantification process and also increase the complexity of analyzing the spectrum peaks. The wetter the sample, the greater the role of secondary reaction of the product ions with H_2O. A dihydrate is usually formed with alcohols, aldehydes and carboxylic acids, while a monohydrate is usually formed with ketones, esters and ethers, as indicate in equation 3.

$$H_3O^+ + H_2O + X \longrightarrow H_3O^+.(H_2O)_n + X \qquad (2)\ X \text{ is third body (He or Ar)}$$

$$H_3O^+.(H_2O)_n + M \longrightarrow MH^+.(H_2O)_n + H_2O \qquad (3)\ \text{ligand switching reaction}$$

$$MH^+ + H_2O \longrightarrow MH^+.(H_2O)_n$$

The molecular species that have a lower PA than water cannot undergo proton transfer reaction and for these analytes other ion precursors are required.

1.3.5.2 NO^+ reactions

The reaction with NO^+ undergoes three types of reactions: association, charge transfer, and hydride ion transfer. The charge transfer reaction occurs when the ionization energy (IE) of the compounds is smaller than the ionization energy of NO^+, 9.26eV. It occurs with aromatic hydrocarbon and organosulfur molecules [14][15] as equation 4 illustrates.

$$NO^+ + C_6H_5CH_3 \longrightarrow C_7H_8^+ + NO \qquad (4)$$

Association reactions, in contrast, commonly occur with some types of polar organic molecules especially carboxylic acids, esters, and ketones. They often occur in parallel with other processes. This reaction is apparently enhanced when there is not much difference between the IE of the NO^+ and the IE of a compound such as some ketone, where the IE of the acetone, for example, is 9.71eV as shown in equation 5 below.

$$NO^+ + CH_3COCH_3 + He \longrightarrow NO^+CH_3COCH_3 + He \qquad (5)$$

Finally, the hydride ion transfer reaction is the only process that occurs specifically with NO^+. This involves the abstraction of H^- from the compound, resulting in HNO and a single ion product, the parent cation molecule with less H (see equation 6), particularly with aldehydes, ethers, and primary and secondary alcohols.

$$NO^+ + CH_3CHO \longrightarrow CH_2CHO^+ + HNO \qquad (6)$$

1.3.5.3 O_2^+ reactions

Most of the O_2^+ reactions are direct charge-transfer reactions (equation 7) and dissociative charge-transfer reactions (equation 8). The O_2 molecule has an IE of 12.06eV. Accordingly, the O_2^+ will react with most molecules having lower IE. As the IE of O_2 is appreciably greater than most organic compounds, it reacts with many molecules via one of the above processes.

$$O_2^+ + M \longrightarrow M^+ + O_2 \qquad (7)$$

$$O_2^+ + C_4H_{10} \longrightarrow C_4H_{10}^+ + O_2 \qquad (8)$$

$$\longrightarrow C_4H_9^+ + O_2 + H$$

$$\longrightarrow C_3H_7^+ + O_2 + CH_3$$

$$\longrightarrow C_3H_6^+ + O_2 + CH_4$$

Using O_2^+ ions in the SIFT-MS reactions leads to multiple ion products and therefore a more complex mass spectrum. It is similar to the mass spectrum obtained by electron impact ionization that results in extensive fragmentation of the parent molecule. The number of products generated by O_2^+ chemical ionization limits the usefulness of this precursor. O_2^+ is most valuable for the detection of inorganic volatile compounds such as NO, NO_2, NH_3 and CS_2 in which it does not undergo dissociative charge transfer with these species. Moreover, it is also useful for checking the identification of the H_3O^+ and NO^+ products.

1.3.6 Kinetics and rate coefficients

A fundamental requirement of the SIFT-MS technique is the knowledge of the kinetic parameters of the reagent ions with the analyte molecules. Consequently, the rate coefficient and the product branching ratios need to be determined for the reagent ions' reactions with all the compounds of interest.

Two methods have been used to measure the rate coefficient. [11] Firstly, the absolute method, in which the rate coefficient is obtained from the slope of the semi-logarithmic plot of ion intensity against an absolute measurement of neutral flow for compounds with vapor pressure greater than ~2.5 Torr at 20 °C.

The rate coefficient from this method can be determined theoretically from the simple chemical reaction equation:

$$A^+ + B \longrightarrow \text{products}$$

The rate reaction between A^+ and B is given by

$$-d[A^+]/dt = k[A^+][B]$$

Because [B] >> [A^+] by typically 5 orders of magnitude. This rate law can be defined as a pseudo-first order rate law.

By integrating this equation, we have:

$[A^+] = [A_0^+]\exp(k[B]t)$

$\ln[A^+] = \ln[A_0^+] - k[B]t$

[B] is the number density of the ion precursor. [B] can be determined from the flow rate as the next equation shows: [7]

$$[B] = B\frac{\Phi R\, P_g}{\Phi c + \Phi R\, Kb\, Tg}$$

[B] = number density, Kb = Boltzmann constant, Tg = carrier gas temperature, ΦR= reactant gas flow rate, Φc= carrier gas flow rate, Pg=carrier gas pressure.

So, the integrated equation can be expressed in terms of the intensity, as shown below.

$\ln I = \ln I_0 - kt[B]$

Then, this equation can be written in terms of the correction, as shown next.

$$\ln I = \ln I_0 - k[B]\frac{l + \varepsilon}{\gamma i}$$

I= count rate of the precursor, I_0= count rate of the precursor in the absence of the analyte, k= rate coefficient, [B]= number density, ε= end correction distance, mixing distance of the reactant gas into o the carrier gas that is typically 2cm, γ^i= ion velocity, l= the distance of the inlet port to the downstream orifice.

Because [B] can be calculated from the flow rate, so the rate coefficient can be determined by plotting the semi-logarithmic function lnI against [B]. k, the rate coefficient is then easily determined from the slope. This method is dependent on an accurate determination of [B], which introduces an error of approximately ± 10%.

The second method is a relative method, which is used for compounds with vapor pressure less than 2.5 Torr at 20 °C. In this method, only the rate coefficient is measured relative to the H_3O^+ reaction, which is assumed to occur at the collision rate. This method depends on the knowledge that exothermic proton transfer reactions proceed at the collision rate and there is extensive laboratory evidence to support this view. The collision rate can be calculated theoretically if the polarizability and the dipole moment of the reactant molecule are known.[16] Then, from the ratio of the decay rates of the NO^+ and O_2^+ reactions compared to the decay of H_3O^+, rate coefficients can be determined for NO^+ and O_2^+.

In summary, if the rate coefficient and product ion ratios are known, then the concentration of the analyte can be determined. Thus, knowledge of the product ions and their kinetic data is loaded into the software database used by the SITF-MS instrument, which then can be used for an analyte concentration measurement.

1.3.7 Modes of operation of SIFT-MS

Two instrument modes can be used in the SIFT-MS experiment: the mass scan mode and selected ion monitoring scan mode (SIM). As mentioned in the *GC-MS A Practical User's Guide Book*, the difference in these two modes can be described as: "it depends on whether we wish to look at the forest or the trees."

1.3.7.1 Mass scan mode

A full mass scan is a continuous scan over a range of masses. It is always used for testing an unknown sample, showing the mass of the various product ions usually from 10-200 amu. At present, the upper limit is typically 200 amu (Voice 100) and 250 amu (Voice 200) due to the poor mass discrimination for large ions [17] and their lower velocity.

1.3.7.2 SIM scan mode

In SIM scan or selected ion-monitoring scan, only pre-selected masses are scanned rather than scanning the full mass range. In other words, it is a jump scan over a discrete number of masses. [18] This mode gives more accuracy in terms of the ability to monitor specific ion amplitude. It can be used for all three-reagent ions during a single SIM scan.

The main advantage of using this mode is the high sensitivity and quantitative analysis result that can be provided by this mode and its usefulness in the detection of only specific desired compounds.

Chapter 2

Preliminary preparations and experiments

1. Introduction

Before performing experiments, a thorough series of calibration checks of the instrument are required. This chapter describes the experimental procedure followed during the course of preparing the instrument prior to use for analysis. This procedure is important in terms of obtaining reliable measurements. Then, this discussion is followed by a brief summary of experiments on some important flavour compounds, and an examination of the validity of using Tedlar bags for air analysis. These introductory experiments provide more insight into instrument-required procedures, and appraise the ability of this technique to cope with potential problems associated with a range of analytes.

2. Preliminary work

This research began from preliminary tests in the laboratory with the SIFT-MS to test the validity of the current parameters of the instrument. This, in fact, included calibrating the instrument, measuring the instrument calibration factors (ICF) and testing the quadrupole stability of the instrument. Then, the compounds of interest were calibrated for better measurement accuracy.

2.1 Instrument calibration

2.1.1 Instrument calibration factors (ICF)

The ICF defines the mass-dependent correction that raw signal measurements are multiplied by, to correct the differences in the transmission and detection efficiencies of different ions.[19] Instrument calibration was performed in order to measure and correct the instrument calibration factors (ICF), using the Constant Cumulative Count (3C method) and the new calibrated cylinder method.

i. The Constant Cumulative Count (3C method)

The 3C method is based on the assumption of normalising the sum of all detected ion signals over the entire mass range, if there was unit transmission and detection efficiency for all ions passing through the instrument, regardless of the product-ion distribution. The 3C method simply involves producing a number of mass spectra with different product-ion distributions and then choosing a function of mass that, when applied to those mass spectra, show a constant sum of all product signals that match the unreacted reagent ion's signals. The outcome of this procedure is that if the ICF is correctly applied, the same ICF will also be true in the presence of mass discrimination effects. The 3C method was performed according to the Syft procedure by making samples of a selection of analytes that result predominantly in a single product ion, at the chosen concentration in the mass range of the instrument. Also, the concentration of these analytes should be concentrated enough to reduce the reagent ion count by more than 20%, but not so concentrated that they influence the diffusion of ions in the flow tube. The following samples were used as they had been shown to give satisfactory results:

a. Sample inlet closed
b. Nitrogen with a trace of moisture
c. Air at the ambient humidity
d. Air at breath humidity
e. Benzene
f. Toluene
g. Xylene
h. Acetone
i. MEK
j. Pentanone
k. Hexanone or MIBK
l. Heptanone

However, this method exhibited some difficulties while trying to control the sample concentrations and depletion of the reagent ions. Therefore, due to its great complications, this method was replaced by the new calibrated cylinder method.

New calibrated cylinder method for determining ICF

The new ICF method is based on using predefined analyte concentrations such as, measuring concentrations present in a Scotty bottle that contains compounds known to a high precision. These compounds have different mass ranges, with the range of compounds used covering the entire mass spectrum required as shown in Table 2.1.

Table 2.1 Scotty bottle compounds that are used for the instrument calibration.

Analyte	M.Wt
C_2H_4	28
C_4H_{10}	58
C_6H_6	78
C_8H_{10}	106
$C_4H_2F_4$	126
C_6F_6	186
C_7F_8	236

The signal intensity can be adjusted according to the mass of the analytes used. Theoretically, this can be explained by the following: first, the concentration of a known analyte is measured; the concentration, as determined by the SIFT-MS instrument, is then adjusted to the correct concentration according to the equation below:

$$[A] = \frac{{}_{ICF}P^{+}}{{}_{ICF}I^{+}kt}$$

Where:

[A] = analyte concentration, ICF= Instrument correction factor for the product and in the dominator for the reagent ion, P^+= product ion intensity, I^+= reagent ion intensity, k= rate coefficient, and t= reaction time.

[A] is known and k, I^+ and P^+ are known parameters. One parameter, t, the time of the reaction in the flow tube, still has to be determined before the ICF can be measured. The reaction time t, can in fact, be measured from the ethene reaction (equation 1) with O_2^+ where ICF is assumed to be 1 for both the O_2^+ and $C_2H_4^+$ ions that have masses of 32 and 28 respectively. This is due to the small mass discrimination between O_2^+ and $C_2H_4^+$, which assumes $ICF_{O2+} \approx ICF_{C2H4+}=1$. Therefore, in this case the only unknown parameter is t, which then can be easily calculated. The reaction time is assumed constant for all reactions, so the only parameter left unknown is the ICF. The ICF product factors are measured for the compounds that are illustrated in Table 1 above, and range up to 186 amu for the Voice 100 instrument.

$$C_2H_4 + O_2^+ \longrightarrow C_2H_4^+ + O_2 \qquad (1)$$

For example, the ICF of the benzene ion products, resulting from the reaction with O_2^+ (equation 2), can be calculated in the same way. As I^+, P^+, k, [A], the ICF of the reagent ion, and t are known, (the ICF of the O_2^+ precursor is assumed to be 1), then the only unknown parameter is the ICF of the product ion, which can be determined. Similarly, from the reaction of benzene with H_3O^+ (equation 3), the ICF of the H_3O^+ precursor can be calculated, due to the availability of the ICF value of the product that is now known from the reaction with O_2^+. Likewise, the ICF of the other analytes up to the instrument mass range limit can be determined using this technique. The measurement of the ICF factors has been aided by using a special spreadsheet that was built for this purpose. The result of the ICF calibration of the LDI1 instrument, for example, is illustrated in Figure 2.1.

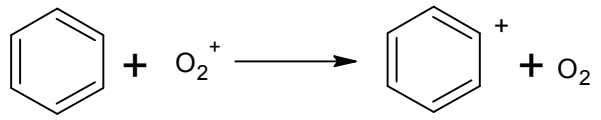

(2)

$$C_6H_6 + H_3O^+ \longrightarrow C_6H_6.H^+ + H_2O \qquad (3)$$

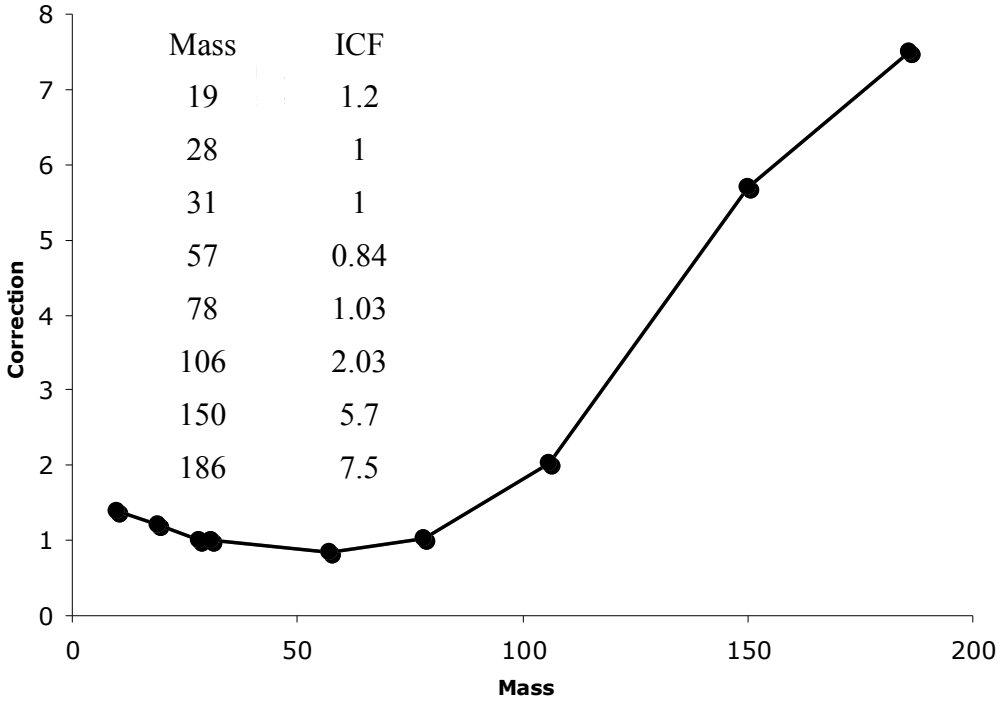

Figure 2.1 ICF diagram result for the LDI1 instrument, using the new cylinder method.

2.1.2 Quadrupole stability

The stability of the quadrupole mass filter is very important in quantitative analysis. This stability was tested on the voice 100 (P1) instrument in order to establish the reliability of the data, by monitoring a specific mass as a function of temperature and time. It is expected that the position in mass spectrum should be constant to within ±0.1 amu. To do this, the mass scan line was first calibrated using tetradecane ($C_{14}H_{30}$). The instrument was then switched

off to allow it to cool down for about 2 hours. It was then turned on again and the quadrupole stability was tested using a repeating scanning method, as a function of time and temperature. Movement in mass peak of more than 0.1 amu, as shown in Figures 2.2 and 2.3, is an example of an unstable quadrupole mass filter as found in the P1 instrument, prior to the adjustment of the RF transforming voltage of the planar with increasing temperature. Figures 2.4 and 2.5 show a good stability of the quadrupole with reproducibility in the mass position better than 0.1 amu.

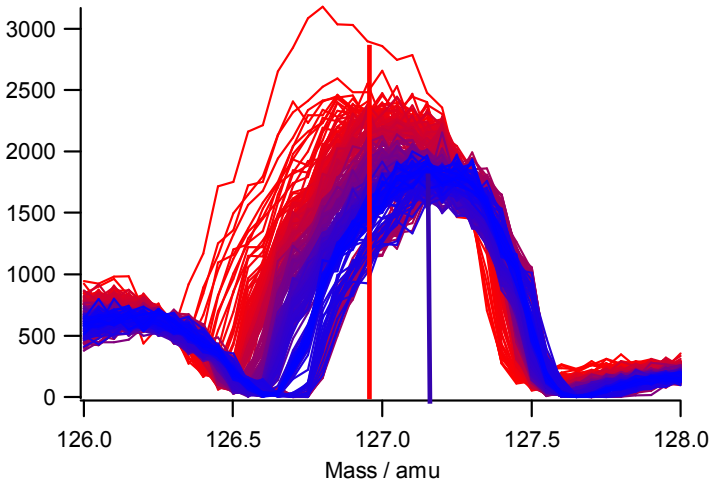

Figure 2.2 Unstable quadrupole, band signal shifts more than 0.1 amu

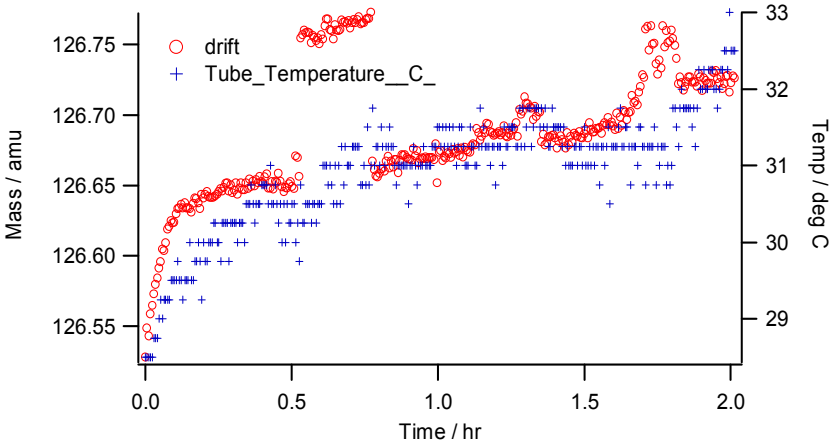

Figure 2.3 Shifts in mass of more than 0.1 amu as a function of time and temperature.

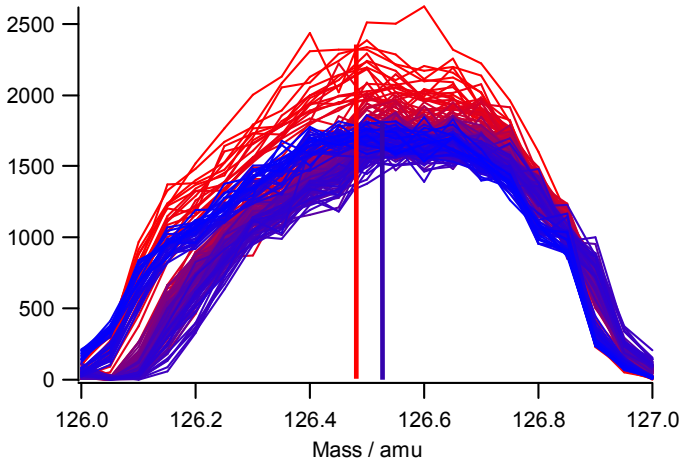

Figure 2.4 Reproducibility of a mass peak in stable quadrupole, showing shifts in the mass of less than 0.1 amu.

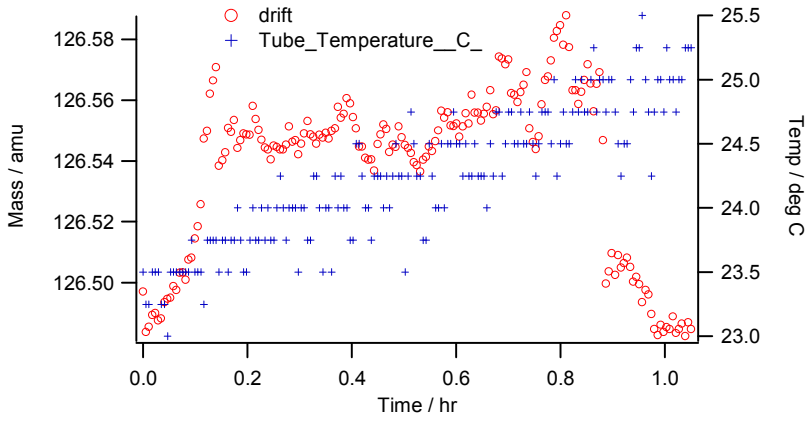

Figure 2.5 Shifts in mass of less than 0.1 amu as a function of time and temperature.

2.2 Analyte calibration

Recently, with the ongoing developments in analytical methods for sampling, a number of different methods is available for preparation of calibration mixtures. Two methods have been used in this work for preparing standards. [20]

2.2.1 Static method

In the static method, the sample is prepared by injecting into a container, a known weight of the target organic compound that is sufficiently volatile to be completely vaporized. This method, nonetheless, shows certain drawbacks in terms of the degree of the stability of the compound in the container; the adsorption process by the container wall and errors introduced in the dilution steps.

2.2.2 Dynamic method (Permeation tube)

In contrast, dynamic methods are generally preferred for generating standard mixtures using permeation tubes. Several advantages have been noted for this method according to Simonetta et al.'s study (2005) [21], such as minimizing the effect of adsorption, the capability of producing precise continuous dilution ranges and the ease of generating flow having different humidity.

The second dynamic method was chosen as the best calibration method in the SIFT-MS instrument with the stated benefits previously described. Using a permeation tube, a test gas mixture, of known concentration, is obtained by controlled permeation of a gaseous analyte out through the Teflon polymer walls of the permeation tube at a precise temperature in an oven. The analyte is transmitted in a carrier gas stream to the SIFT-MS instrument.

Permeation tubes contain gases that have usually condensed to liquids under pressure. The weight loss of vapour through the walls of the tube, at the specified temperature, has been evaluated by the manufacturers. When operated at the temperature specified, they can be used as primary calibration standards.

3. Some important flavour compounds analysis

3.1 Maltol

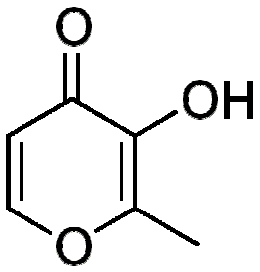

3-hydroxy-2-methyl-4H-pyran-4-one

M.Wt. 126 g/mol

Vapour pressure: 0.00243 mmHg at 25 °C

Maltol is a natural organic compound that is used primarily as a flavour enhancer. It is one of the flavour compounds in milk and cheese and is one of a range of other important flavour volatile compounds that the food and flavour industry are interested in, as shown in Table 2.4. In order to measure its concentration in milk and cheese, using the SIFT-MS technique, we have first to determine the kinetic parameters of the main reagent ions H_3O^+, NO^+ and O_2^+ with maltol. In order to obtain these parameters for maltol, the relative rate method is used because of the low vapour pressure of maltol (2.43×10^{-4} Torr at 25 °C). In this method, a diluted sample of maltol was created in a Tedlar bag full of nitrogen and then sampled into the SIFT-MS. Next, the products arising from the reaction of each reagent ion with maltol, were identified and counted. Relative decay rates were then obtained for each reagent ion. For example, the reaction with the H_3O^+ produces one proton transfer ion product. Further, it

is known that the rate of this exothermic proton transfer reaction equals the collision rate, as this invariably occurs for exothermic proton transfer reactions.[22] This rate can be calculated theoretically with regard to the dipole moment and the polarizability of the maltol.[16] The rate coefficients for the reagent ions NO^+ and O_2^+, cannot be obtained by the same calculation because their reactions do not necessarily occur on every collision. However, their rate coefficients can be obtained by measuring their decay rates, relative to that for H_3O^+. The result is summarised in Tables 2.2 and 2.3.

Table 2.2 The relative decay rate of the three reagent ions with the maltol and the collision rate of the H_3O^+

	H_3O^+	**NO^+**	**O_2^+**
k	5.41	2.42	2.91
%	100%	45%	54%
H_3O^+ Collision Rate			
4.8×10^{-09}			

Table 2.3 The resultant rate coefficients of the three reagent ions.

Precursor	**Rate constant**	
H_3O^+	4.8×10^{-09}	cm^3/molecule/s
NO^+	2.2×10^{-09}	cm^3/molecule/s
O_2^+	2.6×10^{-09}	cm^3/molecule/s

Table 2.4 Some of the milk flavour volatile compounds, including maltol, that are of interest to the food and flavour industry.

Compound	Sensory properties[23]	Chemical structure	M.Wt
Skatole	Flowery	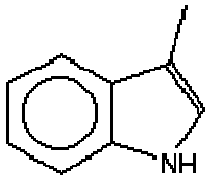	131.17
Acetone		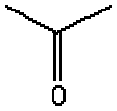	58.08
2-heptanone	Blue cheese		114.19
Maltol	Caramel	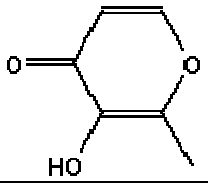	126.11
2-Hepten-1-al	Oily , putty		112.17
2-Heptenal,Z	Oily , putty	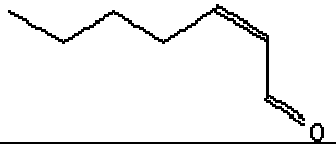	112.17
2-Heptenal,E	Oily , putty		112.17
Ethyl butanoate	Ester, fruity	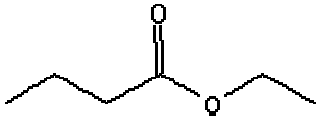	116.16
2-Methyl butanal	Malty , cocoa	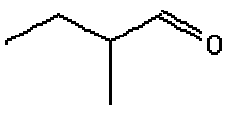	86.13

3-Methyl butanal	Malty, cocoa	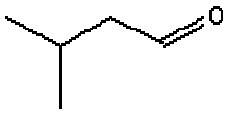	86.13
Dimethyl sulfide	Cowy		62.14
1-Octen-3-one (Vinyl amyl ketone)	Metallic, mushroom		126.20

3.2 Distinguishing between aldhydes and ketones

SIFT-MS has the ability to distinguish between some isobaric compounds. This is a valuable asset when applied to aldhydes and ketones, which are very common components in food flavours. To do this, the selected ion precursor feature is used. Butanal and butanone, which have the same molecular mass of 72 amu, are distinguished by using a particular precursor and looking for different product masses as a consequence of different reactions of aldehydes and ketones with the reagent ions. The reaction with H_3O^+ gives the same product ion mass for both of them at mass 73 and therefore cannot be used for distinguishing between them. However, the reaction with NO^+ gives an association reaction with butanone to give a 102 amu product ion and hydrogen elimination with butanal, giving a product ion at 71 amu. Therefore, the reaction with NO^+ provides a convenient way of distinguishing between these isomers as shown in the following equations:

This distinction between butanone and butanal was utilised when examining a sample of a liquid coffee, which had a complex aroma. Coffee is known to contain over 500 compounds that have been observed in the headspace using different analytical techniques. Two of these compounds are butanone and butanal. A diluted butanone solution was added to a liquid coffee sample and the relationship between an added quantity of butanone in the coffee and in the headspace was measured using the SIM method with NO^+ as the reagent ion. A linear relationship was obtained as shown in Figure 2.6. This linear result confirms the fact that butanone can be distinguished from butanal in a headspace of a liquid coffee mixture and shows the linear response.

The experiment conducted on coffee demonstrates how SIFT-MS is able to distinguish between isobaric compounds with different functional groups such as ketone and aldehyde.

Figure 2.6 MEK detected in a coffee mixture and the linear response resulting from increasing MEK concentration.

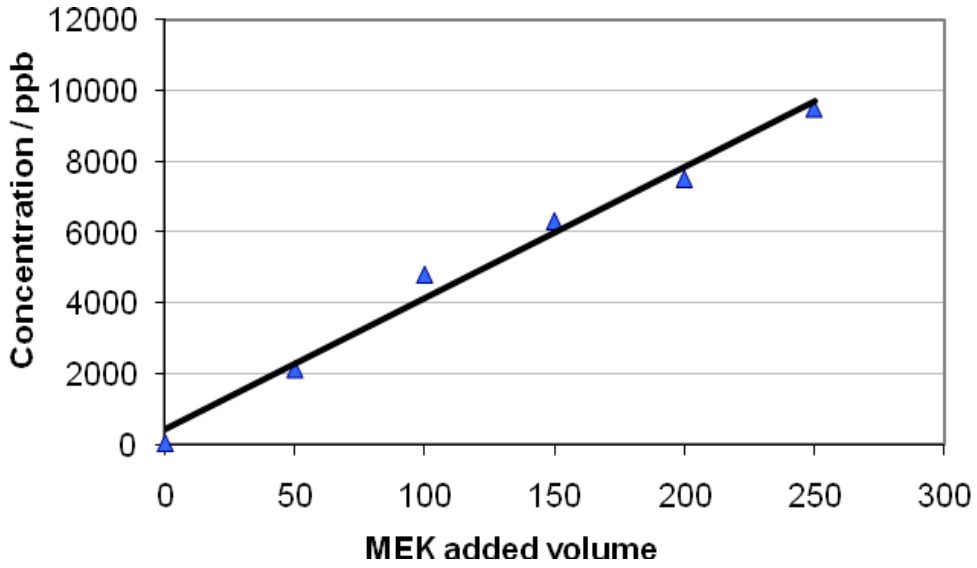

3.3 Vanillin

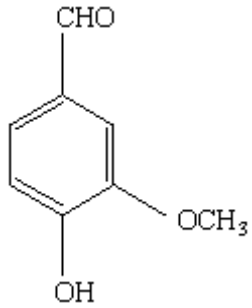

Benzaldehyde, 4-hydroxy-3-methoxy

M.Wt. 152.1473

Some work was done on vanillin, which is one of the compounds that can be found in several different foods. Vanillin is also commonly added as a flavour compound in foods, so having the ability to detect it is very important to the food industry. However, an immediate problem arose when dealing with this compound with its 3 different functional groups. This problem was mainly related to the inability to measure the exact concentration of the compound because of its adsorptive nature on the walls of the inlet. Hence, the sticky property of this compound led to a reduction in the ion count of the product. The degree of adsorption was investigated. A set of different vanillin concentrations, in a range of ppm concentrations, was prepared for quantitative analysis in an attempt to achieve a linear relationship between increasing concentration and the headspace ion count. A short heated inlet was used in this process to avoid the exposure of vanillin to a large surface area, as this tends to reduce the sticky effect of the vanillin. The result, nonetheless, was not satisfactory as illustrated in Figure 2.7. It indicated a significant extent of vanillin adsorption on the inlet walls that increased in proportion to the concentration of vanillin. Significant deviations from headspace concentration and solution concentration were apparent.

Figure 2.7 Vanillin deviating concentration due to adsorption process.

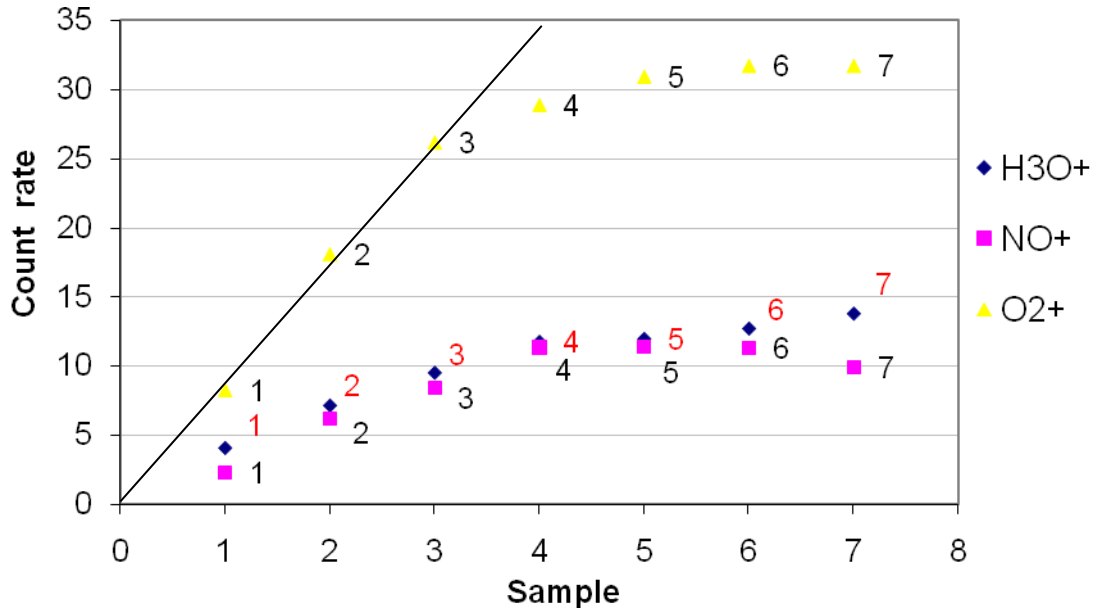

4 Citrus fruits experiment

Some experiments were performed on citrus fruits in order to determine the concentration of specific compounds, in different types of citrus. These compounds make up the distinctive aroma of citrus fruits and many of them are common to a number of citrus fruits. The ratios of the different citrus fruit compounds determine the unique bouquet of the different fruits. The method that was used in these experiments was the selected ion method (SIM). This method scans selected masses of relevance to target compounds. It is suitable for accurately determining the concentration of each targeted analyte. The experiment was done using the same quantities of lemon, orange, grapefruit and mandarin. Roughly, 20 grams of each were placed into 1.5 litre bottles and sealed with a septum. The results are shown in Table 2.5 and graphically in Figure 2.8.

Table 2.5 Citrus compounds of interest and their concentration in different citrus fruits.

Compounds	Concentration (ppm)					
	lab air	background	grapefruit	lemon	orange	mandarin
Geranial	0.005	0.005	0.15	0.005	0.058	0.014
Geraniol	0.002	0	0.092	0.019	0.061	0.014
Linalool	0	0.002	0.3	0.15	0.33	0.12
Acetaldehyde	0.013	0.01	7.6	2.2	6.9	4.8
Ethyl acetate	0.006	0.006	9.4	0.081	0.13	0.27
Ethyl propionate	0.006	0.003	0.17	0.11	0.099	0.12
Ethyl butyrate	0.038	0.026	0.71	0.22	0.17	0.074
Citronellal	0.002	0	0.13	0.005	0.041	0.013
Ethyl 2-methylbutyrate	0	0	0.054	0.014	0	0.004
Ethanol	0.25	0.24	96	11	63	27
Limonene	0.009	0.013	80	29	80	39
Octanal	0.001	0.002	0.021	0.001	0.011	0.008
Thymol	0.001	0.005	0.045	0.022	0.019	0.01
Methyl N-methylanthanilate	0	0	0.048	0	0.017	0
Hexanal	0.006	0.005	1.3	0.12	0.71	0.29
Trans-2-hexenal	0	0.001	0.19	0.043	0.12	0.08
Hexenol	0	0.002	0.016	0.004	0.007	0.009
Isopentyl alcohol	0.003	0.004	0.009	0.002	0.007	0.006
Grapefruit mercaptan	0.007	0.004	0.028	0.004	0.013	0.009

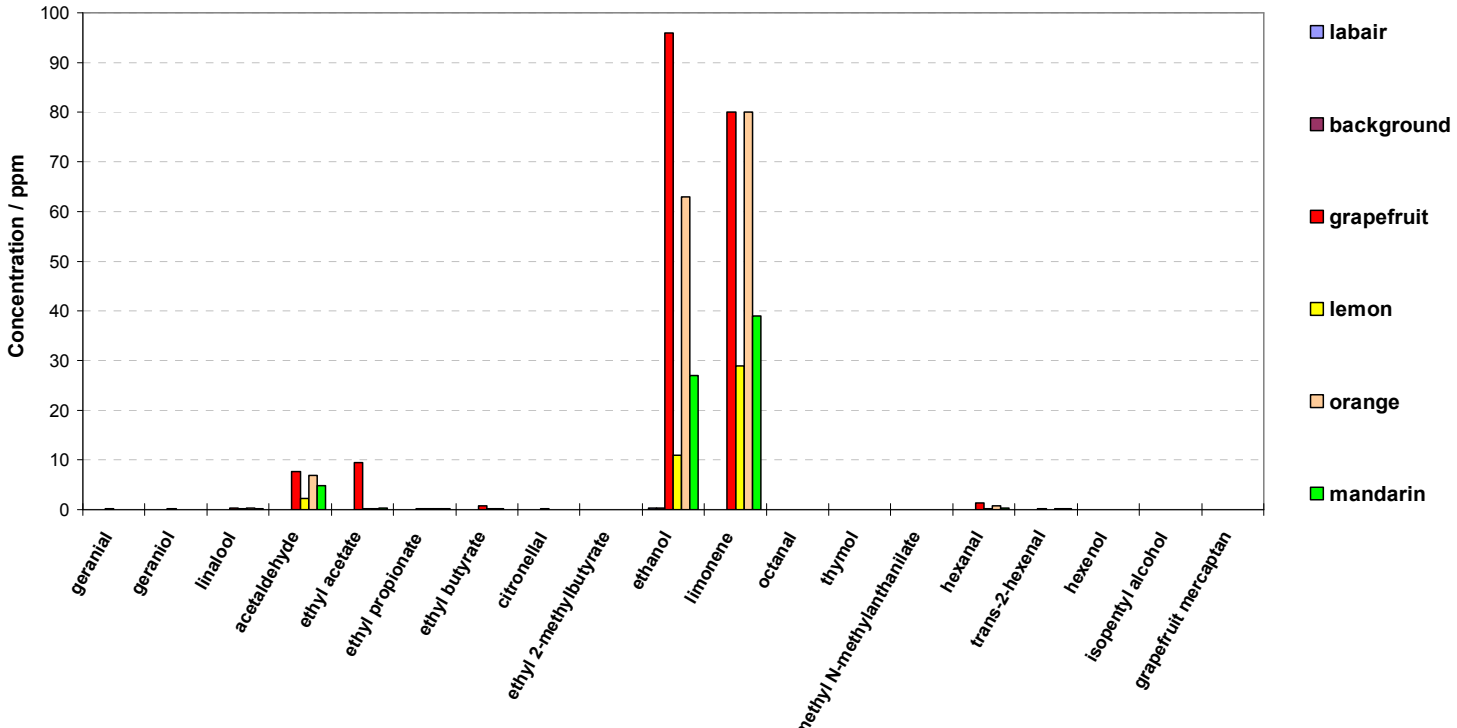

Figure 2.8 Citrus compounds of interest concentrations in different citrus fruits.

5. Tedlar bags

Several methods are used to store samples and transport them to the laboratory such as canisters, cold trapping, Teflon bags and Tedlar bags. Tedlar bags are particularly convenient for holding samples because of their ease to operate, to handle, their low cost, and their re-usability. However, some problems were found when dealing with these bags. Concentration stability of contents in these bags for a number of compounds is not very satisfactory. Some analytes appear to increase their concentration with time but more commonly, others show a decreasing concentration with time. Tedlar bags also have significant concentration of several compounds arising from the bag polymer. For example, some compounds present in the bags are produced by the bag material itself including, N-N-dimethylacetamide (C_4H_9NO solvent used in the production of the Tedlar bags) and phenol at m/z 88 and 95 amu respectively. These compounds also increase with increasing temperature. In their study of monitoring the effect of temperature on Tedlar bags, Marco et al. found an increase in the concentrations of these species 170% (C_4H_9NO) and 88% (phenol).[25] Therefore, this contamination affects the analyses results at the relevant masses.

Increases in the concentrations of some analytes can occur, either by permeation through the walls of the bag or by production from the bag material. Possible loss of concentration can occur by permeation through the bag walls, adsorbtion into the walls or permeation of vapour water through the walls into the bag. Water was found to permeate through the walls as found by Nielsen and co-workers. [24] Tedlar bags have also been found to adsorb some of the BTEX compounds (benzene, toluene, ethyl benzene, xylene and its isomers). Thus, the integrity of samples analyzed for their BTEX composition, may be compromised by sampling into a Tedlar bag, particularly when the concentration ranges are in the low ppbv. It was

therefore necessary to investigate the possibility of using Tedlar bags for the air monitoring purpose, particularly for the BTEX compounds.

Tedlar bags were investigated previously by Marco and co-workers for breath sampling and medical diagnostic research. Some decreases in the concentrations were reported in the Marco et al. study [25], where they were found to be compound dependent. For instance, benzene and toluene were found to lose less than 15% of their initial concentration after 52h and showed no significant diffusion loss within 180h. Consequently, possible loss of concentration then should be related to adsorbtion to the walls and/or permeation of water through the walls. The concentrations of benzene and toluene were also found to increase by 2 to 10% by heating the bag.

5.1 Experimental procedure and results

To test the level of contamination of Tedlar bags on BTEX samples, different sets of empty Tedlar bags were examined for their VOC levels, including the BTEX compounds. Three Tedlar bags were used in the study: a well-purged bag, a fresh purged bag and an unpurged bag. Each of these bags was filled with nitrogen and sampled by the SIFT-MS instrument, using a full mass scan. From the data displayed in Table 2 and Figure 2.9, it is evident there are a lot of compounds in these bags at significant concentrations that influence even the freshly purged one. As a result, the large background will restrict the ability of measuring concentrations lower than the background concentration (see Figure 2.11). The results in Table 2.6 show a high background of compounds of interest that exist in the bags.

Table 2.6 Concentrations in the background of different Tedlar bags, corresponding to the designated analyte in ppbv.

	Lab Air	Well Purged Bag	Fresh Purged Bag	Unpurged Bag
Benzene	0.001	0.003	0.002	0.006
toluene	0.008	0.012	0.014	0.02
ethyl benzene	0.005	0.008	0.009	0.012
formaldehyde	0	0	0	0
acetaldehyde	0.017	0.015	0.009	0.011
3-butadiene	0.004	0.005	0.005	0.005
nitrogen dioxide	0.032	0.024	0.02	0.031
methanol	0.12	0.037	0.058	0.049
ethanol	0.18	0.038	0.042	0.042
n-propyl alcohol	0.006	0.002	0.003	0.005
acetone	0.046	0.015	0.015	0.014
methyl ethyl ketone	0.003	0	0.001	0.001
acetic acid	0.036	0.05	0.036	0.039

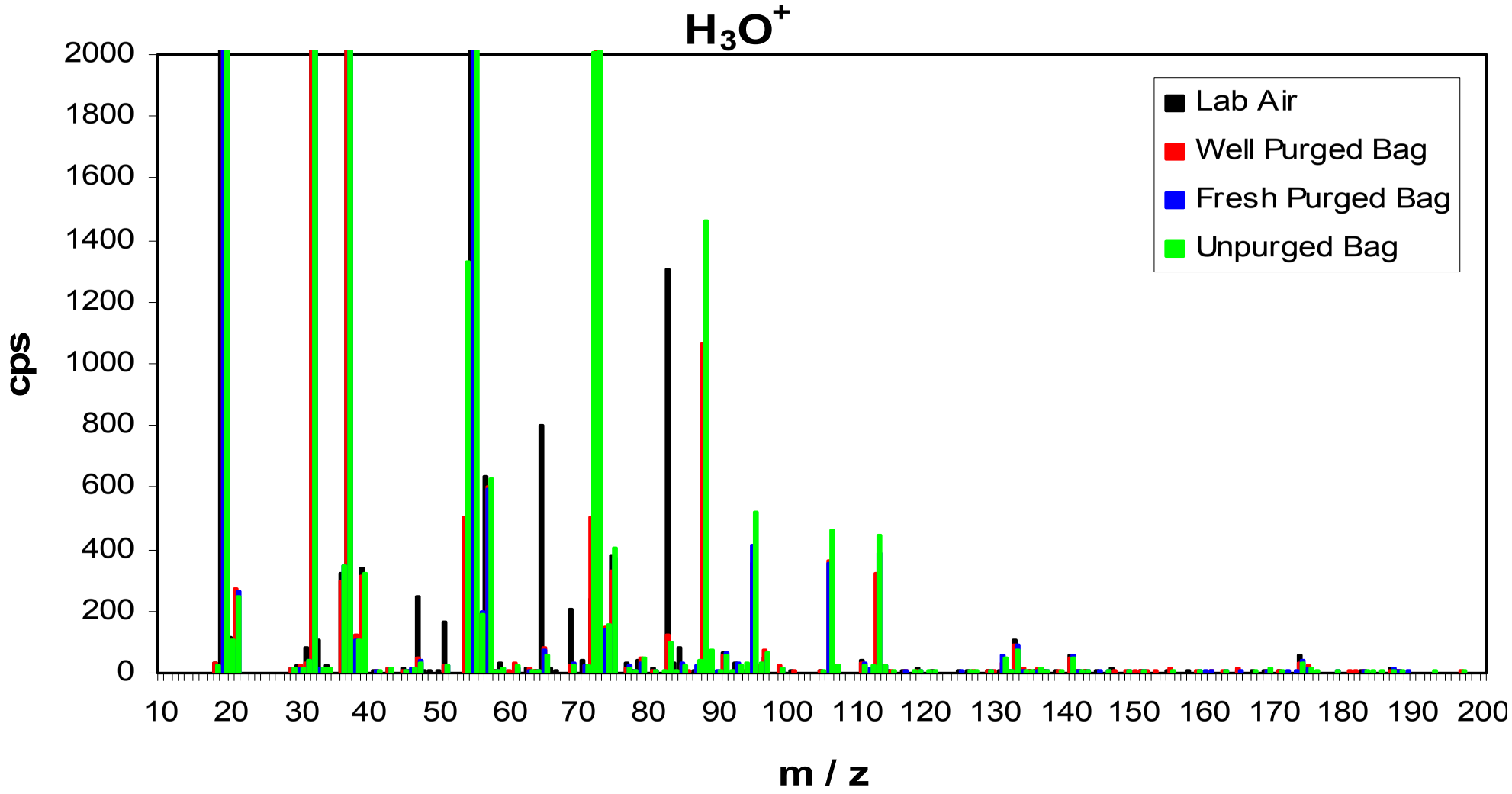
H_3O^+
cps
2000
1800
1600
1400
1200
1000
800
600
400
200
0
10
20
30
40
50
60
70
80
90
100
110
120
130
140
150
160
170
180
190
200
m / z
Lab Air
Well Purged Bag
Fresh Purged Bag
Unpurged Bag

Next, the adsorption characteristics of BTEX compounds in Tedlar bags were tested. A series of known concentrations of BTEX compound samples were prepared in Tedlar bags from a standard cylinder of BTEX compounds present at specified concentrations. Samples of 1 ppm, 100 ppb, and 10 ppb were prepared and used in this experiment and analysed using the BTEX method.

Sampling was also carried out at different times to monitor the change in concentration as a function of time. Each experiment was repeated three times and the average was obtained. The result was quite unclear for xylene because of its product ion interference with ethylbenzene. There was a small decrease in concentration with time as demonstrated in Figure 2.10 in the first 6 days with a range of about 2 to 10 % reduction in the benzene and toluene concentrations. This percentage was in reasonable agreement with the value corresponding to adsorption of these compounds into Tedlar bag walls in the Marco et al. study. [25] It showed that heating Tedlar bags increased the concentration of benzene and toluene from about 2 to 10%, which corresponded to the adsorption into the bag walls. There also were decreases of about 20% and 25%, decreasing on the seventh day for benzene and toluene respectively. Benzene and toluene half-lives were also determined by Marco and his co-workers to be about 8.3± 0.75 days. Xylene+ethyl benzene shows greater adsorption as a function of time. These compounds showed about 5 to 15% reduction in the first six days and about 35% in the seventh day. Figure 8 shows the effect of adsorption and the restricted level of the analysis of benzene.

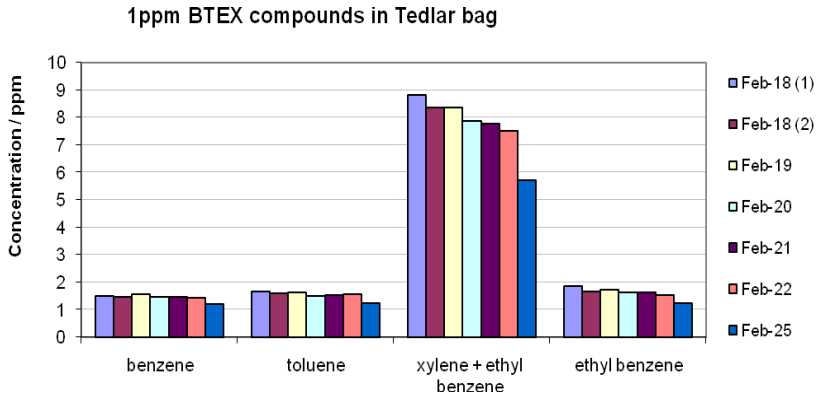

Figure 2.10
The result of sampling a Tedlar bag spiked with 1 ppm BTEX compounds over seven days.

a)

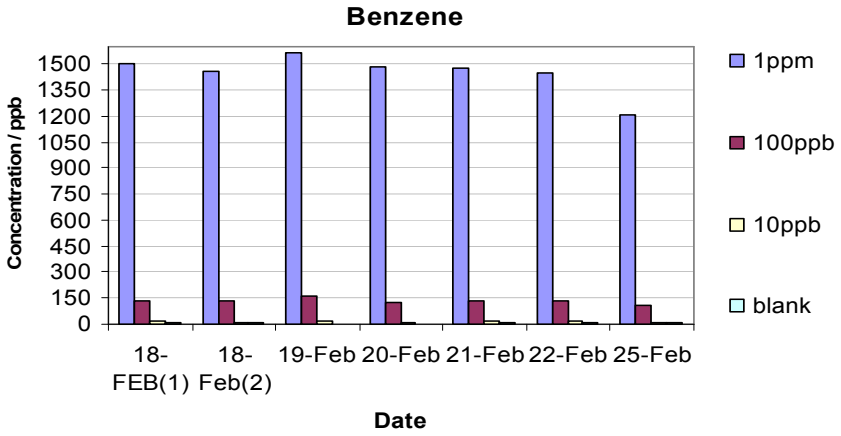

b)

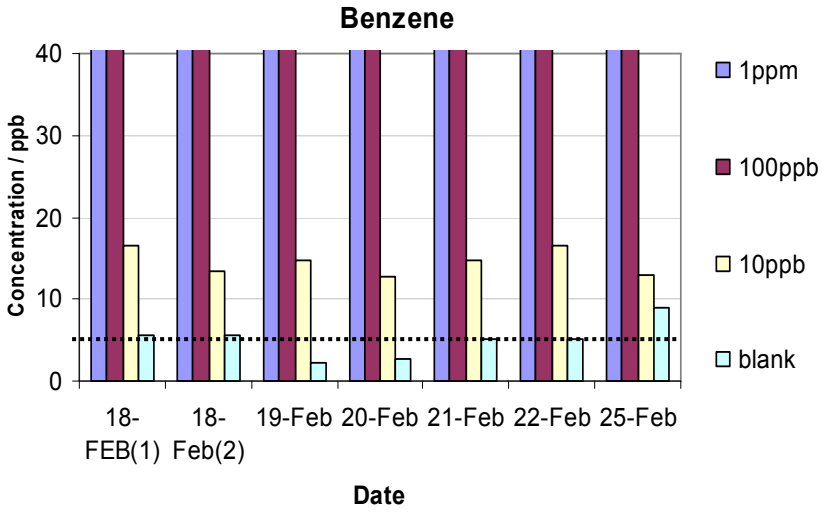

Figure 2.11. a) Analysis of Tedlar bags containing a known benzene concentration at different times. b) A large scale of the figure a showing the 10 ppb, the blank and the restricted concentration of benzene.

To conclude, the practice of using Tedlar bags in ambient air monitoring, according to these results, would be largely restricted to high sample concentrations. This is due to the high background of the relevant compounds in these bags. For example, the effect of the background is obvious for concentrations of 10 ppb or less (Figure 2.11). This background compromises the ability to analyze samples with concentrations lower than ~10 ppb. In addition, there might be a minor contribution of the loss of these compounds from Tedlar bags by diffusion through the bag polymer itself.

Chapter 3

Detection of Sulfur compounds in natural gas

1. Introduction

In this chapter, the potential of using SIFT-MS to detect sulfur compounds, particularly hydrogen sulfide (H_2S) in natural gas and LPG as examples of hydrocarbon mixtures, was investigated. Moreover, general information about natural gas, LPG and H_2S is provided, including some of the problems relating to the presence of H_2S.

1.1 General introduction

Some instrument analyses tend to take a long time and require long sample preparation before yielding results. In addition, careful analyte calibration is required. However, some analyses are crucial and the results are demanded immediately, where they have consequential effects on other procedures and decision-making. For example, it is important to monitor the concentration of sulfur compounds in natural gas and crude oil, because of the ability of these compounds to cause corrosion and their harmful effect on human health. From this perspective, there has been interest in measuring the concentration of these compounds in hydrocarbon mixtures such as natural gas and the headspace of crude oil. In this study, we will use the reaction product ions from chemical ionization reactions of sulfur compounds to monitor sulfide concentration.

Table 3.1 shows the sulfur compounds of interest and their important physical properties.

Table 3.1 Important properties of sulfur compounds of interest according to NIST chemistry webBook database.

Compounds	*Molar mass*	*Proton Affinity*	*Ionization Energy*	*Molecule name*
H_2S	34	705	10.45	Hydrogen sulfide
CH_3SH	48	773.4	9.4	Methanethiol
C_2H_5SH	62	789.6	9.31	Ethanethiol
C_2H_6S	62	830.9	8.69	Dimethyl Sulfide
$C_2H_6S_2$	94	815.3	7.4	Dimethyl Disulfide

1.2 Natural gas

Natural gas is a gaseous fossil fuel. It is found in oil fields either dissolved or isolated in natural gas fields. Petroleum oil and natural gas are the products of thermal conversion of decayed organic matter, called kerogen that is trapped in sedimentary rocks. [26]

In addition, natural gas is not a pure product; the primary component of natural gas is methane accounting for up to 70-90%. In addition, it often contains heavier gaseous hydrocarbons such as ethane, propane and butane accounting up to 20%, as well as other sulfur containing gases, in varying amounts.[27] These sulfur compounds are in fact common contaminants, which must be removed prior to most uses. Nitrogen, helium, carbon dioxide, water, and odorants loaded for ease of detection, can also be present. [28] Mercury is also present in small amounts in some natural gas fields. Natural gas can also be a primary market resource for helium gas. [29] Components of natural gas vary between gas fields, and the exact components of natural gas used in the following experiments are shown in Table 3.2, as certificated by the Southern

Gas Services Limited. [30] Natural gas that contains hydrocarbons, other than methane, is called 'wet' natural gas, while that consisting only of methane is called 'dry' natural gas. Moreover, the presence of H_2S in amounts greater than 5.7 mg/Nm^3 is classified by the Environmental Protection Agency (EPA) [31] as 'sour gas'. These sour gases, besides other resource types such as shale gas, tight gas, and coalbed methane, are increasingly becoming more challenging resources for natural gas industries. Sour gas, for example, is routinely sweetened at desulfurization plants. This involves removing sulfur compounds, including H_2S, by adsorption in amine solution and the Claus process, which is used for synthesis of the element sulfur. [32]

Processed natural gas is odorless and therefore it is odorized by adding small amounts of odorants, such as mixtures of t-butyl mercaptan, isopropyl mercaptanthiol, tetrahydrothiophene, dimethyl sulfide and other sulfur compounds, for leak detection before it is distributed to customers.

Table 3.2 Natural gas analysis components certificate, according to Southern Gas Services Limited.[30]

Sample identification	Data result
Moisture Content	**90 mg/Sm^3**
Carbon dioxide	**5.7**
Nitrogen	**2.04**
Methane	**80.1%**
Ethane	**8.3%**
Propane	**2.78%**
iso-Butane	**0.47**
n-Butane	**0.43**
Neo-Pentane	**BLD of 0.001***
iso-Pentane	**0.11**
n-Pentane	**0.069**
Hexanes	**0.033**
Heptanes	**0.024**
Octanes+	**0.013**
Real Superior Cal Value	**39.857**
Real Inferior Cal Value	**36.048**
Real Specific Gravity	**0.702**

* BLD: Below level of detection.

1.3 LPG

Liquefied petroleum gas (LPG) is a mixture of hydrocarbon gases. It primarily contains propane and butane. Propylene and butylenes are usually present also in small concentrations. Ethanethiol is also added as a powerful odorant so that leaks can be detected easily.

This gas is normally used as a fuel in heating appliances. Further, it is increasingly replacing chlorofluorocarbons as an aerosol propellant and a refrigerant, to reduce damage to the ozone layer. This gas is manufactured during the refining of crude oil, or extracted from gas streams. LPG was included here because of its similar mixtures of hydrocarbons to the natural gas. It can be used in a similar reaction environment to natural gas.

1.4 H_2S

Hydrogen sulfide is naturally present in crude oil and natural gas. It is found as a large component of natural gas (up to 90%), in volcanic regions, and in certain sulfur springs. Moreover, it is considered as the main toxic substance that can be found in livestock rearing systems with manure storage. [33] It is also considered a hazard at waste treatment facilities.

Approximately 90% of hydrogen sulfide originates from natural sources. [34] About 10% of total global emissions of H_2S are due to human activity. Anthropogenic releases of H_2S into the air result primarily from the desulfurization process of oil and natural gas, where sulfur is generally produced from H_2S by using the method that is known as the Claus process. Moreover, it can be released from paper and pulp manufacturing. [26] Its normal concentration in clean air is about 0.0001-0.0002ppm.[35]

Hydrogen sulfide is weakly acidic and has a smell of rotten eggs. It dissociates in aqueous solution into hydrogen cations H^+ and the hydrosulfide anion HS^- as shown in the following equation:

$$H_2S \rightarrow HS^- + H^+$$

$$K_a = 6.9\times10^{-7} \text{ mol/L}; \quad pK_a = 6.89$$

H_2S is separated by adsorption with a solution of weak bases, which take up hydrogen sulfide when cold and then release it when heated, regenerating the adsorption agent. H_2S decomposes slowly when exposed to air and light, even at room temperature.[32] This is illustrated by the following equation:

$$H_2S + 3/2\ O_2 \longrightarrow H_2O + SO_2$$

H_2S is very soluble in water. At 0°C 4.651 L of H_2S dissolve in 1L of water, and at 20°C 2.61 L dissolve in 1L of water. [36]

Hydrogen sulfide, in addition, is corrosive and its presence can result in some steel becoming brittle. This leads to sulfide stress cracking. This is of great concern especially when handling ‘sour gas’ and sour crude oil in the oil industries.

Additionally, some bacteria such as Salmonella can liberate hydrogen sulfide when they digest sulfur-containing amino acids.[37] H_2S-producing bacteria also operate in the human colon, and the odor of flatulence is largely due to trace amounts of the gas. Evidence exists that hydrogen sulfide, produced by bacteria in the colon, may cause or contribute to ulcerative colitis. Furthermore, hydrogen sulfide can be present naturally in well water, where ozone or a filter with manganese dioxide is often used for its removal.

From a health perspective, hydrogen sulfide is highly toxic. It is heavier than air, so it tends to accumulate at the bottom of poorly ventilated spaces. It is more poisonous than HCN with a maximum allowed concentration of 15 mg m^{-3} (10 ppm). Long exposure to air containing 0.0035% (35 ppm) of H_2S is potentially fatal. [27] Collapse, unconsciousness and death can occur following exposure to concentrations of just a few hundred ppm for 2 minutes, or 100 – 150 ppm for 8 to 48 hours. [38] The recognition threshold is 0.0047 ppm at which 50% of humans can detect the characteristic odor of hydrogen sulfide. [39] Nevertheless, at high concentration, it quickly deadens the sense of smell, so potential victims may be unaware of its presence until it is too late. The effect of H_2S was evaluated in 1995 by Schiffman et al. Their study concluded that continuous smelling of odors from H_2S is associated with significantly more tension, more depression, less vigour, more fatigue and more confusion. [33] The next table (Table 3.3) presents the effects of different concentrations of H_2S on human health.

***Table 3.3** Hydrogen sulfide established dose-effect relationships.

H2S concentration (ppm)	*Effect*	*Reference*
1000-2000	Rabid collapse and death	[33]
530-1000	Strong Central Nervous System stimulation, hyperpnoea followed by respiratory arrest	[33]
320-530	Pulmonary oedema with risk of death	[40]
150-250	Loss of olfactory sense	[40]
50-100	Serious eye damage	[33]
10-20	Threshold for eye irritation	[38]

2. Corrosion problem of sulfur compounds

Sulfur compounds have been found to create some problems in terms of their ability to cause corrosion. As mentioned previously, H_2S is corrosive and therefore it is

usually removed at the natural gas processing plants to reduce corrosion of pipelines and compression equipment. [41] Thiosulfate and aqueous sulfide have been shown to accelerate metal dissolution when added to the bulk electrolyte, as found in Marcus' study (1991). [42]

Although sulfur compounds have been found to appear in oil with varying concentrations, the corrosion phenomenon has been found to be restricted to oil containing concentrations above minimum levels. These sulfide compounds react with steel leading to corrosion damage to hardware that is not properly prepared. Therefore, it is important to determine the concentration of these sulfur compounds in order to diagnose what sort of preparation is required. Choosing whether some protection of hardware is necessary or not, is clearly important in terms of saving oil companies' money.

It is important then that a reliable analytical technique is developed to determine the concentration of these compounds in real time, for instance during drilling, which allows appropriate preparations to be made based on the levels of sulfide detected. The SIFT-MS has the ability to detect these compounds in real time with good accuracy. Moreover, the number of sour wells will likely increase as more natural gas development occurs. The new drilling is increasingly focused on deep gas formation that tends to be sour. [43] Further, the EPA concedes that the potential of routine H_2S emission at oil and gas wells is significant. [44] In addition, the American Petroleum Institute (API) and the oil and gas industry technical organization, publish recommendations for practices that help prevent hazardous H_2S concentrations from occurring in the workplace. [45] Based on these factors, a requirement for an instrument such as the SIFT-MS is necessary.

3. Reactions of SIFT-MS reagent ions with sulfur compounds in natural gas and LPG

The hydronium ion (H_3O^+) is a well-suited ion reagent for analysing sulfur compounds of highly concentrated samples containing light hydrocarbons, because it is largely unreactive with the light hydrocarbons. Of the other reagent ions, NO^+ reacts rapidly with the light-branched hydrocarbons, while O_2^+ reacts rapidly with all hydrocarbons, except methane, with which it reacts only slowly. Also, NO^+ is unreactive with H_2S while O_2^+ reacts to form H_2S^+ that reacts rapidly with H_2O [46]. More information about the reaction of SIFT-MS reagent ions with hydrocarbons is given later in chapter 4 (section 3).

Figures 3.1 and 3.2 show full mass spectra for the H_3O^+, NO^+ and O_2^+ reagent ions over a limited mass range, for 1% sample mixtures of natural gas and LPG in nitrogen, respectively. These figures also show significantly more product formation in the LPG because of the much higher level of non-methane hydrocarbons in LPG than in natural gas. The reason for using a 1% dilution of natural gas and LPG will be explained later. Thus, the dominant product masses of the commonly produced sulfur compounds are also shown in Figures 3.1 and 3.2 for the H_3O^+ and NO^+ reagent ions. For most masses, the background was suitable for low ppb detection. The reaction of the sulfur compounds of interest with H_3O^+ is illustrated in the following equations. These compounds have been found to react mainly by exothermic proton transfer reaction with H_3O^+ due to their higher PA value than H_2O, as was previously shown in Table3.1. Furthermore, all of the $H_3O^+(H_2O)_{0,1}$ reactions, as found in the Williams et al.'s study [47] proceed close to the collision rate, despite the obvious endothermic behavior of these compounds being driven by entropy, except for the H_2S reaction with $H_3O^+.H_2O$, which does not occur. [47]

$H_2S + H_3O^+ \underset{}{\overset{k= 1.65 \times 10^{-9}}{\rightleftharpoons}} H_3S^+ + H_2O$ $\Delta H^\circ = -3.3$ kcal mol^{-1} kcoll= 1.9×10^{-9}

$H_2S + H_3O^+.H_2O \longrightarrow H_3S^+.H_2O + H_2O$ $\Delta H^\circ =$ **28.9** kcal mol^{-1}

$C_2H_5SH + H_3O^+ \xrightarrow{k= 2.6 \times 10^{-9}} C_2H_5SH_2^+ + H_2O$ $\Delta H^\circ = -23.4$ kcal mol^{-1} kcoll= 2.60×10^{-09}

$C_2H_5SH + H_3O^+.H_2O \longrightarrow C_2H_5SH_2^+.H_2O + H_2O$ $\Delta H^\circ = 8.8$ kcal mol^{-1}

$CH_3SH + H_3O^+ \xrightarrow{k= 1.75 \times 10^{-9}} CH_3SH_2^+ + H_2O$ $\Delta H^\circ = -19.6$ kcal mol^{-1} kcoll= 2.00×10^{-09}

$CH_3SH + H_3O^+.H_2O \longrightarrow CH_3SH_2^+.H_2O + H_2O$ $\Delta H^\circ = 12.6$ kcal mol^{-1}

$(CH_3)_2S + H_3O^+ \xrightarrow{k= 2.5 \times 10^{-9}} (CH_3)_2SH^+ + H_2O$ $\Delta H^\circ = -33.4$ kcal mol^{-1} kcoll= 2.5×10^{-09}

$(CH_3)_2S + H_3O^+.H_2O \longrightarrow (CH_3)_2SH^+ + H_2O$ $\Delta H^\circ = -33.4$ kcal mol^{-1} kcoll= 2×10^{-09}

$(CH_3)_2S_2 + H_3O^+ \xrightarrow{k= 2.6 \times 10^{-9}} CH_3)_2S_2H^+ + H_2O$ kcoll= 2.60×10^{-09}

$(CH_3)_2S_2 + H_3O^+.H_2O \longrightarrow CH_3)_2S_2H^+.H_2O + H_2O$ kcoll= 2×10^{-09}

Figure 3.1 SIFT-MS (Voice100) full scan data of the 1% natural gas mixture in nitrogen for the three ion reagents: (a) H_3O^+, (b) NO^+ and (c) $O2^+$ respectively. 1,2,3, and 4 corresponding to ion product mass peak position for hydrogen sulfide, methanethiol, ethanethiol plus dimethyl sulfide, and dimethyl disulfide. The grey lines indicate peaks arising from reagent ions and their cluster with H_2O.

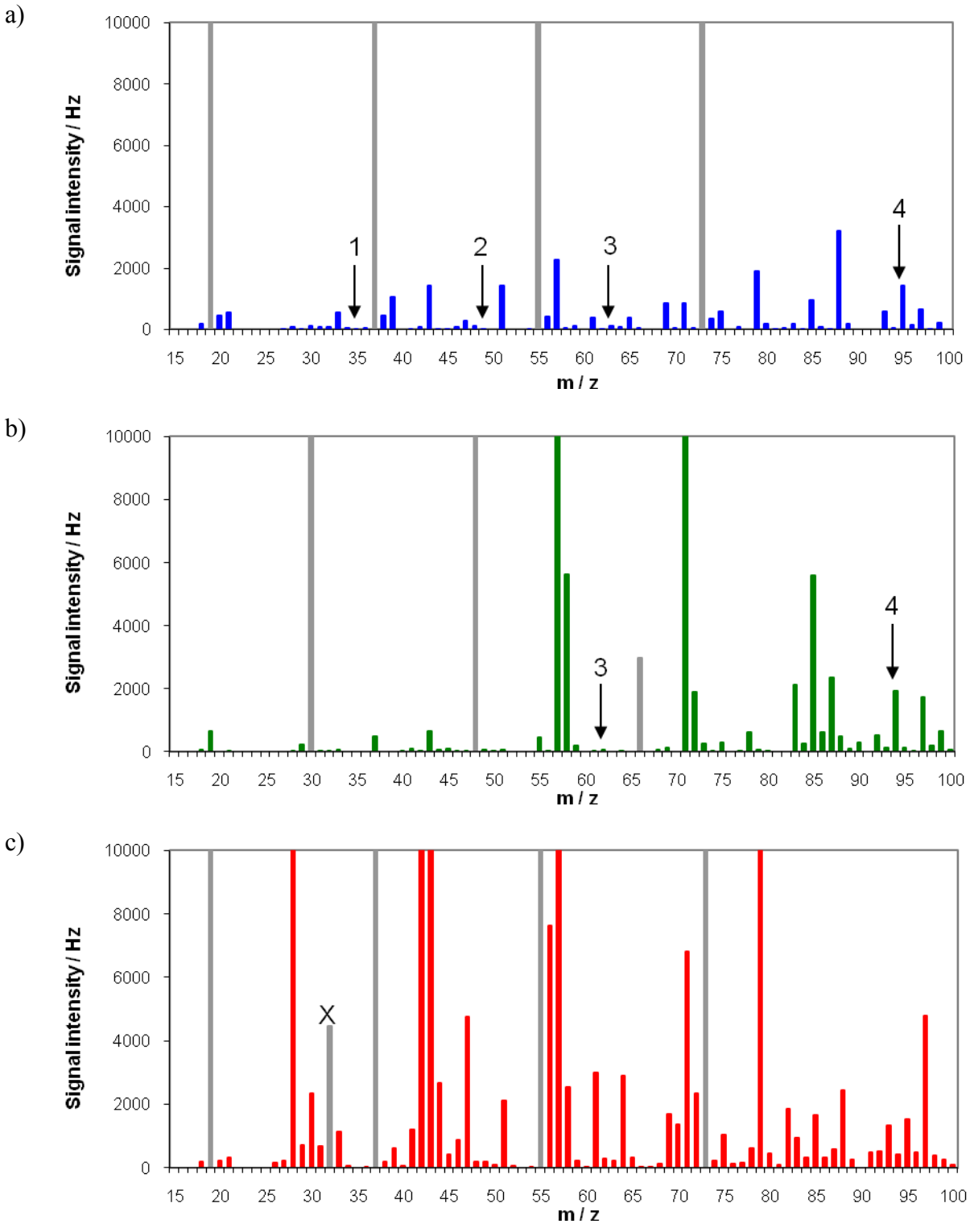

Figure 3.2 SIFT-MS (Voice100) full mass scan for liquefied petroleum gas (1% in nitrogen) for the three ion reagents: (a) H_3O^+, (b) NO^+ and (c) O_2^+, respectively. The number 1,2,3, and 4 correspond to ion product mass peak positions for hydrogen sulfide, methanethiol, ethanethiol plus dimethyl sulfide, and dimethyl disulfide. The grey lines indicate peaks arising from reagent ions with H_2O. The "X" in (c) shows the severely depleted O_2^+ reagent ion signal.

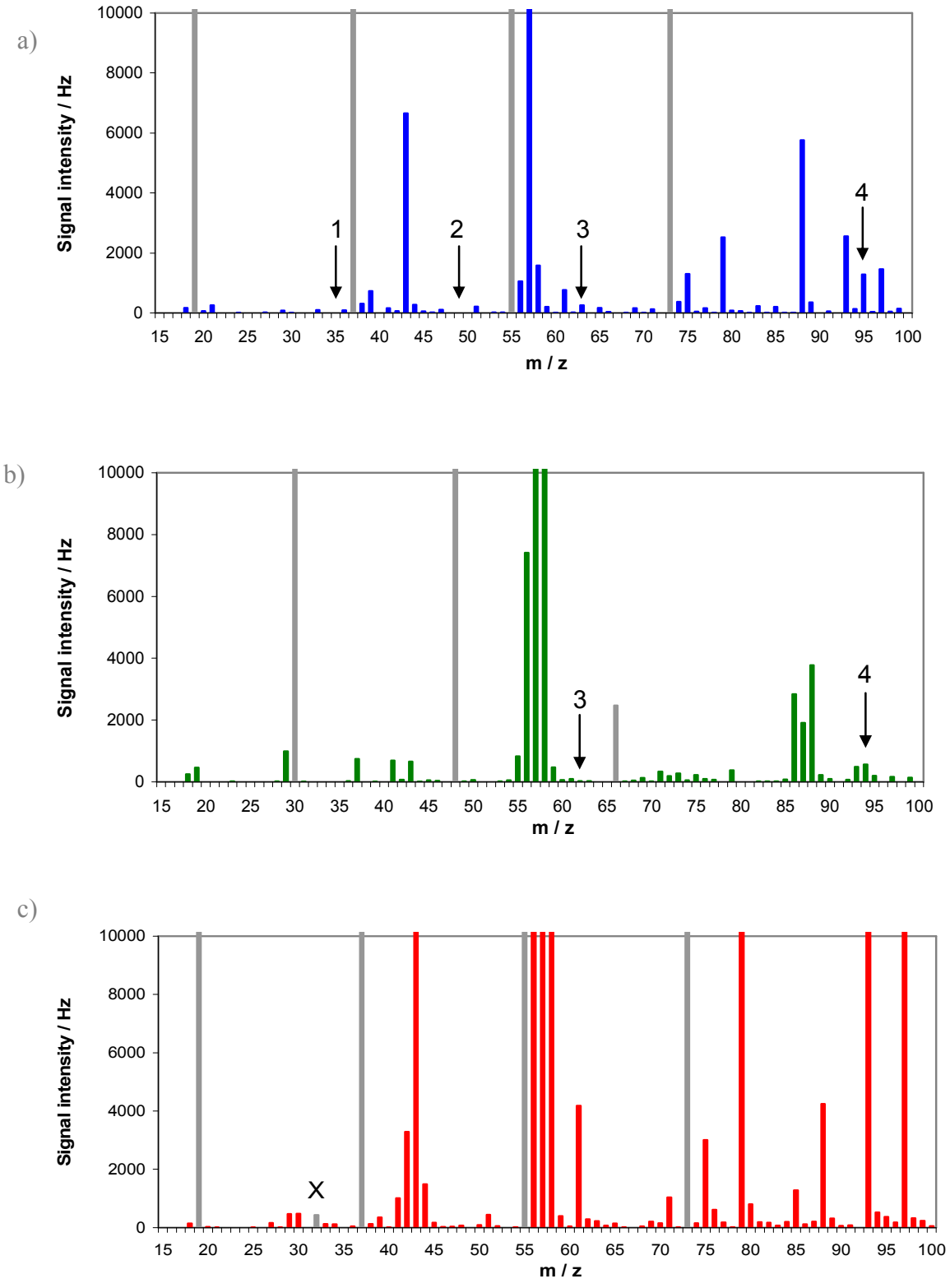

4. Experiment and results

The SIFT-MS was prepared to measure a set of the most important sulfur compounds that could contribute to the corrosion problem as indicated in Table 4.

These compounds were calibrated in the SIFT-MS instrument using standard permeation tubes. The correction factors were measured for each of these compounds, with the aim of increasing the measurement accuracy. These experiments were repeated several times and the average value was obtained. Because of instrument calibration effect, it was necessary to multiply the rate coefficients by the instrument calibration factor for that compound. The correction factors for these compounds represent the rate coefficient for each compound multiplied by a measured factor. More information about the permeation method is given next.

4.1 H_2S calibration using the Permeation method

The dynamic method is an ideal calibration method in the SIFT-MS instrument for the sulfur compounds of interest. It provides a sample of the sulfur compounds at known concentration in the ppm concentration range. This method provides controlled permeation of a gaseous analyte out of a permeation tube through a Teflon polymer, into a nitrogen gas stream. These devices, as noted before, contain certain condensable gases, so when operated at a specific temperature they can be used as a primary standard.

The permeation tube delivers a known concentration of analyte at specific oven temperature. The result of H_2S calibration using the standard permeation tube is shown in Figure 3.3. The result obtained presents a good linear response with the changing of concentration that was made by changing the ratio of N_2 which passed through the permeation oven. Furthermore, the H_2S concentration measured by the

SIFT-MS instrument accurately monitored the known concentration of H_2S as shown in Table 3.4.

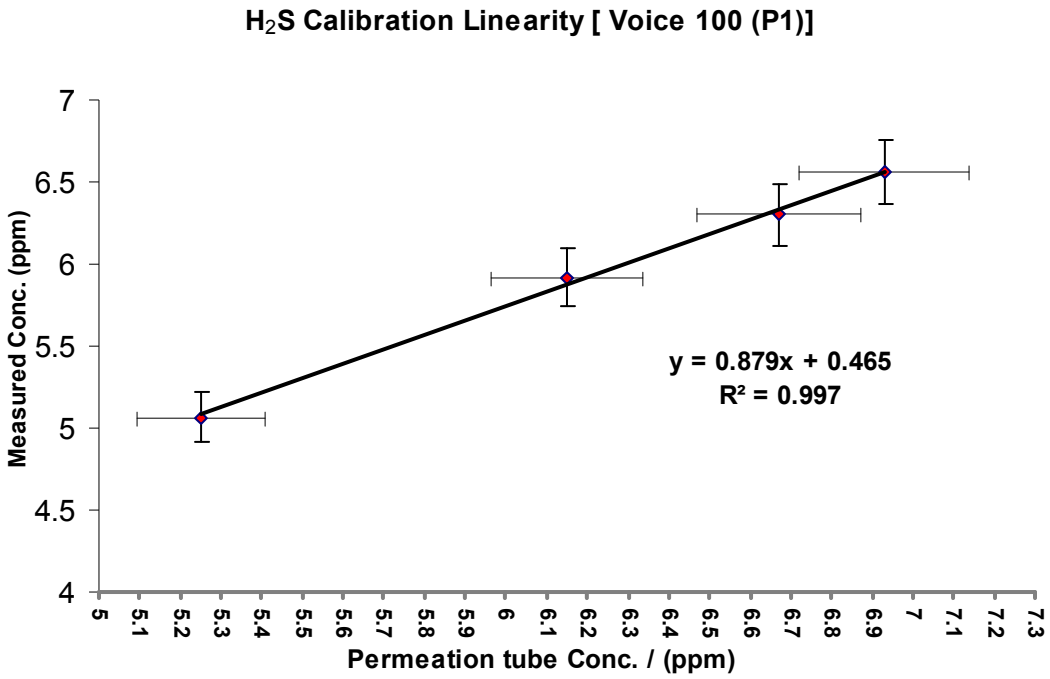

Figure 3.3 H_2S calibration result, using the H_2S permeation tube as a standard concentration.

Table 3.4 H_2S measured concentrations of the three systems by SIFT-MS comparing with the prepared concentrations in Tedlar bag.

Prepared concentration	Measured concentration (ppm)		
	H_2S / N_2	H_2S / LPG	H_2S / Natural gas
2 ppm	1.99	2.13	2.06
0.035 ppm	0.034	0.039	0.041

4.2 Experimental procedure and discussion

The experimental procedure can be summarised as follows:

- Calibration of the Voice 100 (P1) instrument for these compounds using the permeation tubes (dynamic method) that were described earlier.
- Sampling the natural gas and LPG by SIFT-MS and establishing the ion reagents' count rate in a range that is suitable for analysis. Undiluted natural gas consumed nearly all the ion reagents, as shown in Figure 3.4. However, if a 100 fold (1%) dilution of natural gas is made, a workable count rate of the reagent ions can be used for analysis, as shown in Figures 3.1 and 3.2.

Figure 3.4 Mass scan (Voice100) of **undiluted natural gas** for a) H_3O^+ b) NO^+ and c) O_2^+, showing the high depletion of the reagent ions, and increasing number of the H_3O^+ cluster ions in part a. Figure 6.b is the chemical ionisation spectrum of NO^+ and Figure 6.c has the same spectrum for O_2^+.

a)

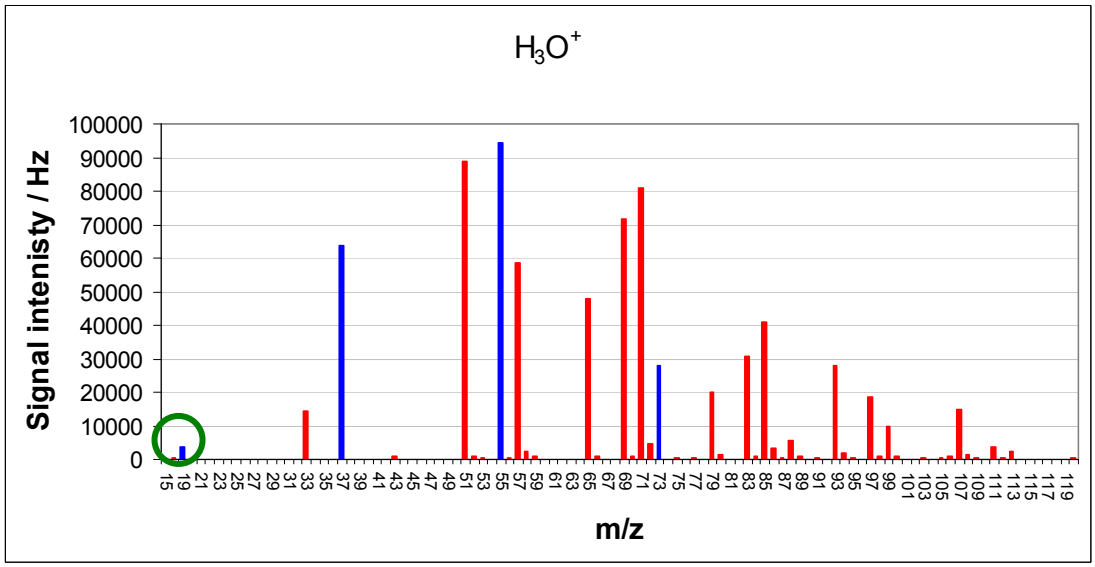

b)

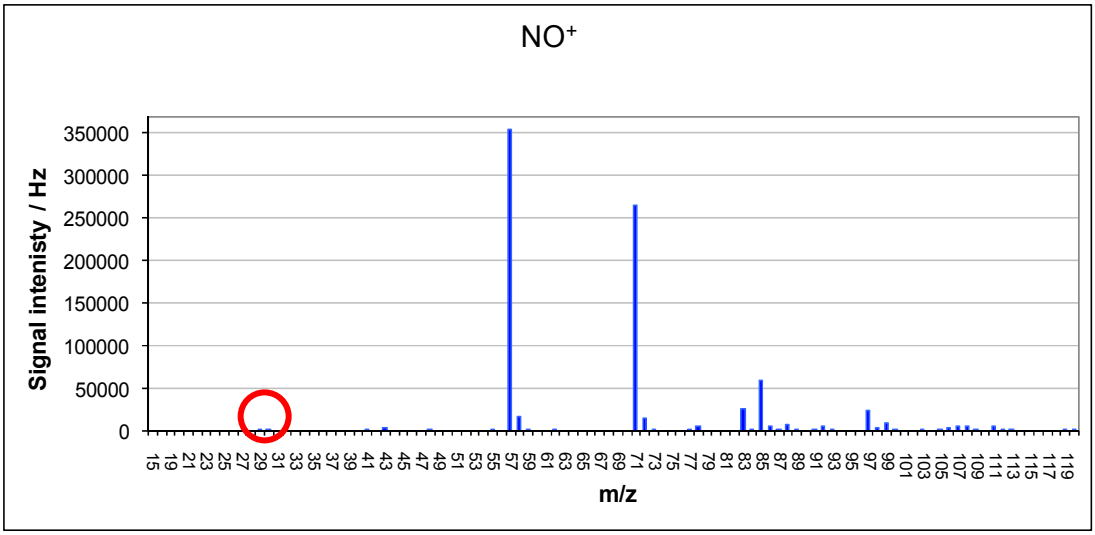

c)

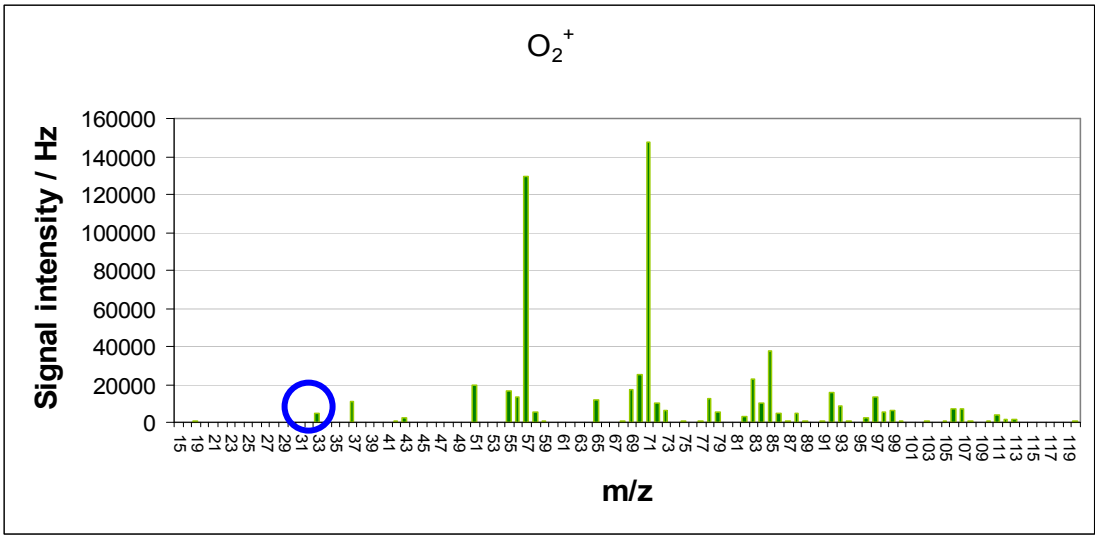

- Full mass scan was carried out on two diluted samples of 1% LPG mixture in N_2 and 1% natural gas mixture in N_2 in order to obtain an insight about the possibility of measuring the concentration of sulfides in the samples. The results are shown in previous Figures 3.1 and 3.2.
- A 1% H_2S stock mixture of hydrogen sulfide in nitrogen was prepared in a custom-built 300-mL glass bulb, using standard gas handling techniques. The bulb included a Suba-seal septum (Aldrich) through which gas could be sampled using a gas syringe. The 1% mixture of H_2S in nitrogen was used to prepare a more dilute 100 ppm mixture of H_2S in nitrogen. It was then employed for preparation of the serial dilutions of H_2S in 1% natural gas, LPG and N_2 mixtures.
- H_2S was spiked into the Tedlar bags containing the solvent (LPG, natural gas and N_2) separately, allowing three systems to be investigated at varying concentrations. Then, these sulfur compounds were sampled by SIFT-MS using the method already described.
- The samples were analysed twice. In addition, this process was undertaken rapidly, with the duplicate measurements being completed within one hour. The reason for that was to reduce losses due to the rather reactive nature of H_2S and the slightly permeable behaviour of Tedlar bags, especially with respect to methane. The response of increasing the concentration of the H_2S in these systems was determined and is shown in Figure 3.5. The responses of the three systems were linear with concentration and the SIFT-MS instrument still had high instrument sensitivity for measuring the H_2S concentration. The H_2S concentration response gave a linear relationship to the largest concentration prepared, 100 ppm. Figure 3.6 shows the large range of linear response of H_2S in 1% natural gas.

- H_2S/LPG

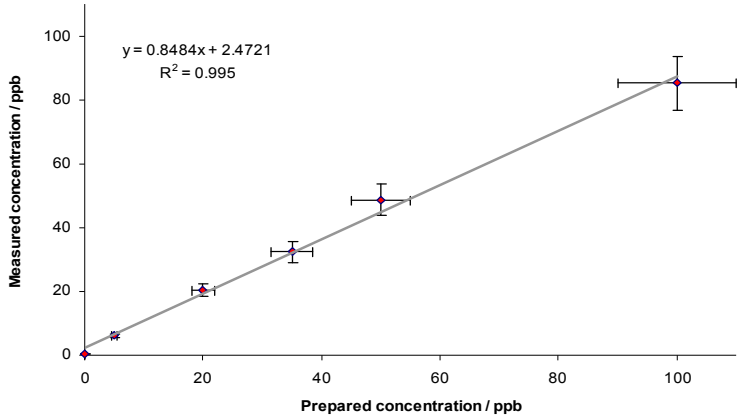

Figure 3.5. a) The linear relationship result of H_2S in a 1% mixture of LPG.

- H_2S / N_2

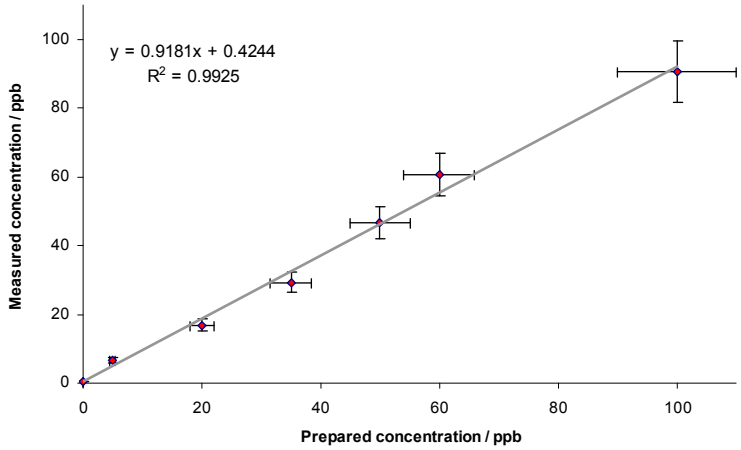

Figure 3.5. b) The linear relationship exhibited for dilution of H_2S in N_2

- H_2S/ Natural gas

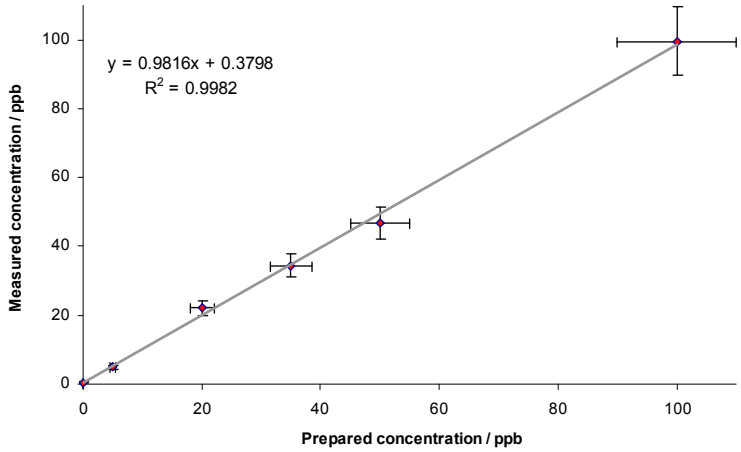

Figure 3.5. c) The linear relationship exhibited for dilution of H_2S in a 1% mixture of natural gas.

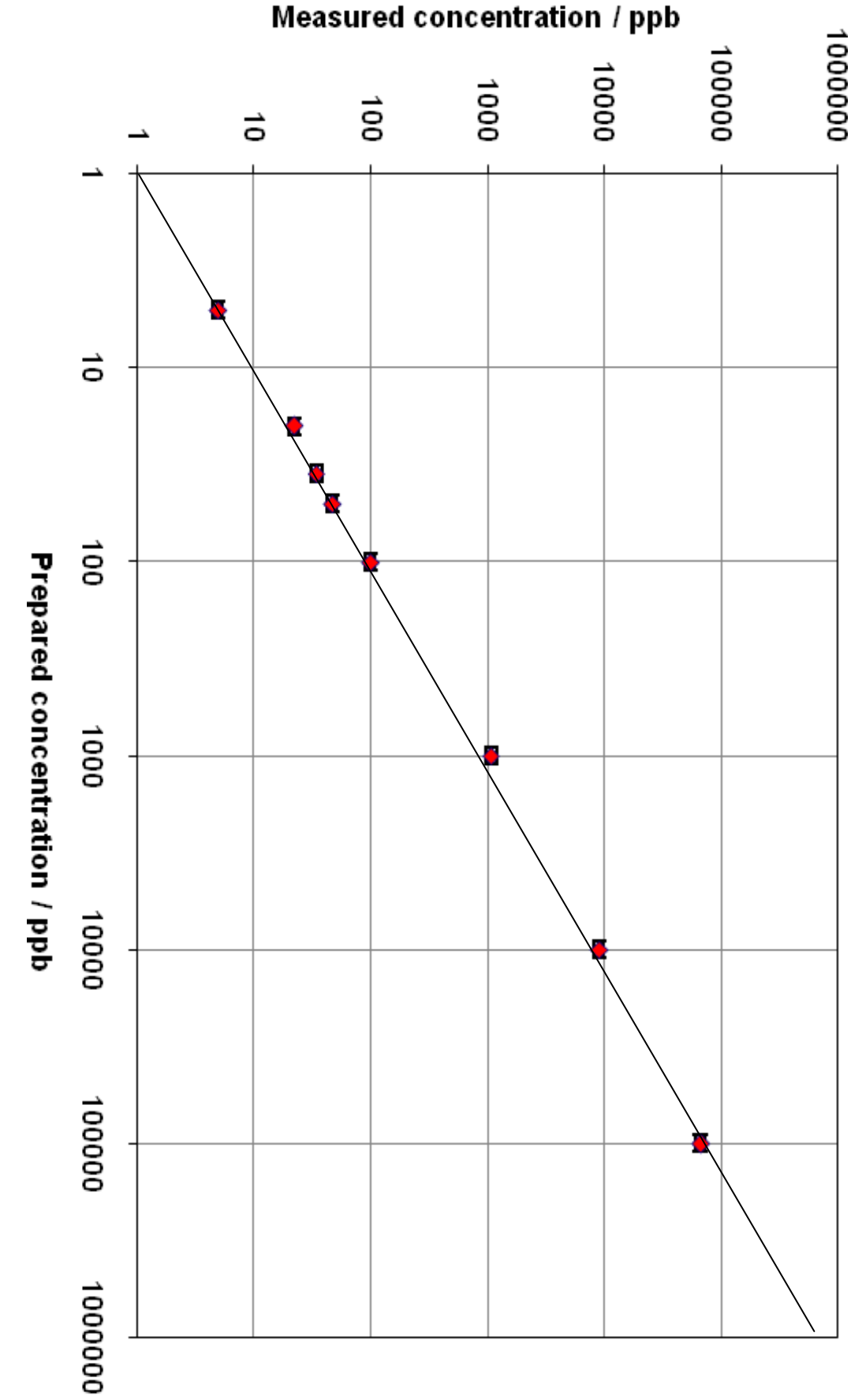

Figure 3. 6. SIFT-MS quantitation of hydrogen sulfide in natural gas (1% in nitrogen) using the H_3O^+ reagent ion. Note that logarithmic scales are used.

As mentioned previously, it was necessary for these experiments to be performed using a 1% mixture of natural gas in nitrogen, because the sample flow rate used in the Voice 100 (P1) instrument, leaded to a near complete reduction of the reagent ions' signals, especially for H_3O^+. This in fact can be attributed to the presence of a high concentration of methane that can work as a third body, increasing the rate of the three-body reaction process. [48] The three-body reaction usually results in the association of H_3O^+ ion with the neutral collision partner H_2O. It is then stabilized by subsequent collision with methane as the third body, before dissociation back to the reactants occurs. The following equations show the processes of H_3O^+ reaction with H_2O in the presence of the third body.

$$H_3O^+ + H_2O + M \longrightarrow H_3O^+.H_2O + M$$

$$H3O^+.(H_2O)_{n-1} + H_2O + M \longrightarrow H_3O^+.(H_2O)_n + M$$

Substituting CH_4 for He, as the third body M, accelerated the process of generating the water cluster ions of H_3O^+. It increased the intensity of the H_3O^+ cluster ions signals 37, 55, 73 amu as shown in the equations above and in Figures 3.2 and 3.1. The measured concentration of the sulfur compounds in the 1% hydrocarbon mixtures were appropriately scaled to account for the dilution.

An alternative to dilution to a 1% mixture of hydrocarbon in nitrogen, was to reduce the flow of hydrocarbon into the flow tube and using an undiluted mixture. This approach was used on the Voice 100 (LDI1) instrument and the result was satisfying, enabling the analysis of undiluted natural gas without the need for a dilution.

Consequently, the method can be adjusted by changing the inlet capillary, thereby altering the flow of analyte into the flow tube. The result of using low sample flows provided different concentrations due to the calibration that was not performed on the LDI1 instrument for H_2S. The resultant linear relationship response is shown in Figure 3.8 for H_2S in undiluted natural gas.

4.3 Limit of detection (LOD)

LOD is defined as the minimum confidence level of analyte concentration that can be detected. The LOD of H_2S in natural gas was determined by following the Syft Analytics Limited Standard Operating Procedure. [49] The LOD was experimentally determined for the 1% natural gas mixture in N_2, resulting in 7.5 ppb of hydrogen sulfide in natural gas. This was performed by calculating the mean blank concentration of 20 natural gas samples (C_b) and their standard deviation (C_{sd}). These data were used to calculate the detected limit concentration of H_2S with the following equation:

$$C_m = C_b + k\, C_{sd}$$

Where C_m is the LOD and the k is a multiplier that specifies at what concentration level, above the blank concentration, is considered. The generally accepted value is k=3.

Figure 3.7 Full mass scan of undiluted natural gas by (LDI1) using the low sample flow rate capillary for each of the three ion reagents (H_3O^+, NO^+, and O_2^+). The mass scans derived form H_3O^+ and NO^+ show good ion signals and are suitable for analysis. The mass scan, arising form O_2^+ , shows depleted reagent signal at m/z 32, indicated by red color.

a)

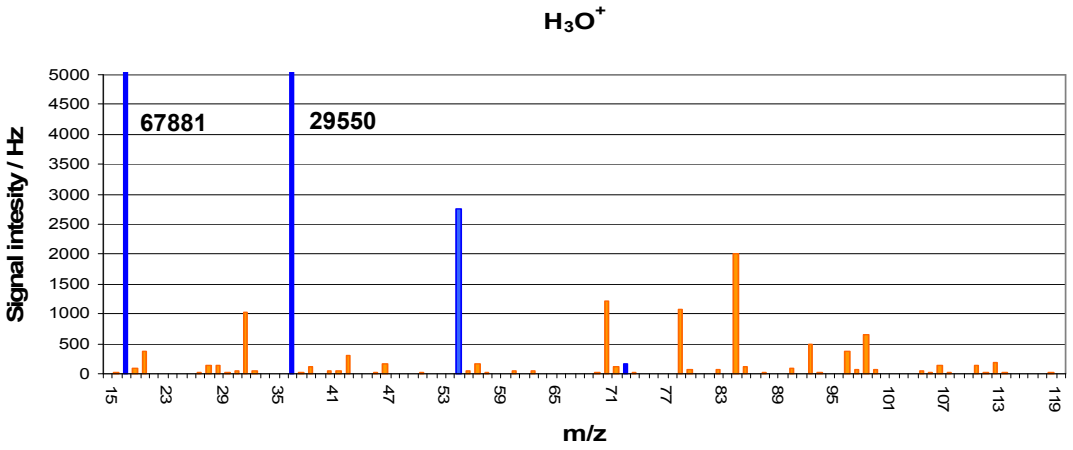

b)

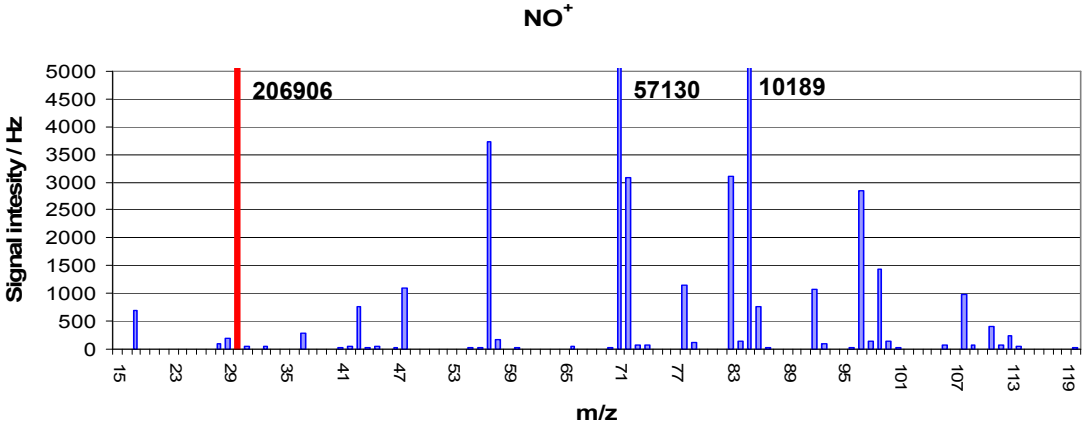

c)

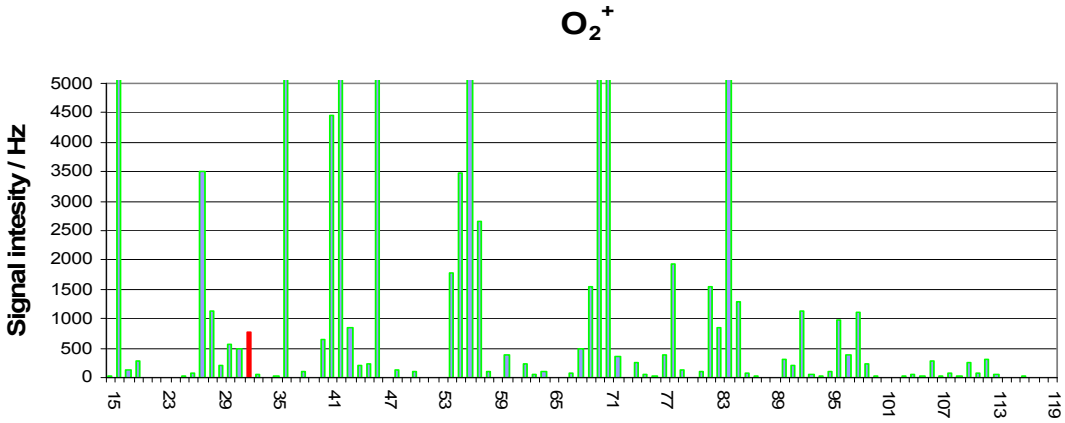

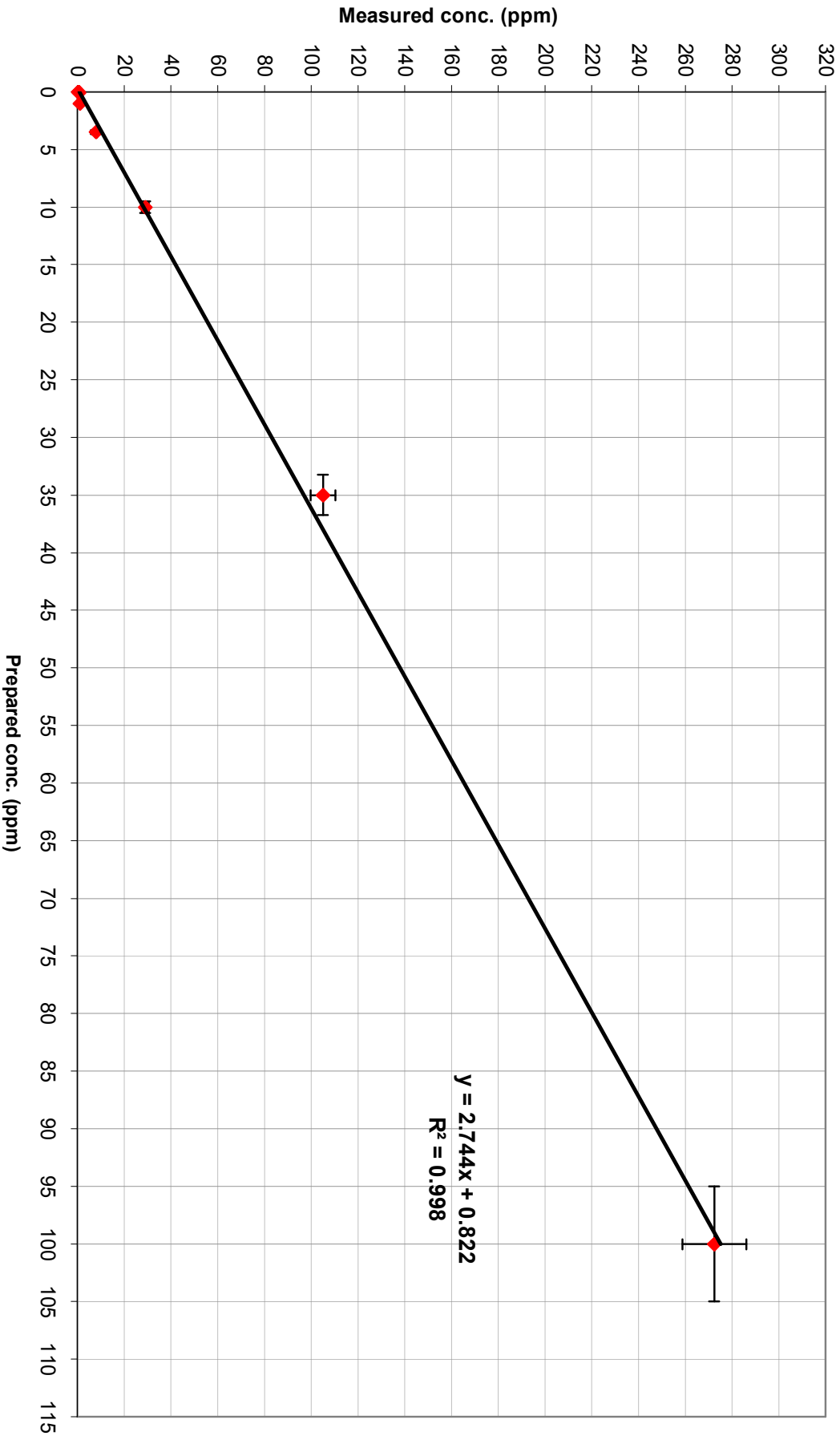

Figure 3.8 The different concentrations of H_2S mixture with undiluted natural gas response on LDI1, using the low sample flow rate capillary. LDI 1 has not been calibrated for H_2S, rationalising the different of the concentration measured.

4.4 Other sulfur compounds

The work on the detection of sulfur compounds in hydrocarbons is extended in this section. The experiments discussed here were completed on the commercial version of the SIFT-MS (Voice 200), expanding the compounds of interest to include methyl mercaptan (CH_3SH), ethyl mercaptan (CH_3CH_2SH) and dimethyl sulfide (CH_3SCH_3). Dimethyl disulfide (CH_3SSCH_3) was not included because of its very large interference with the background of natural gas and LPG at an m/z 95, compared with other sulfur compounds as indicated earlier in Figure 1.

First, the voice 200 instrument (3007) was calibrated for these sulfur compounds. Second, a mixture of the relevant sulfur compounds, with a known concentration, was prepared in a Tedlar bag, using permeation tubes. This mixture was subsequently used to make several dilution series. Three systems of pure N_2, 1% LPG mixture in N_2, and 1% natural gas mixture in N_2 were used as was done with the previous H_2S experiment.

4.4.1 Ion chemistry of the additional sulfur compounds

4.4.1.1 Methyl mercaptan

Methyl mercaptan (CH_3SH) reacts with NO^+ slowly, relative to H_3O^+ and O_2^+ as stated in Spanel et al.'s study [50]. In addition, the major product ion of the methyl mercaptan and NO^+ is the charge exchange product CH_3SH^+. This overlaps in mass with the $NO^+.H_2O$ adduct ion at m/z 48 that is efficiently formed when humid samples are analyzed using NO^+ ions. The same ion ($NO^+.H_2O$) is always present in a small amount, using the O_2^+ reagent ion, arising from the ion injection process.

Therefore, NO^+ and O_2^+ will provide less sensitive analysis because of the much larger background at m/z 48 in their mass spectra. H_3O^+ was thus used for the analysis of CH_3SH, which resulted in the $CH_3SH_2^+$ product ion at an m/z value of 49, which also has no serious contamination by other isobaric ions. This product ion formed hydration products at m/z 67 and 85 in humid samples [50], which was not the case in this experiment. Therefore, the product ion at the m/z value of 49 was only measured because of the low humidity of the sample and a high background interference that appeared at m/z 85 in natural gas. H_3O^+ was therefore chosen to be used in the analysis of CH_3SH for the above reasons, and also because of the low reactivity of H_3O^+ with light hydrocarbons in LPG and natural gas, providing a simple analysis method.

4.4.1.2 Ethyl mercaptan

Ethyl mercaptan (C_2H_5SH) reacts with H_3O^+ rapidly at the collision rate by proton trasfer. The reaction resulted in a single product ion at m/z 63 ($C_2H_5SH_2^+$). It also reacts with NO^+ to produce, via dissociative charge transfer and hydrogen elimination, two major product ions at m/z 61 and 62 with product ratios of 0.2 and 0.5 respectively. The reaction of NO^+ however, offered an attractive option to analyse ethyl mercaptan. Although NO^+ was therefore the preferred reagent ion to analyse the C_2H_5SH, large background interference at m/z 61 especially with LPG in natural gas prevented the use of this reagent ion in the experiment. H_3O^+ was thus the reagent ion selected to measure C_2H_5SH in hydrocarbons.

4.4.1.3 Dimethyl sulfide (DMS)

H_3O^+ and NO^+ ion reagents can be used to analyse this compound; they react rapidly at the collision rate. H_3O^+ produces an ion product at m/z 63, which overlaps with the

adduct ion $H_3O^+ .CO_2$ which is made via a three body reaction. [50] The amplitude of the $H_3O^+.CO_2$ signal depends on the amount of CO_2 present in the natural gas that was used. The reaction of NO^+ however, offered an attractive option in that a single parent cation is produced at m/z 62. Although NO^+ was therefore the preferred reagent ion to analyse the DMS, it also overlapped with ethyl mercatpan product at m/z 62. O_2^+ so could not be used here because of the presence of hydrocarbons, with which O_2^+ reacts rapidly, resulting in extensive consumption of the O_2^+ reagent ion.

4.4.1.4 Distinguishing Dimethyl sulfide and Ethylmercaptan using SIFT-MS

Dimethyl sulfide, DMS, ion products at m/z 63 (from H_3O^+) and 62 (from NO^+) overlapped with the products of ethyl mercaptan. Despite this overlap problem, it was possible to distinguish ethyl mercaptan, using only the m/z 61 product ion produced from the NO^+ reagent ion. However, this method can be useful only if there was no large background interference at that mass. Systems such as natural gas and LPG have a large interference at m/z 61. Consequently, great care must be taken when distinguishing ethyl mercaptan from DMS in natural gas and LPG.

In the experiment, the distinction was based on the known knowledge of the sample contents. The standard concentration of both DMS and ethyl mercaptan were relatively the same, and they reacted with H_3O^+ reagent ion at similar rates to produce a single product at m/z 63. The instrument was calibrated for both compounds. The concentration was therefore obtained roughly by dividing the 63 H_3O^+ product ion, which corresponded equally to both DMS and C_2H_5SH, by 2. Experiments published elsewhere [51], suggest that another reagent ion such as $CH_3OCH_2^+$, may have greater ability to discriminate DMS and C_2H_5SH as illustrated by the following equations (a and b).[52]

a) $C_2H_5SH + CH_3OCH_2^+ \longrightarrow [C_2H_5SH+CH]^+ (0.85) + CH3OH$
Ethyl mercaptan

$\longrightarrow [C_2H_5SH+CH_3OCH_2]^+ (0.15)$

b) $(CH_3)_2SH + CH_3OCH_2^+ \longrightarrow [C_2H_5SH+CH_3]^+ (0.05) + HCHO$
DMS

$\longrightarrow [C_2H_5SH+CH_3OCH_2]^+ (0.95)$

4.4.2 Results

Nitrogen mixtures

Figures 3.11, 3.12 and 3.13 show the linear relationship of these compounds in pure N_2, in a 1% mixture of LPG in N_2 and in a 1% mixture of natural gas in N_2. These results showed good linear responses. Nevertheless, they showed less consistency with actual concentrations even in the pure N_2 system, which was probably evidence of calibration-related problems. Moreover, the concentrations of the sulfur compound mixtures that were prepared, had a total uncertainty of about ±15%, and they were supposed to have a standard concentration of 4.7 ppm.

LPG mixture

The LPG system also showed good results. Methyl mercaptan showed lower concentration (Figure 3.12) compared with H_2S and both DMS and C_2H_5SH. In fact, it presented a slightly lower concentration because of its slightly lower standard concentration as shown in Figure 3.9.

Natural gas mixture

Natural gas mixtures (Figure 3.13) showed good results in terms of the linearity and consistency of the relevant sulfur compounds with each other.

The differences found between prepared and measured concentrations were suspected to be related to the lower stability of these sulfur compounds in Tedlar bags. Therefore, the stability of these compounds in Tedlar bags, as a function of time was

examined. However, the sulfur compounds showed good stability in Tedlar bags within the time required for an experiment. Figure 3.9 shows the stability of the prepared standard H_2S, DMS, C_2H_5SH, and CH_3SH mixture. These stable mixtures suggest there was a calibration problem. The concentration appeared to be stable within 10% error. The apparent increase in the concentrations of these compounds after three days was, to some extent, accounted for by a changing ICF function over the three days, particularly affecting the H_3O^+ levels (Figure 3.10-a). Nevertheless, the total time of the experiment was less than 2 days. Figure 3.10-b shows the stability of C_2H_5SH, DMS, and H_2S in the 1% LPG mixture in N_2 over 4 hours. Finally, the limit of detection of the relevant sulfur compounds was determined and is illustrated in Table 3.5.

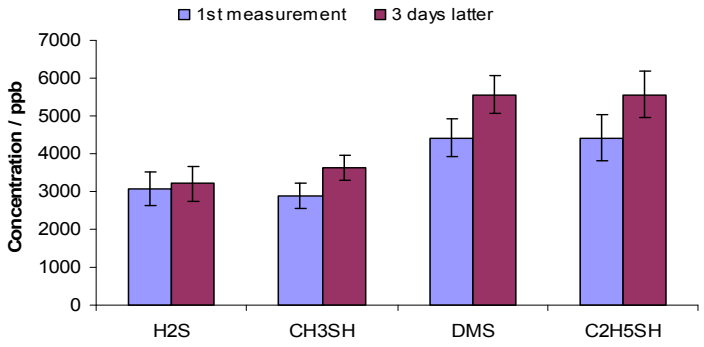

Figure 3.9 Stability of the Standard 4.7 ppm concentration of the relevant compounds over 3 days.

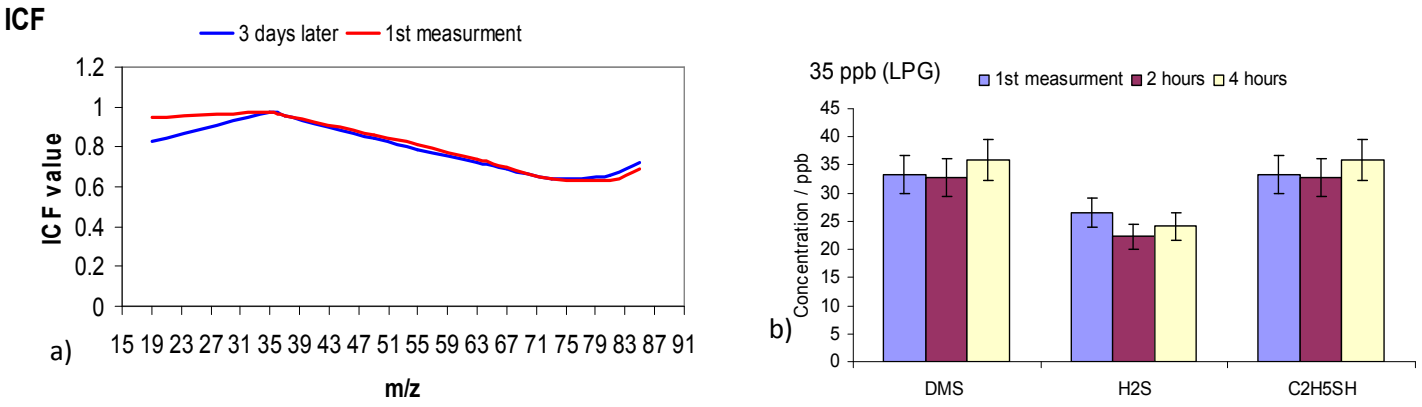

Figure 3.10 a) The ICF function measurement 3 days apart. b) Stability of the 35 Ppb concentration of the relevant compounds over 4 hours in 1% LPG mixture in N_2.

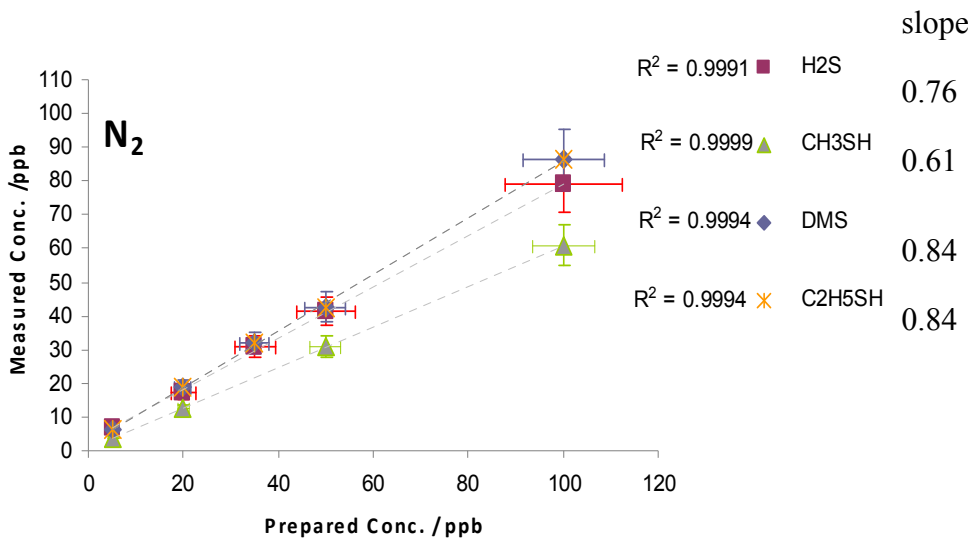

Figure 3.11 The linear relationship result exhibited for dilution of H_2S, DMS, C_2H_5SH, and CH_3SH in N_2.

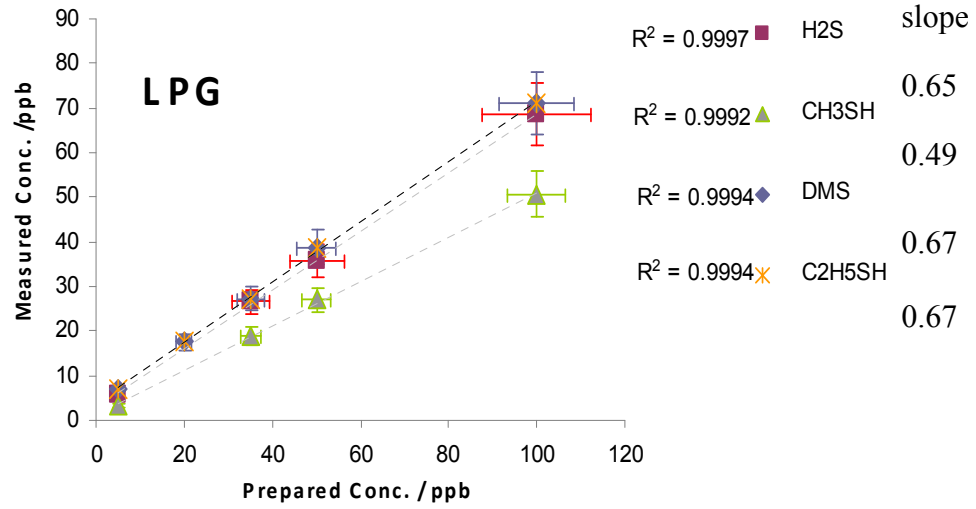

Figure 3.12 The linear relationship result exhibited for dilution of H_2S, DMS, C_2H_5SH, and CH_3SH in 1% mixture of LPG.

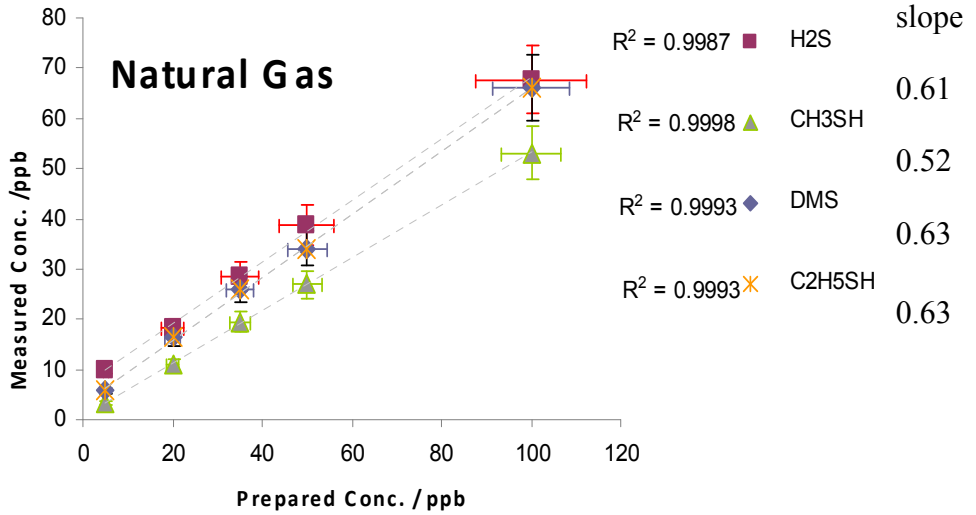

Figure 3.13 The linear relationship result exhibited for dilution of H_2S, DMS, C_2H_5SH, and CH_3SH in 1% mixture of natural gas.

Table 3.5 The LOD of the sulfur compounds of interest in natural gas (Voice 200)

Compound	**H_2S**	**CH_3SH**	**DMS**	**C_2H_5SH**
LOD (ppb)	11.8	1.2	10.9	10.9

5. **Conclusion**

The results elucidate the potential of using SIFT-MS to measure H_2S, CH_3SH and the combined concentration of C_2H_5SH and DMS in LPG and natural gas hydrocarbon mixtures. The SIFT-MS instrument effectively detects and quantifies hydrogen sulfide to the low part-per-billion levels in diluted natural gas and LPG. The results illustrate the linear response of monitoring sulfur compounds in N_2, natural gas and LPG across a wide concentration range. This linear response shows the ability of measuring the concentration of H_2S in three systems including natural gas. The range of sulfur compounds in hydrocarbons was extended using the Voice 200 instrument to include dimethyl sulfide, ethyl mercaptan and methyl mercaptan.

Chapter 4

Further SIFT-MS petroleum applications

1. Introduction

In this chapter, the SIFT-MS project on petroleum was extended to other applications. First, the SIFT-MS capacity of tracing chemical tracer compounds, such as bromobenzene and chlorobenzene, which might be added in very low concentration to hydrocarbons systems, was investigated. The linearity with concentration and the LOD of these compounds were determined. Second, the SIFT-MS capacity to analyze qualitatively some of hydrocarbon mixtures produced by oil refineries was examined. The aim of this second experiment was to explore the potential of using SIFT-MS for qualitative analysis of hydrocarbon mixtures.

2. Tracers in the Oil and Gas Industry

2.1 Overview

Tracers are identifiable substances that can be followed through the course of process. They provide information on the pattern of events in the process or on the redistribution of parts or elements involved. [53] The uses of tracers throughout different industries are diverse and widespread. In the oil industries, tracers are often used to estimate residual oil saturation and volumetric sweep efficiency. They are often added to hydrocarbons to track the migration of seawater, oil and gas through the reservoir.

In drilling, for example, tracers are used to identify lost circulation zones. This is an expensive and frequent problem when drilling into geothermal formations. In hydraulic fracturing, tracers provide information on the location and orientation of fractures. They are used also for orientation and depth correlation of perforators, holes that are punched in the casing or liner of an oil well to connect them to the reservoir. The use of tracers has applications for enhanced oil recovery, by understanding the migration properties of the well.

Tracers can be divided into two general groups: 1) chemical tracers and 2) radioactive tracers. Chemical tracers are those, which can be identified and measured quantitatively by general analytical methods such as conductivity and GC-MS. Radioactive tracers however, are detected by their emitted beta or gamma radiation. In this research, only chemical tracers will be considered.

Various types of reactions can occur to chemical tracers at a microscopic level. This leads to changes in tracer concentration, as the fluid containing the tracer flows through a porous medium. Important knowledge of each tracer, such as analytical detectability and retention characteristics in reservoir rock, must also be known in order to gain more knowledge of the reservoir characteristics.

Currently, online monitoring and detection of tracer compounds on oil-rigs, has interested some oil companies, such as the Norwegian Institute for Nuclear Energy (IFE). IFE originally started work in the field of tracer technology, as the original tracers were radioactively tagged hydrocarbons (such as mono-tritiated methane). IFE is now looking to develop new tracers, which can be monitored on an oil-rig. A requirement for such development is an ability to detect the compounds in the presence of natural gas. Currently, cyclic perfluorocarbons are preferred as tracers by IFE and other companies due to their very low detection limits in natural gas, using standard laboratory GC-MS. However, GC-MS cannot easily be used in the same way on an oil-rig because of the slower time response. Therefore, IFE is interested in looking at a simple and fast online solution on an oil-rig to monitor compounds that can be easily measured. IFE wants to be able to detect bromobenzene and chlorobenzene in a natural gas matrix. By using such compounds, a much more in-depth picture of the reservoir migration patterns can be gained.

This chapter is concerned with the quantification of the chemical tracers (bromobenzene and chlorobenzene) in natural gas and LPG at very low concentrations (ppbv) using the SIFT-MS technique. By being able to monitor these compounds on an oil-rig, more information regarding the density, rate and flow and migration between different well sites can be gained.

2.2 Reactions of the SIFT-MS reagent ions with tracers of interest

The presence of hydrocarbon mixtures, such as natural gas in the analysis medium, will require a consideration of the side reactions that could occur during the course of the analysis. These side reactions could affect the sensitivity and the accuracy of the analysis. Accordingly, a greater understanding of the reagent ion chemistry with the hydrocarbons will be necessary to choose the best reagent ion for the analysis. Small hydrocarbons undergo endothermic reaction with H_3O^+, whilst the large hydrocarbons undergo a slow association reaction, which produces $M.H_3O^+$ ions. The NO^+ ion reactions proceed largely via hydride ion transfer producing $(M-H)^+$ ions with large hydrocarbons ($\geq$C5) and branched hydrocarbons. However, partial incorporation of the NO^+ into the large hydrocarbon with subsequent fragmentation may produce minority ions like $RHNO^+$ ($R \geq C_3$). In contrast, the O_2^+ reagent ion reacts with all hydrocarbons (but only very slowly with methane) by rapid dissociative charge transfer. Figure 4.1 demonstrates the reactions of the main SIFT-MS reagent ions with a branched hydrocarbon (2-methylbutane).

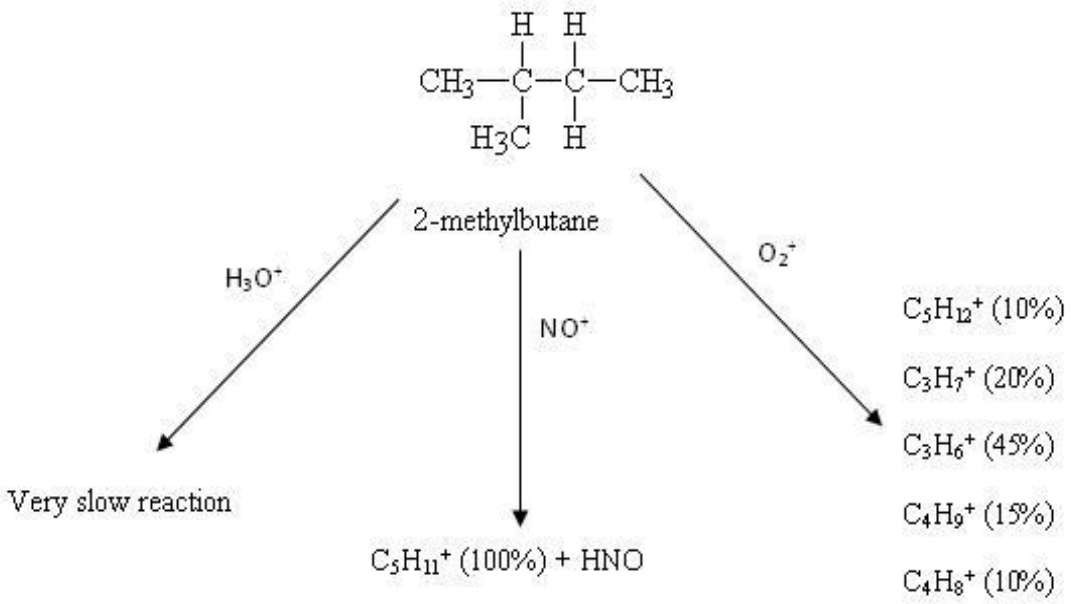

Figure 4.1 The reaction of 2-methylbutane with H_3O^+, NO^+ and O_2^+(SIFT-MS reagent ions).

The rapid reaction of O_2^+ with hydrocarbons makes it unsuitable as a reagent ion for the detection of tracers. Instead, the H_3O^+ was selected for analysis of both bromobenzene and chlorobenzen because of its low reactivity with the light hydrocarbons. The NO^+ can be used as well but it seems to give a low sensitivity for the tracers especially with LPG, due to its reactivity with the branched hydrocarbons.

Bromobenzene has a proton affinity (PA) of 754.1 kJ/mol and an ionisation energy (IE) of 9.00eV. Therefore, it reacts with the H_3O^+ at the collision rate and produces two product ions corresponding to the two isotopes of Br in $C_6H_5BrH^+$ at 157 m/z and 159 m/z with a 0.5 product ratio (equation 1).

$$C_6H_5Br + H_3O^+ \longrightarrow C_6H_5Br.H^+ + H_2O \quad (1)$$

Bromobenzene reacts also with the NO^+ to produce the charge exchange parent ion product of $C_6H_5BrH^+$ again with a 0.5 product ratio corresponding to the two Br isotopes (equation 2).

$$C_6H_5Br + NO^+ \longrightarrow C_6H_5Br^+ + NO \qquad (2)$$

Chlorobenzene has a PA of 753.1 kJ/mol and an IE of 9.07 eV. Consequently, it reacts also with the H_3O^+ at the collision rate to produce the proton transfer product ion $C_6H_5ClH^+$ at m/z 113 and 115 in the product ratio of 0.75 and 0.25 corresponding to the abundance ratio of the Cl isotopes (equation 3). Also, it reacts with NO^+ to produce via charge transfer $C_6H_5Cl^+$, in the same abundance ratio as the Cl isotopes. (Equation 4).

$$C_6H_5Cl + H_3O^+ \longrightarrow C_6H_5Cl.H^+ + H_2O \qquad (3)$$

$$C_6H_5Cl + NO^+ \longrightarrow C_6H_5Cl^+ + NO \qquad (4)$$

2.3 Experimental procedure

A 3L and 250 ml glass bulb was used in this experiment. Each bulb included a Suba-seal septum through which gas could be sampled using a gas syringe. The flasks were used instead of the Tedlar bags because of the strong adsorption of bromobenzene and chlorobenzene onto the bag walls. Three systems of pure N_2, 1% LPG mixture in N_2, and 1% natural gas mixture in N_2 were used in this experiment. Bromobenzene and chlorobenzene were prepared in the 250 ml bulb as a mixture with N_2. The bulb concentrations were calibrated for greater accuracy. This calibrated mixture was then used as a standard for a series of subsequent dilutions. The standard concentration had an uncertainty of ± 25%. However, a problem was experienced when preparing the bulb standard. The concentrations were found to vary. This variation was attributed to both bromobenzene and chlorobenzene

becoming adsorbed onto the bulb rubber septum. As a result, this strong adsorption lowered the concentration in the standard bulb mixtures, and gave concentration measurements that showed a decrease with time.

To minimise the adsorption problem, the standard was prepared and used directly. In addition, the rubber septum was covered with PARAFILM (laboratory film) to reduce the adsorbtion process into the septum. Next, a 5 ppb solution was prepared initially in the 3L bulb. After that, the concentration was increased by adding an additional quantity from the stock mixture to the first 5 ppb concentration. Further, one measurement was carried out to decrease the effect of lowering the pressure inside the bulb that could affect the sample flow rate. The same procedure was followed for the three mixtures, which were then monitored by SIFT-MS, using the Voice 200 instrument.

2.4 Results and discussion

Initial information was obtained about the background and viability of measuring the target compounds in the natural gas. Figure 4.2 shows the full mass scan of the H_3O^+ and NO^+ reagent ions used for the natural gas, using the voice 200 instrument in which the mass was progressed stepwise in integer units. These full mass scans exhibited a suitable background count, indicating the ability of detecting the relevant compounds at low concentration levels.

The experiments on the halobenzene mixtures were carried out on the Voice 200 (3007), based only on the known bromobenzene and chlorobenzene's kinetic parameters, without calibrating the instrument for the target compounds.

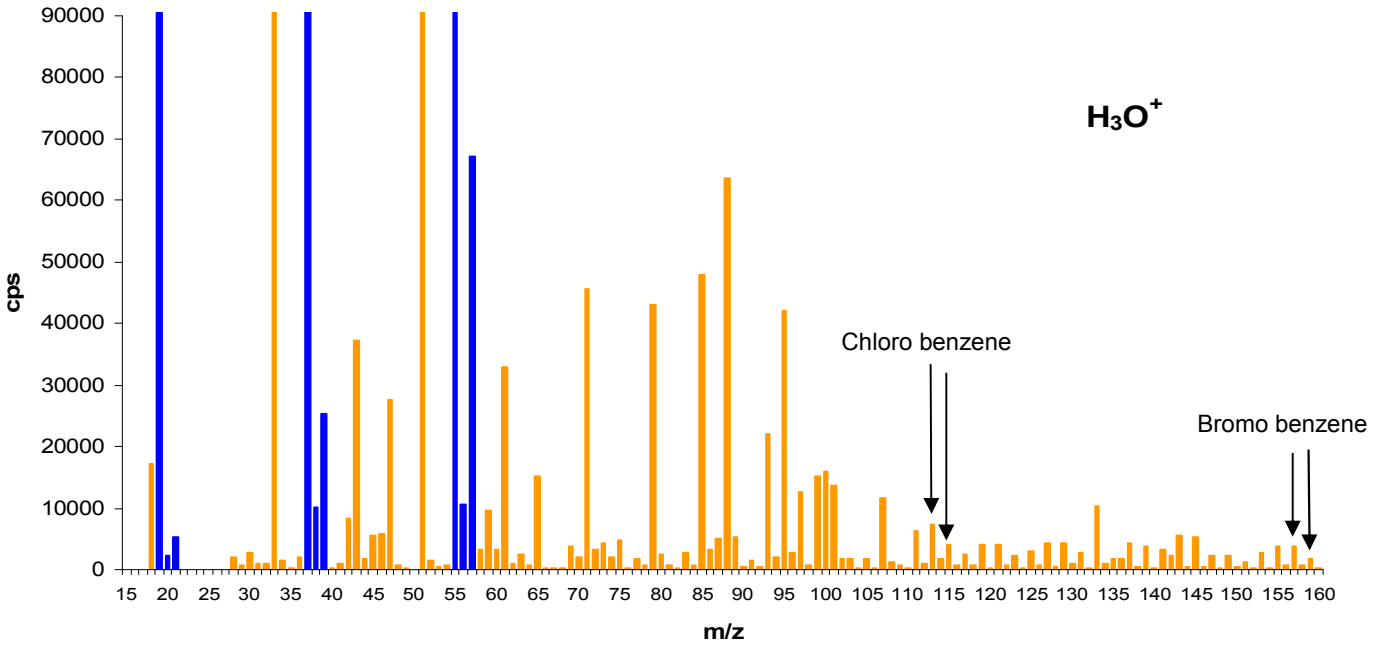

Figure 4.2.a) The H_3O^+ full mass scan of 1% natural gas mixture in N_2 using the Voice 200 instrument in which no halobenzenes were added (background). The blue lines represent the reagent ions.

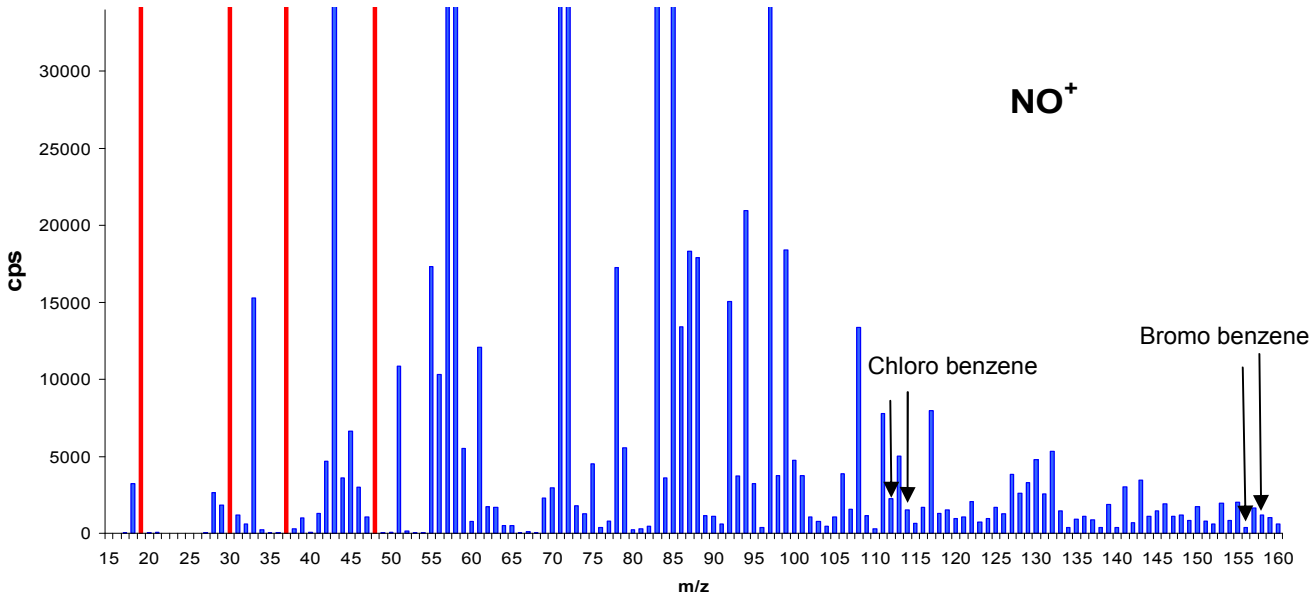

Figure 4.2. b) The NO^+ full mass scan of 1% natural gas mixture in N_2 , using the Voice 200 instrument in which no halobenzenes were added (background). The red lines represent the reagent ions.

The results, as shown in Figures 4.3, 4.4 and 4.5, showed good linear responses of both chlorobenzene and bromobenzene with good concentration agreement within the range of the total uncertainty of the experiments. These results demonstrated the ability of the SIFT-MS technique for tracing the relevant compounds in the three systems including natural gas. Moreover, the results gave further information about the ability of using the NO^+ reagent ions to detect the target compounds except for the LPG system, where the NO^+ measured concentration were higher than that measured using the H_3O^+ (see Figure 4.4). This difference was accounted for by the high depletion of the NO^+ reagent ion count. This depletion was due to the greater reactivity of NO^+ with branched hydrocarbons that are present in the LPG, as was noted previously in the sulfur compounds experiment. Finally, the LOD of bromobenzene and chlorobenzene in the natural gas was determined and the results are shown in Table 4.1. The LOD of these compounds provided a higher detection limit compared with the sulfur compounds that were reported in chapter 3.

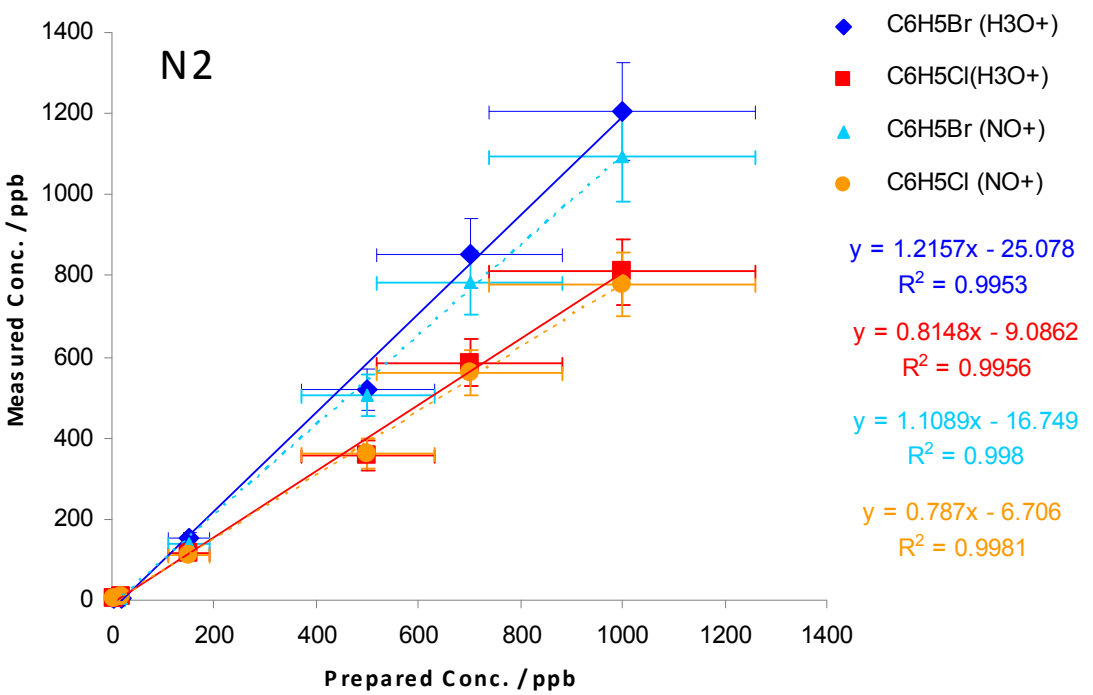

Figure 4.3 The linear relationship between measured concentration and prepared concentration for a mixture of bromobenzene and chlorobenzene in pure N_2.

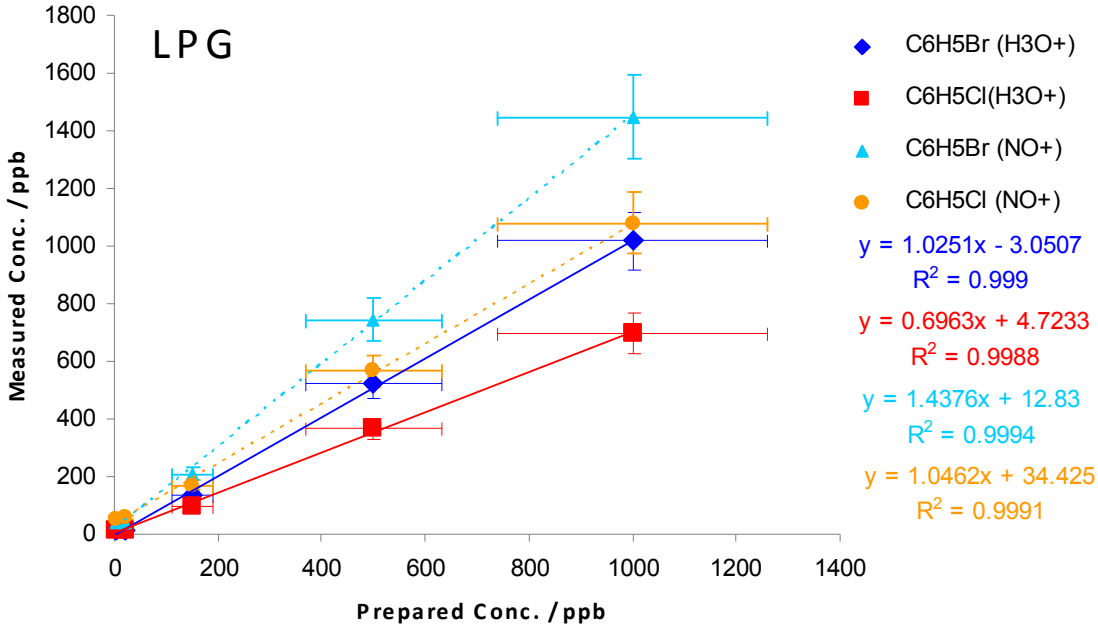

Figure 4.4 The linear relationship between measured concentration and prepared concentration for a mixture of bromobenzene and chlorobenzene in a 1% LPG mixture in N_2.

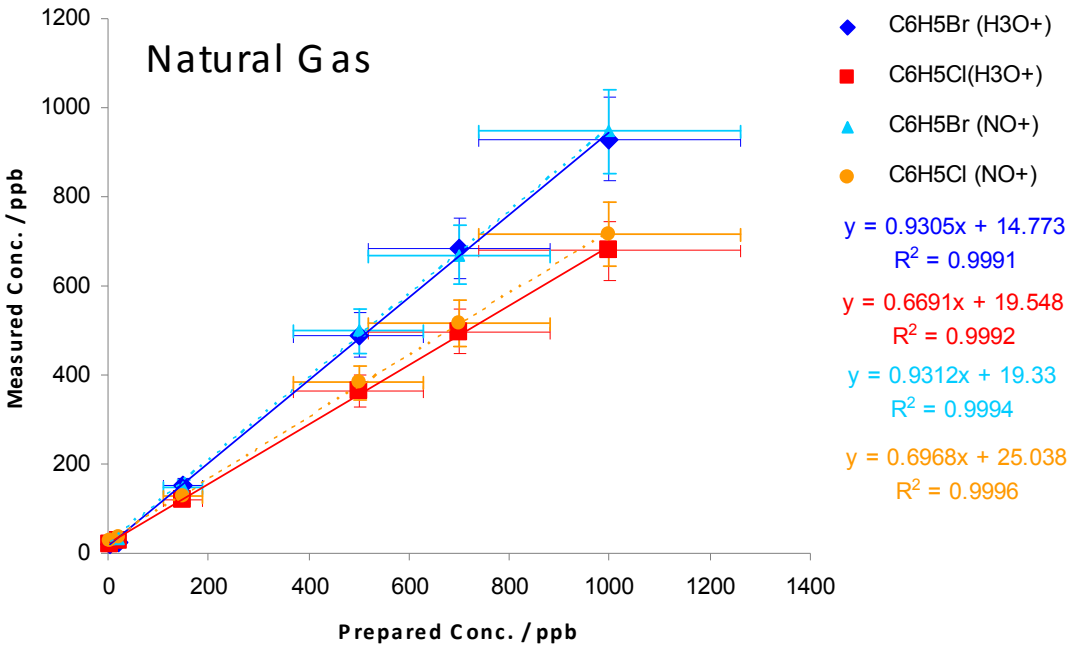

Figure 4.5 The linear relationship between measured concentration and prepared concentration for a mixture of bromobenzene and chlorobenzene in a 1% natural gas mixture in N_2 .

Table 4.1 LOD values of bromobenzene and chlorobenzene in natural gas.

Compounds	C_6H_5Br (NO+)	C_6H_5Cl (NO^+)	C_6H_5Br (H_3O^+)	C_6H_5Cl (H_3O^+)
LOD (ppb)	29.3	40.3	28.8	40.0

To conclude, in examining the detection of both halobenzenes in gas mixtures, it was found that both NO^+ and H_3O^+ reagent ions might be used in natural gas, but only H_3O^+ in LPG. In summary, this study clearly showed the capacity of using the SIFT-MS for the purpose of tracing the relevant compounds in an oil-rig situation to follow added tracers, at concentrations in the low ppbv range as indicated by their LODs.

3. Hydrocarbon qualitative analysis

3.1 Overview

The SIFT-MS analysis for hydrocarbons is not so simple. Hydrocarbons react with SIFT-MS reagent ions differently, depending on the size of the hydrocarbons. For example, the small n-alkanes have PAs smaller than H_2O (PA=691 kJ mol^{-1}) and thus cannot undergo proton transfer with H_3O^+ at thermal energy. Consequently, we do not expect the small alkanes to react rapidly with H_3O^+. Although small hydrocarbons may undergo slow endoergic reactions with H_3O^+, large hydrocarbons exhibit an association reaction, producing $M.H_3O^+$ ions, as observed in the Spanel and Smith study. [15] The rate of the association reaction furthermore, has been found to accelerate as the alkane chain increases and becomes equal to the collision rate with dodecane and larger n-alkanes. In these larger alkane reactions, every collision is stabilized by the reaction with a third body. These observations are illustrated by the following examples, where k is the experimental rate coefficient and k_c is the collision rate coefficient.

n-heptane $k \sim 0.2k_c$

n-octane $k \sim 0.5k_c$

n-decane $k \sim 0.8k_c$

n-dodecane $k = k_c$

This association reaction can be thought of as distributing the bond energy of the excited transient complex ions $(M.H_3O^+)^*$ into the vibrational degrees of freedom of the transient ion. The more degrees of freedom the hydrocarbon has, the larger is the lifetime of the complex ion against unimolecular dissociation. This interesting characteristic of the reactions with H_3O^+ has an ambiguous outcome. The association reactions are followed by a very rapid

ligand switching reaction that occurs in the presence of trace water vapour. This rapid reaction produces neutral HC + $H_3O^+.H_2O$ ion at the collision rate as shown in the following equations. Here HC refers to hydrocarbon compounds.

$$HC + H_3O^+ + M \longrightarrow HC.H_3O^+ + M \qquad (M = \text{Third body})$$

$$HC.H_3O^+ + H_2O \longrightarrow HC + H_3O^+.H_2O \qquad (\text{Bimolecular switching reactions})$$

This ligand switching reaction then has been found to catalyze the production of hydrated hydronium ions as proved in other studies. [11] Hence, there is a need for the use of a dryer such as Nafion™ , if the H_3O^+ reagent ion is used for hydrocarbon analysis.

The O_2^+ reagent ion on the other hand, reacts via efficient dissociative charge transfer at the collision rate, except for methane. The O_2^+ reacts mainly by rapid dissociative charge transfer reactions. However, because of the extensive fragmentation, the use of O_2^+ as a reagent ion does not often provide definitive identification for hydrocarbons as there are many common product ions from the different hydrocarbons.

The NO^+ reagent ion reactions proceed largely via hydride ion transfer. This produces $(M-H)^+$ ions with a minor pathway, leading to partial incorporation of the NO^+ into the large hydrocarbons, producing minority ions like $RHNO^+$ (R= C_3H_7, C_4H_9, etc). This was observed also in the Spanel and Smith study where $RHNO^+$ products for linear hydrocarbons, larger than C5, were found. Further, the NO^+ reagent ion does not react completely with n-alkanes <C6 because of their large IE (> 9.25 eV). However, with n-alkanes > C6, the reaction with NO^+ proceeds largely via a hydride transfer reaction with some small channels leading to fragmentation. The n-alkanes ≥ C6 react with NO^+, but the rate coefficients are all measurably smaller than k_c.[15] In contrast, the branched small hydrocarbons react faster than the n-alkanes [54] with rate coefficients close or equal to the collision rate, as shown previously with the 2-ethylbutane example (section 2).

3.2 Experimental procedure

Different quantitative and qualitative hydrocarbon standard calibration mixtures supplied by SUPELCO were used in this experiment. The components of these mixtures were formerly determined by GC-MS from the supplier. These components had, in general, above 99% purity. In this experiment, six hydrocarbon standard mixtures were analyzed. The complexity level of these mixtures was gradually increased from samples numbered 1 to 6. The first three samples had only simple mixtures of hydrocarbons, whereas the remaining samples represented real refinery hydrocarbon mixtures. The GC-MS spectrum that was provided by the supplier of each sample is shown next to its relevant SIFT-MS spectrum.

These samples were analyzed after containment in Tedlar bags. They were diluted by an appropriate factor to get suitable spectrum intensity. The samples then were analyzed on the Voice 200 instrument, using a full mass scan method. A full mass scan of a blank bag background was performed first, before the sample was injected into the bag. The product ions signals from the hydrocarbons then could be distinguished from the Tedlar bags compounds and could be easily identified. After that, some larger hydrocarbon compounds, n-alkanes (C8-C18) and some cyclohydrocarbons, were analyzed individually in order to understand their fragmentation product ions and to facilitate the hydrocarbon mixtures spectrum analysis.

3.3 Results and discussion

The major process that occurred with the NO^+ reagent ion and hydrocarbons was hydride ion transfer. This observation made NO^+ the reagent ion of choice in the analysis of hydrocarbon mixtures. Large hydrocarbons reacted with NO^+ to give hydride ion transfer as their major product ion with > 65 % product ratio. In addition, further product ions arising from fragmentation of the parent ion also occurred (Table 4.2). Octane, for example, reacted with NO^+ to give its major product ion at m/z 113 and a series of fragmentation product ions of the

kind $RHNO^+$ and R^+ at m/z 71, 88, 57, 74 and 102 (see Figure 4.6). It was also interesting to note that some of the R^+ product ions formed at m/z 57, 71, 85, and 99 in the reaction with NO^+ were not reported in the Spanel and Smith study.[15] Both the product ions $RHNO^+$ and R^+ were observed in this study as ion products of the larger n-alkanes. Nonane also reacted to produce a major product ion at m/z 127 with a similar fragmentation pattern to octane, plus a further fragment ion at m/z 113 (see Figure 4.7). Since the major product ion of these hydrocarbons from NO^+ was at the parent mass less 1, then the mixture analysis becomes plausible. A sample SIFT-MS product ion spectrum for the reagent ions H_3O^+, NO^+ and O_2^+ in their reaction with undecane (Figure 4.8) showed the many ion products of this reaction and this is typical for all the higher-order alkanes. In this spectrum, some fragmentations also occurred with the H_3O^+ reagent ion. Some of these fragmentations may resulted from the small amounts of O_2^+ also present as an impurity peak, in the H_3O^+ mass spectrum.

An indication of the product ions arising from NO^+ for C8-C14 hydrocarbons and some cyclohydrocarbons, supported with their branching ratios that were determined in this study, are displayed in Table 4.2

The cyclohydrocarbons were also found to react with NO^+ via hydride ion transfer as the major product channel. With substituted cyclohydrocarbons, the presence of a large substituent group, such as the butyl group, was found to result in fragmentation. The butyl group dissociated and left the parent cyclo compounds (equation 5).

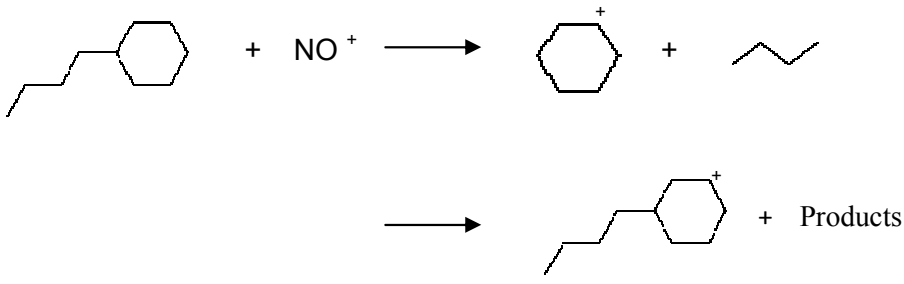

(5)

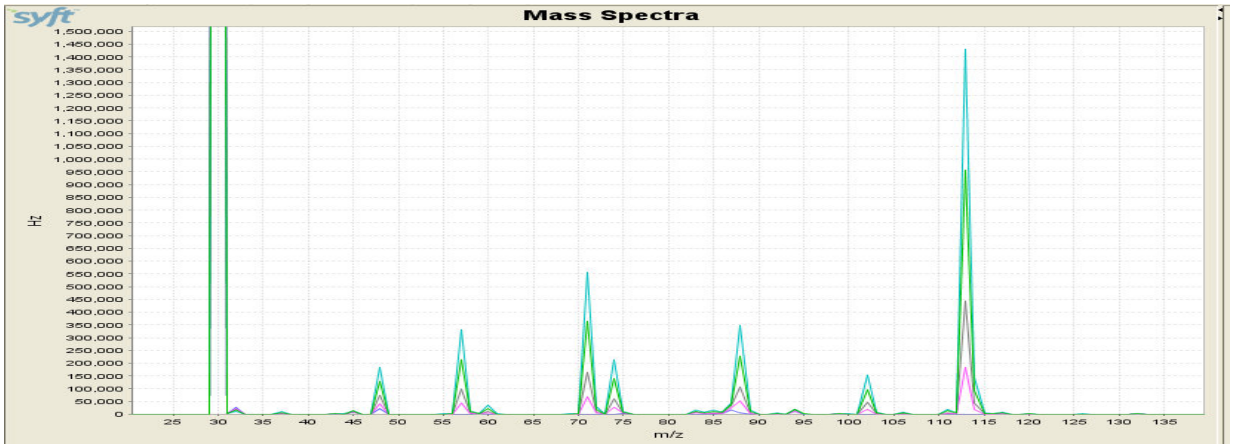

Figure 4.6 The NO^+ full mass scan for octane (C_8H_{18}). Different colors represent different concentrations.

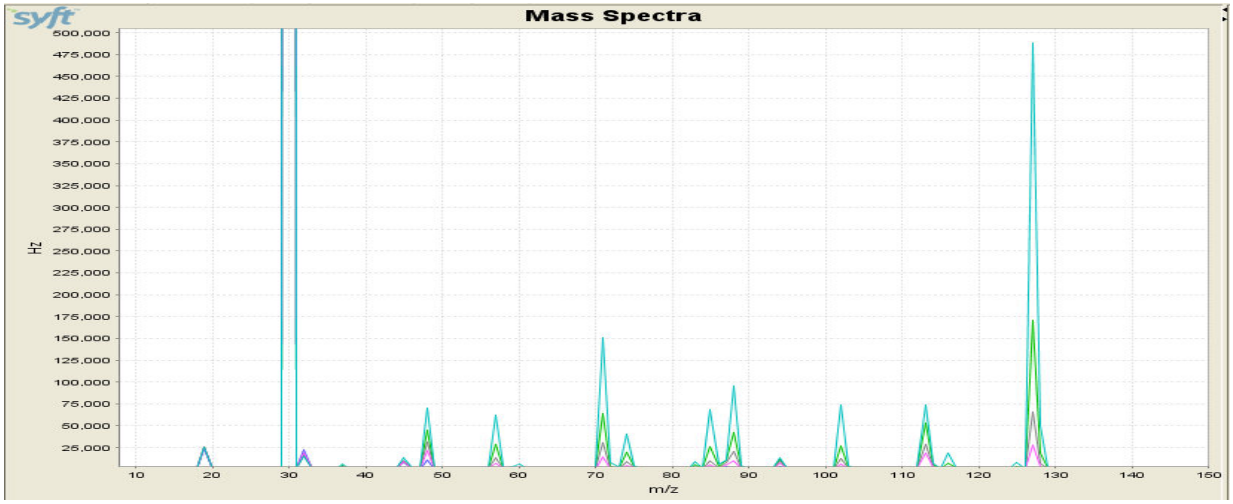

Figure 4.7 The NO^+ full mass scan for nonane (C_9H_{20}). Different colors represent different concentrations.

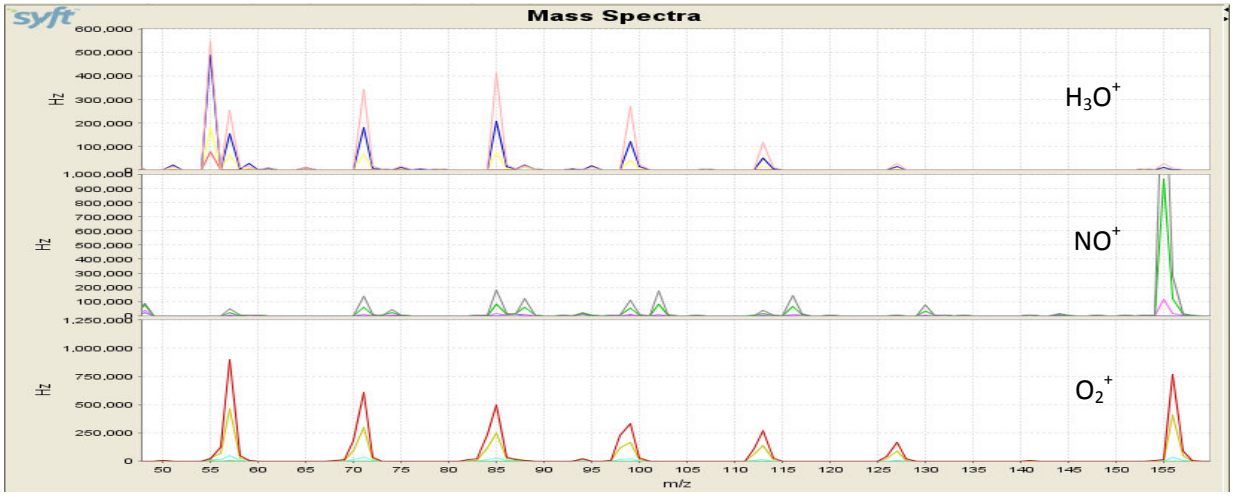

Figure 4.8 Full mass scan for undecane ($C_{11}H_{24}$). Different colors represent different concentrations.

Table 4.2 Products of the reactions of NO^+ with the given hydrocarbons. The Percentage of each ion product is given in brackets (See the text for further explanation)

Compounds	Molecular structure	Formula	Molecular weight	Major product ion (NO^+)	Minor product ions (NO+)	
						< 0.05
n-octane		C_8H_{18}	114	113 (0.65)	71 (0.11), 57(0.06)	$\sum RHNO^+ + R^+$
n-nonane		C_9H_{20}	128	127 (0.62)	113 (0.14), 88 (0.05), 71(0.07),	$\sum RHNO^+ + R^+$
n-decane		$C_{10}H_{22}$	142	141 (0.82)		$\sum RHNO^+ + R^+$
n-undecane		$C_{11}H_{24}$	156	155 (0.86)		$\sum RHNO^+ + R^+$
n-dodecane		$C_{12}H_{26}$	170	169 (0.62)	155 (0.1), 88 (0.09),	$\sum RHNO^+ + R^+$
n-tetradecane		$C_{14}H_{30}$	198	197 (0.11)	117 (0.12), 94 (0.16), 87(0.33), 62(0.06)	$\sum RHNO^+ + R^+$
Cyclohexane		C_6H_{12}	84	83 (0.78)	114 (0.11) 139 (0.1)	
Ethycyclo hexane	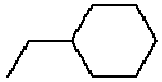	C_8H_{16}	112	111 (1)		
Butylcyclo hexane	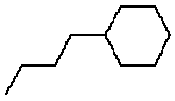	$C_{10}H_{20}$	140	83 (0.7)	139(0.3)	
Methycyclo pentane		C_6H_{12}	84	83 (1)		

Subsequently, analyses of the actual hydrocarbons mixtures obtained from SUPELCO were carried out. Six samples of hydrocarbon mixture samples were qualitatively analyzed. A detailed explanation of each sample and its qualitative analysis result is given next. It was apparent that the clarity of the mass spectra were noticeably affected, apparently by the isotopic variants of the products.

Sample 1:

Sample 1 contained a mixture of n-alkane (C3-C9) as indicated in the GC-MS spectrum (Figure 4.9). It shows the SIFT-MS analysis result of sample 1. Propane, butane and pentane react very slowly with the NO^+ reagent ion as mentioned previously, and so their product ions were not expected to give rise to large intensity in the spectrum. Although propane, butane and pentane react very slowly with the NO^+ reagent ion, small peaks still appeared at their m/z product ion values of 43, 57 and 71. However, these peaks were believed to correspond to the fragmentation products produced from large hydrocarbons as shown for instance in octane and nonane spectra (Figures 4.6 and 4.7). The presence of a product at m/z 43 was also suspected to arise from a reagent ion impurity in the NO^+ signal as well as the ion products at m/z 57 and 71. The appearance of these product ions was clearly due to the presence of the O_2^+ ion impurity. This was obvious from the reduction of the O_2^+ signal at m/z 32 compared to the blank signal. Other ion products in the sample were easily identified. However, smaller fragment ions were produced and these contributed to several masses as indicated by the dashed faint arrows in Figure 4.9. This will in consequence, introduce an error in the quantitative analysis of the smaller n-alkanes without further substantial testing using calibrated mixtures.

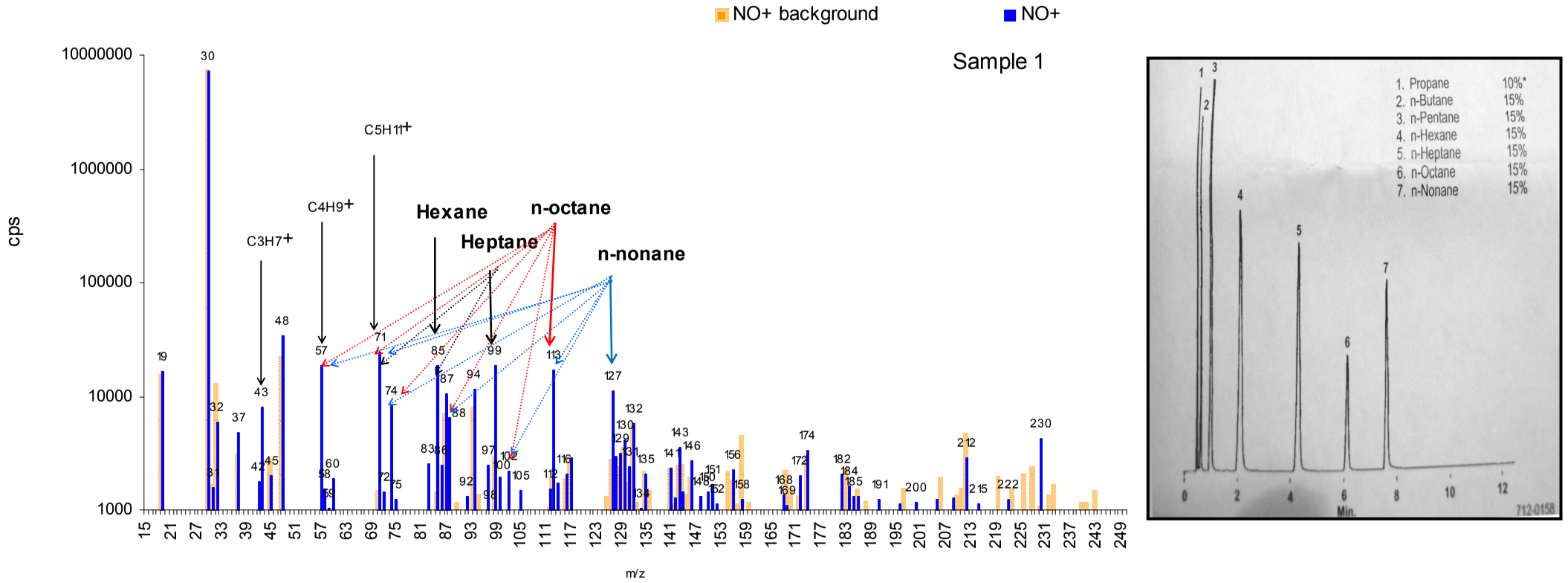

Figure 4.9 The NO^+ chemical ionization spectrum of sample 1. The GC-MS spectrum of sample 1 is also shown.

Sample 2:

Sample 2 contained larger n-alkanes (C10-C18) and some other larger alkanes. Figure 4.10 shows the analysis result for sample 2. Analysis of the large n-alkanes was restricted by the volatility of these compounds at room temperature. To achieve acceptable concentrations, it was necessary to suitably dilute the sample by a factor for recognition, but with regard to the other n-alkanes present in the sample. In this experiment n-alkanes smaller than tetradecane (< C14) could be identified. n-alkanes larger than C13 could not be because of their low volatility at room temperature. For instance, Tetradecane vapour pressure is 1 Torr at 76.4°C. Increasing the length of the hydrocarbons chain reduced the volatility of the hydrocarbons, and this was clearly apparent by looking at the (parent-1) m/z intensity of these n-alkanes as they increased in size (Figure 4.10). A range of fragmentation ions appeared in the low mass range of the spectrum, corresponding, as noted earlier, to the R^+ and $RHNO^+$ fragmentations. These fragmentations will, in fact, affect the ability to make quantitative analysis without careful calibration over a range of concentrations.

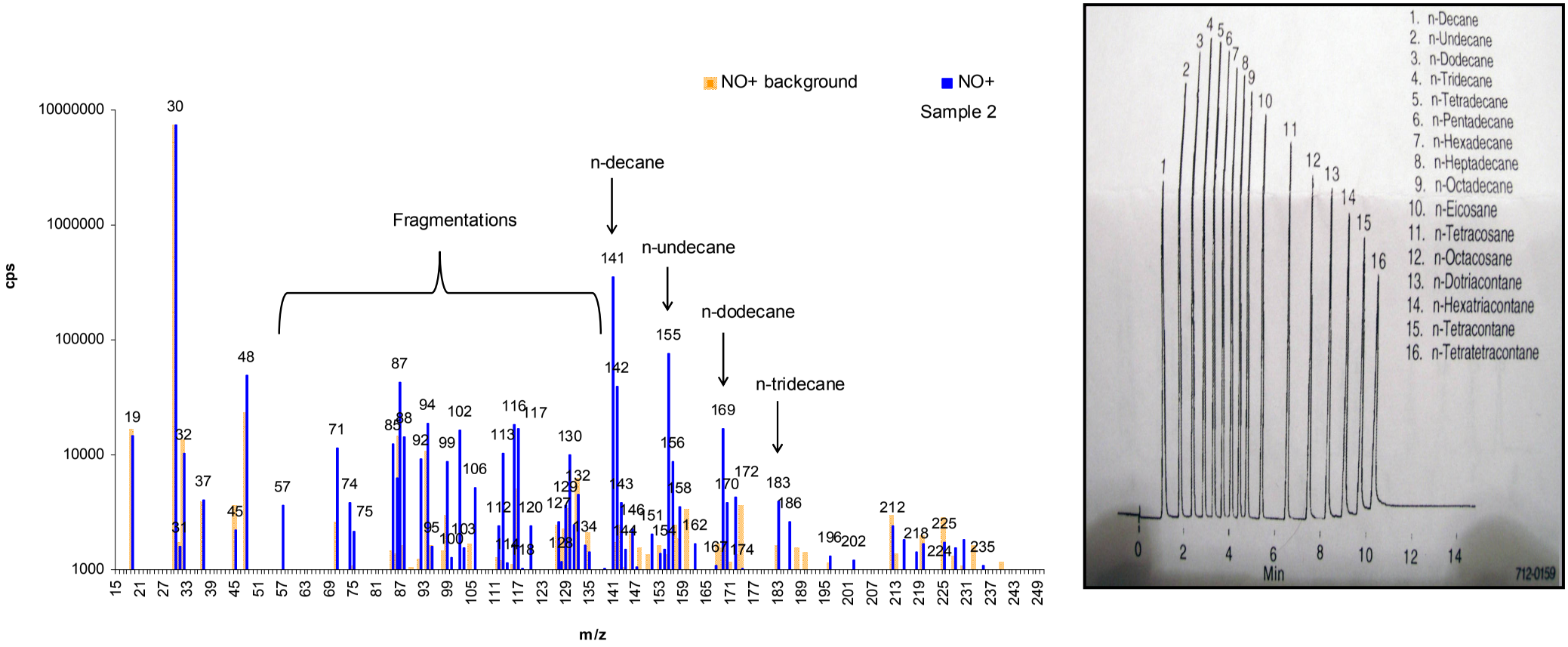

Figure 4.10 The NO^+ chemical ionization spectrum of sample 2. The GC-MS spectrum of sample 2 is also shown.

Sample 3:

Sample 3 contained different hydrocarbon mixtures of both aromatic and aliphatic hydrocarbons (linear and branching) (see GC-MS spectrum Figure 4.11). This sample enabled the ability to identify both types of hydrocarbons, aliphatic and aromatic, in the presence of each other. In addition, it presented the effects of the presence of the branching alkanes on the signal intensity. It was clear that branched alkanes reacted faster than n-alkanes with NO^+, so their signals were large at m/z 71 and 85 and higher than the fragment ion singles in intensity. This made them easy to identify. Figure 4.11 shows the sample 3 analysis result.

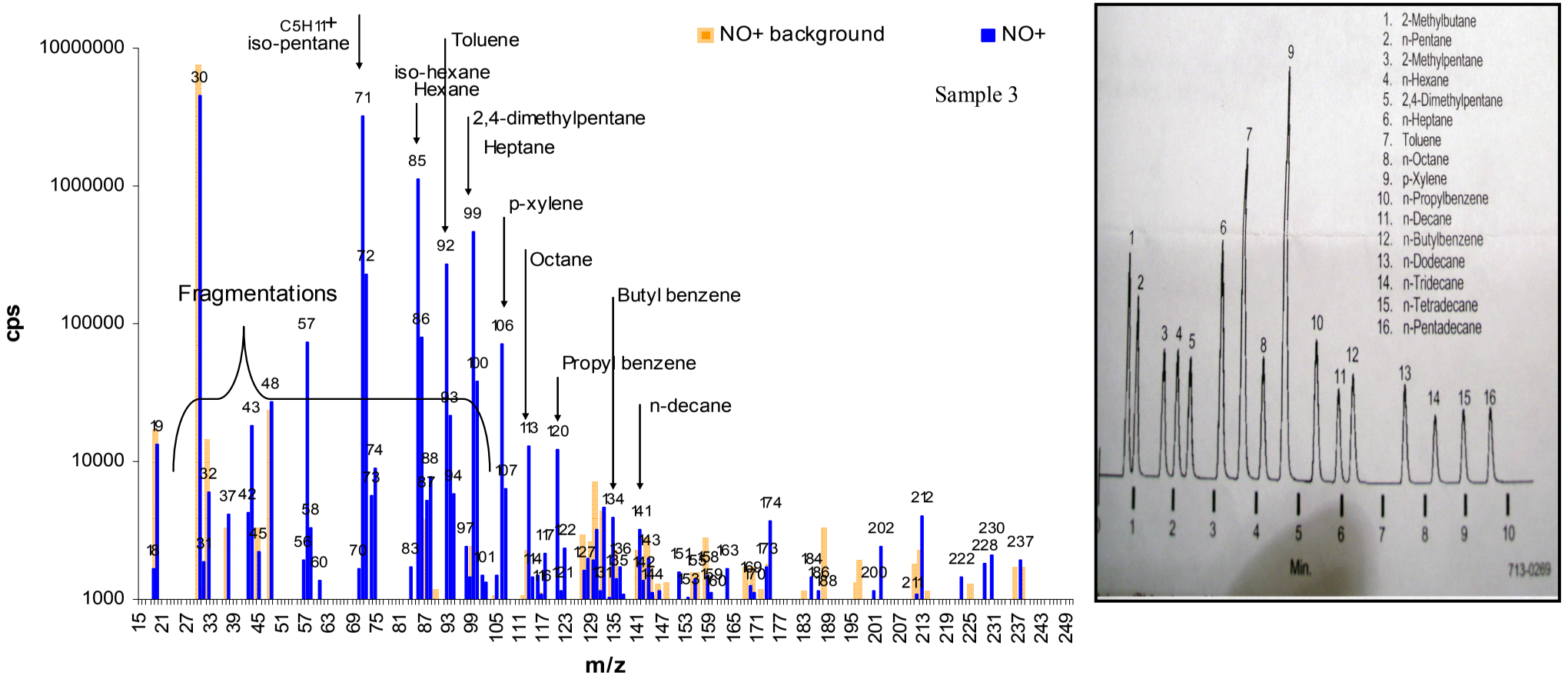

Figure 4.11 The NO^+ chemical ionization spectrum of sample 3. The GC-MS spectrum of sample 3 is also shown.

Sample 4, 5 and 6:

Sample 4, 5 and 6 can be described as real refinery hydrocarbon mixtures with different complexities as follows:

Sample 4 = branching alkane mixture - a total of 34 hydrocarbons.

Sample 5 = sample 4 + larger n-alkanes + cyclohydrocarbons and aromatic hydrocarbons – a total of 63 hydrocarbons.

Sample 6 = sample 5 + more larger n-alkanes – a total of 89 hydrocarbons.

The SIFT-MS analysis results of these complicated mixtures are shown in Figures 4.12, 4.13 and 4.14.

The analysis of sample 4 showed a relatively simple spectrum for the 34 hydrocarbons present in the sample 4 mixture. The sample contents were therefore quite easily identified due to the absence of large n-alkanes, which react to produce a range of ion products from fragmentation. It was clear that the signal intensity at m/z 57 and m/z 71 was large and corresponded to iso-butane and iso-propane, respectively. The sample 5 mixture contained 63 hydrocarbons and was more complex (Figure 4.13.a). Nevertheless, some analyses were achievable for the sample mixture, except for any isomers and some unidentifiable compounds at m/z 108 and 120. Lastly, the sample 6 mixture, containing 89 hydrocarbons (Figure 4.14.a), showed a noticeable increase in the complexity of the spectrum with quite a number of peaks corresponding to product ions of different m/z ratios. The NO^+ chemical ionization spectrum of sample 6 is shown in Figure 4.14. There were some unidentified masses, such 108 and 120 as in sample 5, plus another product ion at m/z 151. The ion products of m/z 87 and 94 are compounds arising from the Tedlar bags polymer and they

vary with the bag and are temperature dependent. The presence of these two ion products in Tedlar bags was discussed in an earlier chapter (chapter 2, section 5) of this thesis.

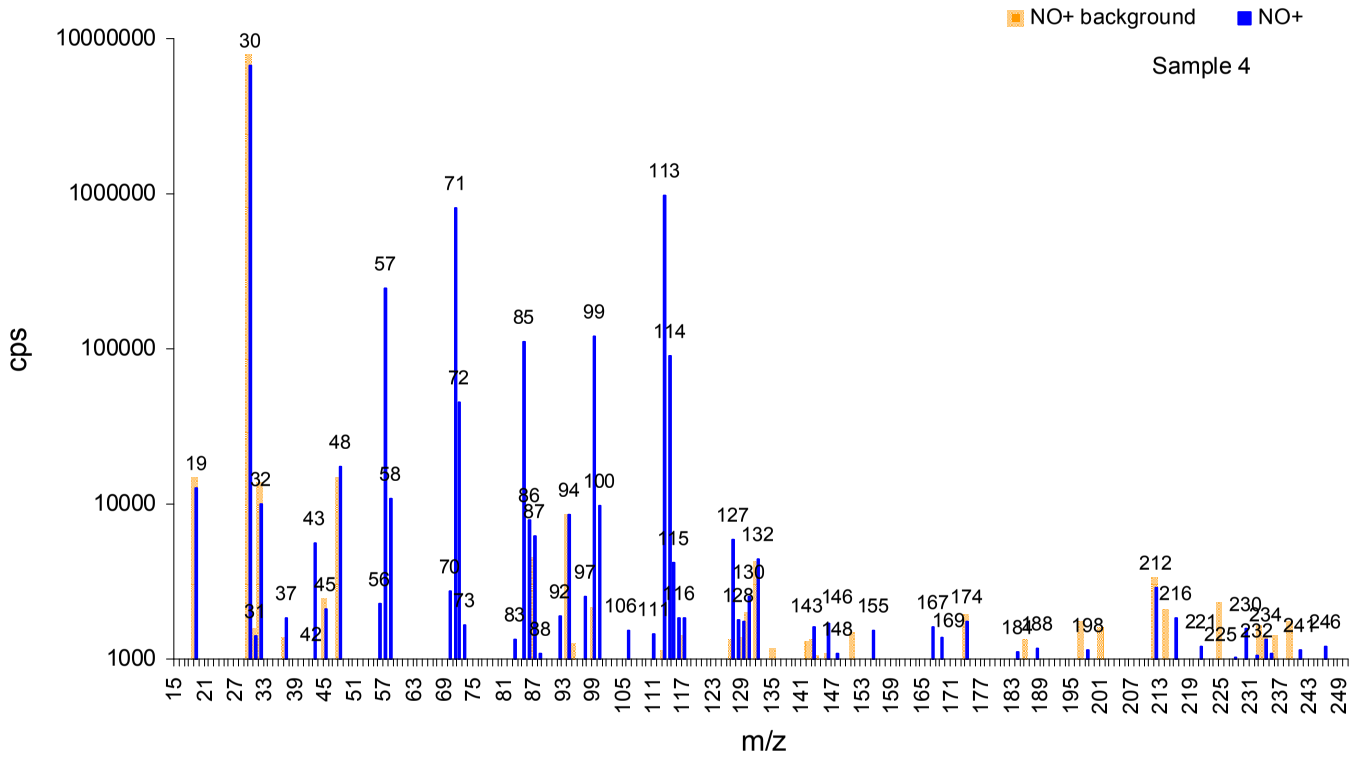

m/z	Product ions			
57	iso-butane			
71	iso-pentane			
85	methyl pentane	dimethyl butane		
99	methyl hexane	dimethyl pentane	trimethyl butane	ethyl pentane
113	trimethyl pentane	Methyl heptane	dimethyl hexane	
127	dimethyl heptane	methyl octane	ethyl heptane	trimethyl hexane

1. iso-Butane
2. n-Butane
3. iso-Pentane
4. n-Pentane
5. 2,3-Dimethylbutane
6. 2-Methylpentane
7. 3-Methylpentane
8. 2,4-Dimethylpentane
9. 2,2,3-Trimethylbutane
10. 2,3-Dimethylpentane
11. 3-Methylhexane
12. 2,2,4-Trimethylpentane
13. 2,5-Dimethylhexane & 2,2,3-Trimethylpentane
14. 2,4-Dimethylhexane
15. 2,3,4-Trimethylpentane
16. 2,3,3-Trimethylpentane
17. 2,3-Dimethylhexane
18. 2-Methylheptane
19. 4-Methylheptane & 3,4-Dimethylhexane**
20. 3,4-Dimethylhexane**
21. 3-Methylheptane
22. 2,2,5-Trimethylhexane
23. 2,2,4-Trimethylhexane
24. 2,4,4-Trimethylhexane
25. 2,3,5-Trimethylhexane
26. 2,4-Dimethylheptane
27. 2,6-Dimethylheptane
28. 2,5-Dimethylheptane
29. 2,3,4-Trimethylhexane
30. 2,3-Dimethylheptane
31. 2,4,6-Trimethylhexane
32. Unidentified trimethylhexane
33. Unidentified trimethylhexane
34. Unidentified trimethylhexane

**Stereoisomers.

Figure 4.12 The NO^+ chemical ionization spectrum and table of sample 4 product ions identified. The 34 hydrocarbons in the sample are shown in the table.

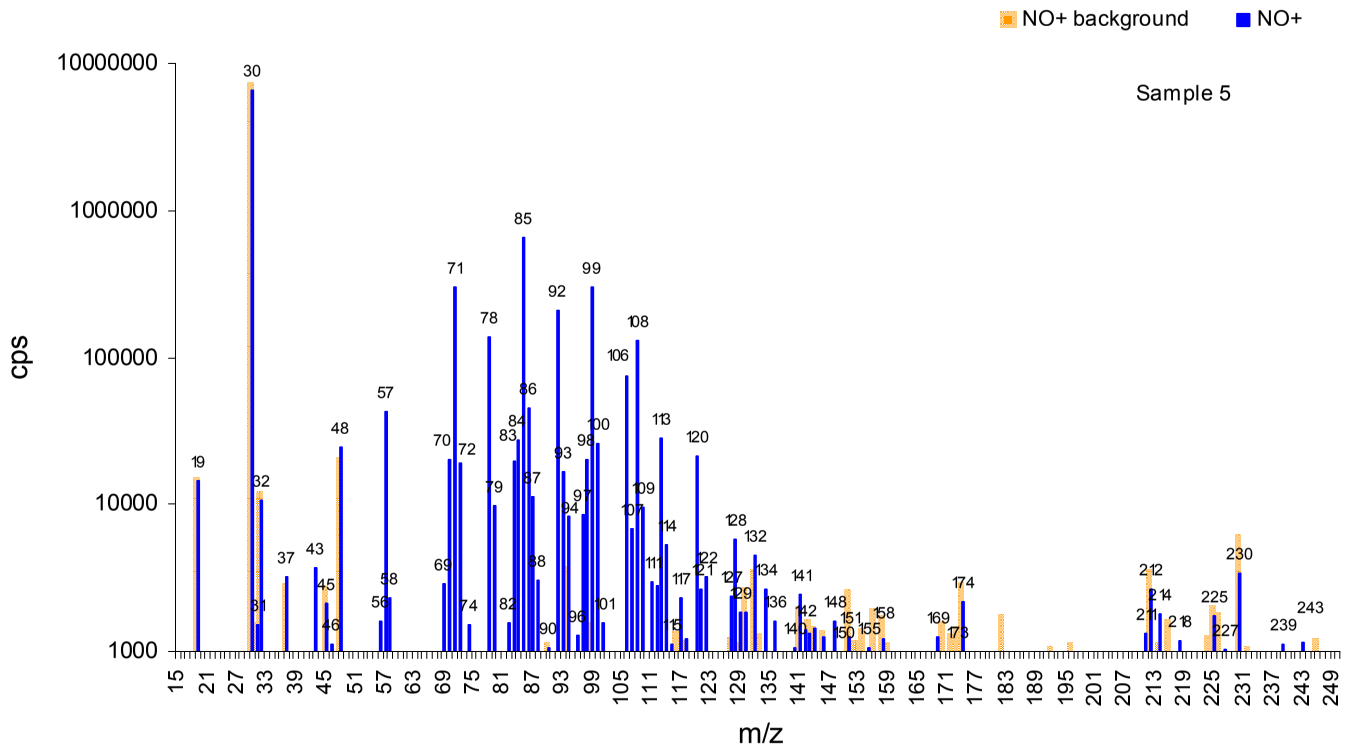

Figure 4.13 The NO^+ chemical ionization spectrum and table of sample 5 product ions identified.

m/z	Product ions			
57	iso-butane	$C_4H_9^+$		
69	cyclopentane			
71	ios-pentane	$C_5H_{11}^+$		
78	benzene			
83	cyclohexane	methylcyclo pentane		
85	methyl pentane	dimethyl butane	hexane	
92	toluene			
97	methylcyclo hexane	dimethylcyclo pentane	ethylcyclo pentane	
99	methyl hexane	heptane	dimethy pentane	
106	xylene	ethylbenzene		
108	?			
111	trimethylcyclo pentane	dimethylcyclo hexane		
113	octane	ethylhexane	methylethyl pentane	
120	?			
127	nonane	methyoctane	ethylheptane	trimethyl hexane

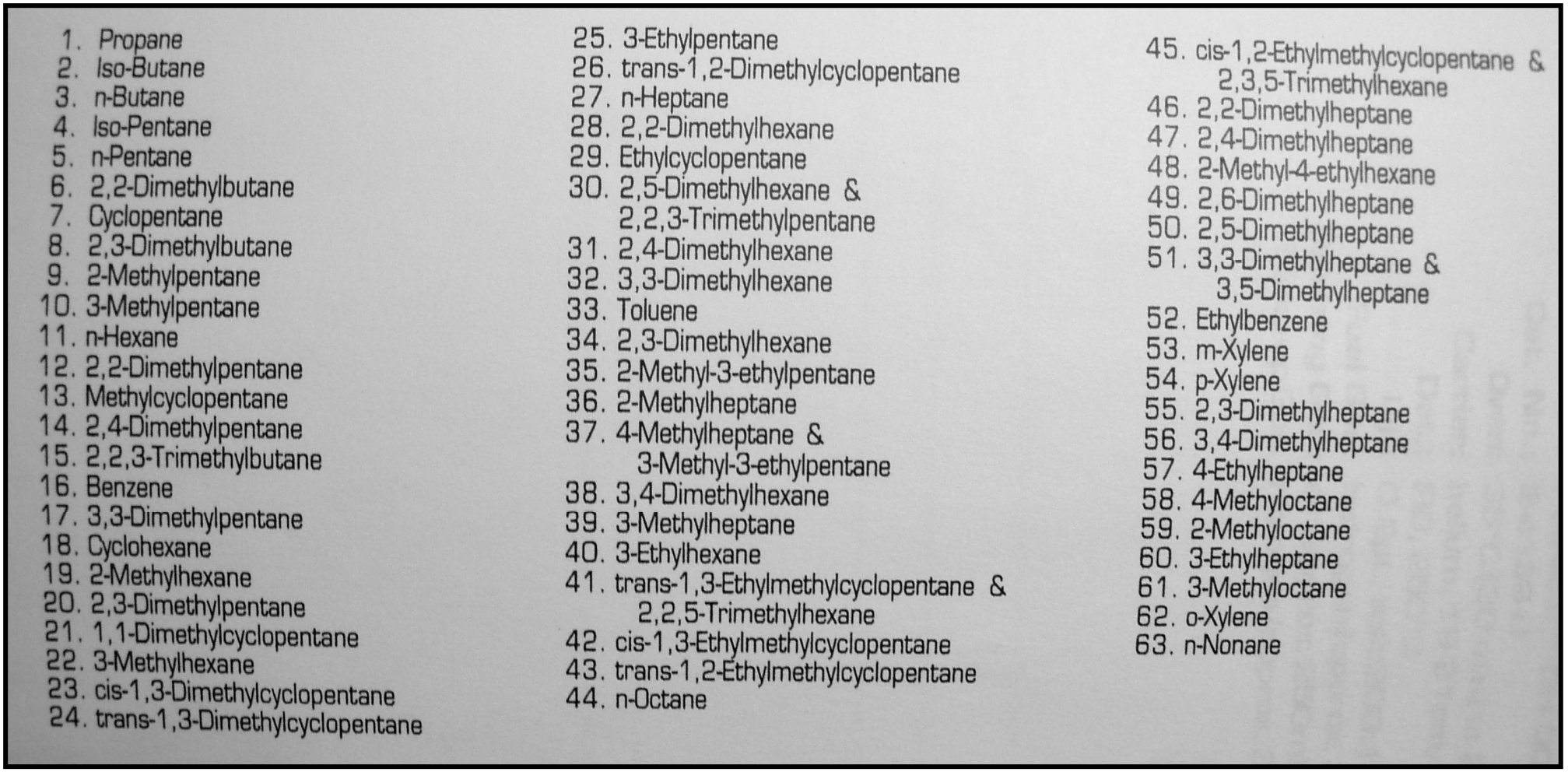

Figure 4.13.a. A summary of the 63 hydrocarbons present in sample 5.

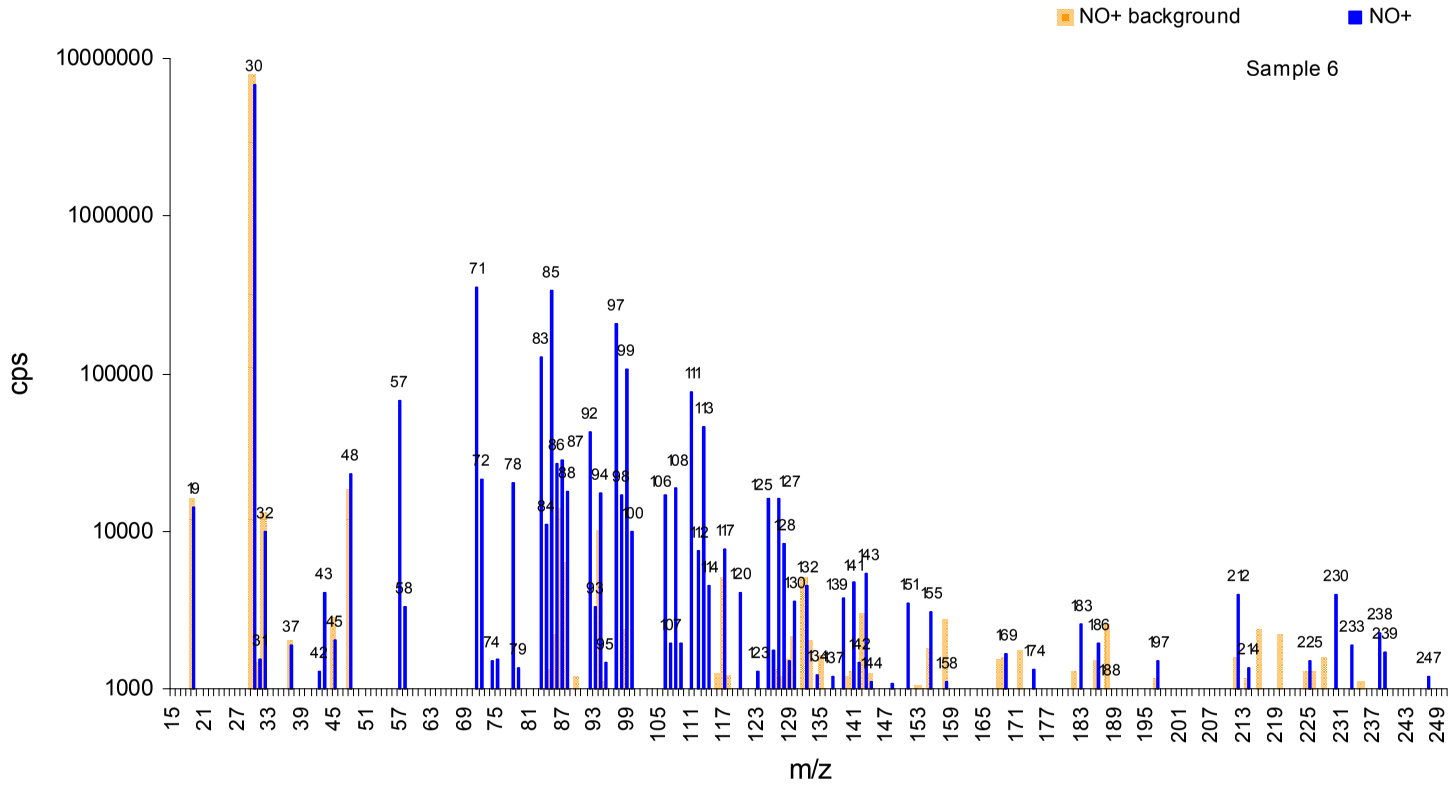

Figure 4.14 The NO^+ chemical ionization spectrum and table of sample 6 product ions identified.

m/z	Product ions			
57	iso-butane	$C_4H_9^+$		
69	cyclopentane			
71	ios-pentane	$C_5H_{11}^+$		
78	benzene			
83	cyclohexane	methylcyclo pentane		
85	methyl pentane	dimethylbutane	hexane	
92	toluene			
97	methylcyclo hexane	dimethylcyclo pentane	ethylcyclo pentane	
99	methyl hexane	heptane	dimethyl pentane	
106	xylene	ethylbenzene		
108	?			
111	trimethyl cyclopentane	dimethylcyclo hexane		
113	octane	ethylhexane	methylethyl pentane	
120	?			
125	trimethyl cyclohexane			
127	nonane	methyloctane	Ethyl heptane	trimethyl hexane
141	decane			
155	undecane			
169	Dodecane			

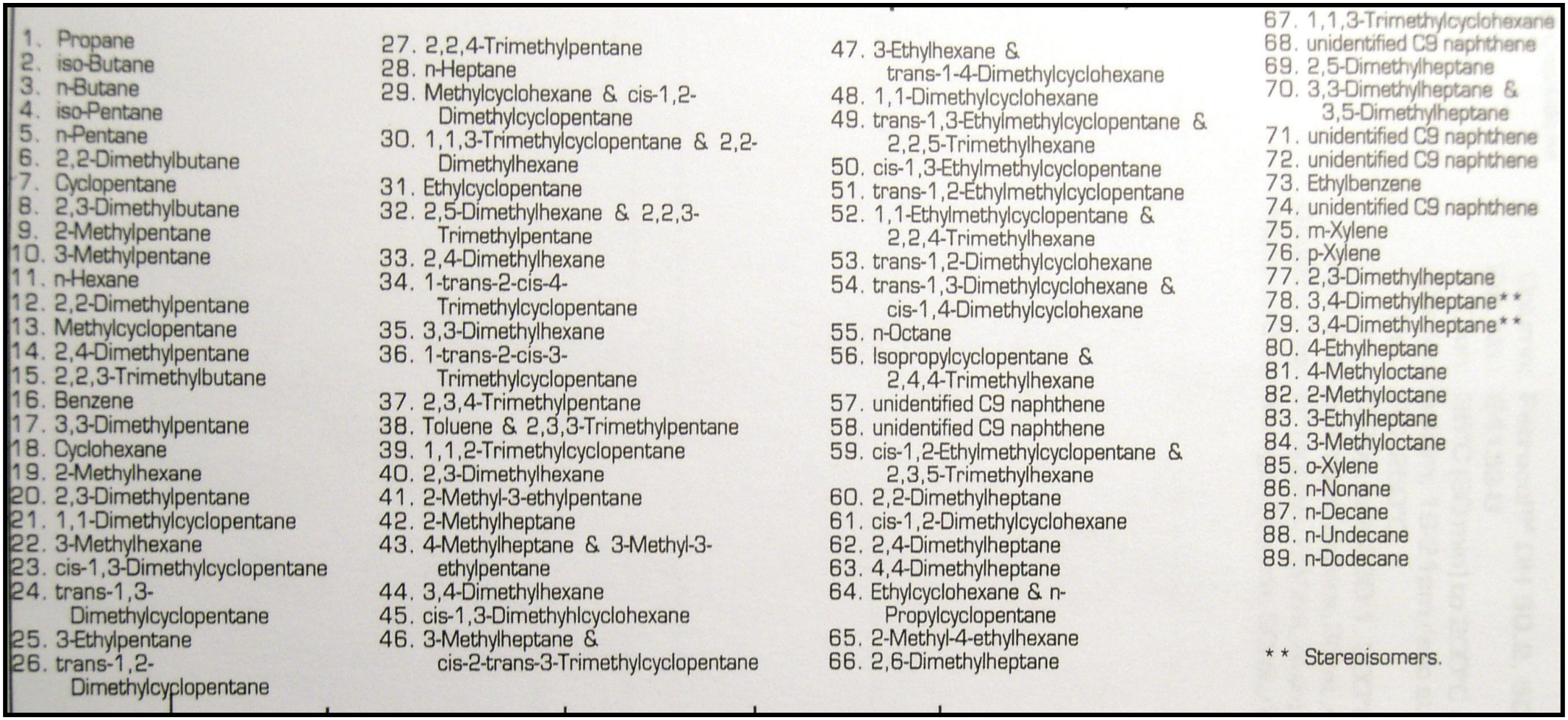

1. Propane
2. iso-Butane
3. n-Butane
4. iso-Pentane
5. n-Pentane
6. 2,2-Dimethylbutane
7. Cyclopentane
8. 2,3-Dimethylbutane
9. 2-Methylpentane
10. 3-Methylpentane
11. n-Hexane
12. 2,2-Dimethylpentane
13. Methylcyclopentane
14. 2,4-Dimethylpentane
15. 2,2,3-Trimethylbutane
16. Benzene
17. 3,3-Dimethylpentane
18. Cyclohexane
19. 2-Methylhexane
20. 2,3-Dimethylpentane
21. 1,1-Dimethylcyclopentane
22. 3-Methylhexane
23. cis-1,3-Dimethylcyclopentane
24. trans-1,3-Dimethylcyclopentane
25. 3-Ethylpentane
26. trans-1,2-Dimethylcyclopentane
27. 2,2,4-Trimethylpentane
28. n-Heptane
29. Methylcyclohexane & cis-1,2-Dimethylcyclopentane
30. 1,1,3-Trimethylcyclopentane & 2,2-Dimethylhexane
31. Ethylcyclopentane
32. 2,5-Dimethylhexane & 2,2,3-Trimethylpentane
33. 2,4-Dimethylhexane
34. 1-trans-2-cis-4-Trimethylcyclopentane
35. 3,3-Dimethylhexane
36. 1-trans-2-cis-3-Trimethylcyclopentane
37. 2,3,4-Trimethylpentane
38. Toluene & 2,3,3-Trimethylpentane
39. 1,1,2-Trimethylcyclopentane
40. 2,3-Dimethylhexane
41. 2-Methyl-3-ethylpentane
42. 2-Methylheptane
43. 4-Methylheptane & 3-Methyl-3-ethylpentane
44. 3,4-Dimethylhexane
45. cis-1,3-Dimethyhlcyclohexane
46. 3-Methylheptane & cis-2-trans-3-Trimethylcyclopentane
47. 3-Ethylhexane & trans-1-4-Dimethylcyclohexane
48. 1,1-Dimethylcyclohexane
49. trans-1,3-Ethylmethylcyclopentane & 2,2,5-Trimethylhexane
50. cis-1,3-Ethylmethylcyclopentane
51. trans-1,2-Ethylmethylcyclopentane
52. 1,1-Ethylmethylcyclopentane & 2,2,4-Trimethylhexane
53. trans-1,2-Dimethylcyclohexane
54. trans-1,3-Dimethylcyclohexane & cis-1,4-Dimethylcyclohexane
55. n-Octane
56. Isopropylcyclopentane & 2,4,4-Trimethylhexane
57. unidentified C9 naphthene
58. unidentified C9 naphthene
59. cis-1,2-Ethylmethylcyclopentane & 2,3,5-Trimethylhexane
60. 2,2-Dimethylheptane
61. cis-1,2-Dimethylcyclohexane
62. 2,4-Dimethylheptane
63. 4,4-Dimethylheptane
64. Ethylcyclohexane & n-Propylcyclopentane
65. 2-Methyl-4-ethylhexane
66. 2,6-Dimethylheptane
67. 1,1,3-Trimethylcyclohexane
68. unidentified C9 naphthene
69. 2,5-Dimethylheptane
70. 3,3-Dimethylheptane & 3,5-Dimethylheptane
71. unidentified C9 naphthene
72. unidentified C9 naphthene
73. Ethylbenzene
74. unidentified C9 naphthene
75. m-Xylene
76. p-Xylene
77. 2,3-Dimethylheptane
78. 3,4-Dimethylheptane**
79. 3,4-Dimethylheptane**
80. 4-Ethylheptane
81. 4-Methyloctane
82. 2-Methyloctane
83. 3-Ethylheptane
84. 3-Methyloctane
85. o-Xylene
86. n-Nonane
87. n-Decane
88. n-Undecane
89. n-Dodecane

** Stereoisomers.

Figure 4.14.a. A summary of the 89 hydrocarbons present in sample 1.

3.4 Conclusion

This study indicates the utility of the NO^+ reagent ion to detect qualitatively, some of the large hydrocarbons in complex mixtures of hydrocarbons. Unfortunately, however, the SIFT-MS reactions cannot distinguish between the structural isomers of most aromatic and aliphatic hydrocarbons. In addition, a number of the smaller hydrocarbons yield common fragment ions and the overlap with isotopic ions from ^{13}C leads to the necessity for more attention when quantitative analysis is required. In these circumstances, an additional analytical support is necessary and one way of doing this is to utilize the SIFT-MS advantage of other reagent ions. The reagent ion H_3O^+ with its interesting association reactions, for example, should be useful for large n-alkanes with the use of Nafion to dry the hydrocarbons. [11] The H_3O^+ will eliminate the fragmentation ion products but its application will be restricted only to the large hydrocarbons. Thus, a combination of NO^+ and H_3O^+ would be very useful for quantitative analysis in mixtures containing the larger n-alkanes.

Chapter 5

TD-SIFT-MS potential for air monitoring

1. Introduction

In this chapter, the potential of using the SIFT-MS coupled with a thermal desorber (TD) to be used for air monitoring was explored, using passive sampling methodology. The aim of this part of my project was to examine the suitability of SIFT-MS to monitor VOCs that had been adsorbed on a substrate and to compare the results of the analysis with those of a GC-MS.

2. Air pollutions

2.1 Overview

The recent development in the industrial sector with increasing environmental damage, coupled with the rising number of cars and airplanes around the world, have exacerbated the problem of air quality. Air pollution can be defined, according to Spronken-Smith et al., as substances which, when present in the atmosphere under certain conditions, may become injurious to humans, animals, plants, microbial life and property. [55] These pollutants can lead to some extremely damaging effects, depending on the concentration and the duration of pollution. Some of these effects are hazardous to both the environment and humans. Many diseases and mortalities have been linked to poor air quality. For instance, the following problems have been linked to air pollution: climate change, droughts, floods, ozone layer depletion that leads to excessive UV radiation, acid rain and photochemical smog. The air pollution problem may, furthermore, have an impact on social activity in the sense of community concerns about health and quality of life. [56]

It is clear that, monitoring this dilemma, by examining the concentration of emitted gases in urban air, is becoming crucial. Moreover, workplaces also have to be monitored in order to

demonstrate this compatibility with regulatory safety conditions. A number of regulations have been established for the purpose of controlling emitted toxic gases. One example is “Control of Substances Hazardous to Health Regulations (COSHH)".

To monitor air pollution, research methodologies have been established that incorporate accurate analytical techniques for determining the concentration of most hazardous air pollutants (HAPs). These HAPs compounds are defined, as stated in United States Environmental Protection (USEPA), 2004a as, “those pollutants that cause or may cause cancer or other serious health effects, such as reproductive effects or birth defects, or adverse environmental and ecological effects”.[57] These pollutants were listed by the USEPA in 1990 [11] and include 189 different compounds, of which, 108 compounds were found to be volatile organic compounds.

The analytical methods endorsed by USEPA for these compounds have different degrees of rapidity, accuracy, stability and difficulty. What makes the monitoring of these compounds particularly challenging is that their concentrations are very low in ambient air, with most being in very low ppbv. Therefore, an appropriate level of quality control has to be employed when detecting them. The main objective of much current research aims to provide a technology with high accuracy, rapidity, and at low cost, enabling air quality surveys in different areas, for short and long sampling periods. Moreover, this technology has to be suitable for measuring concentrations of individual compounds in the presence of other volatile organic compounds. Here we describe the application of SIFT-MS technology to the problem because it has the ability to detect trace VOCs in the presence of the bulk components of air. It does this by utilising well characterised gas-phase reactions of the soft chemical ionisation reagents, H_3O^+, NO^+, and O_2^+.

2.2 Volatile organic compounds (VOCs)

Volatile organic compounds (VOCs) are generated in the atmosphere from a variety of anthropogenic sources, including petroleum refineries, factories, natural gas plants, bio-organic sources and automobile exhausts. Air pollution may also arise from natural processes such as volcanic eruptions and forest fires. Many of these compounds released into the air are toxic; 108 of them listed by USEPA are volatile. Consequently, a reliable, accurate and daily monitoring method for these toxic compounds has become essential in order to assess the human health impact.

This research was focused on monitoring benzene, toluene, ethyl benzene and xylene (BTEX), monitored particularly for air quality firstly because of their frequent association with human activities, such as industry and vehicle emissions. Secondly, monitoring is necessary because of their implications to human-health: benzene for example is known to be carcinogenic. [58] It is therefore important to minimise people's exposure to them. This, in fact, may be difficult when, for example, up to 82% of volatile emissions are from motor vehicles. [57] Guideline values of benzene and toluene compounds in New Zealand and the United States are shown in Table 5.1. Also, other VOCs including 1,3-butadiene, mesitlyene, and vinyl chloride will be monitored.

Table 5.1 Guideline value of benzene and toluene compounds.

BTEX compounds	USEPA µg/m^3	New Zealand Ambient Air Quality guide line µg/m^3
Benzene	10	10*
Toluene	400	190

*This value is the national guideline value as an annual average, reducing to 3.6 µg/m^3 by 2010

3. Compounds of interest

3.1 BTEX compounds

3.1.1 Benzene

Benzene is a volatile aromatic hydrocarbon compound. Its vapor pressure at 20ºC is 80.85Torr. Even though it is an important industrial solvent and precursor in the production of drugs, plastics, synthetic rubber and dyes, it is also a natural constituent of crude oil and one of the most hazardous compounds to health, according to the EPA. Benzene is found in the air from emissions from burning coal, oil and gasoline. It is concentrated mainly in the heavy motor vehicle traffic area and around gas stations. Further, it has been classified as a high carcinogenic risk as group 1 and A by both the Cancer Agency and USEPA.

Exposure to benzene has serious health effects. Breathing high levels of benzene can result in death, while low levels can cause drowsiness, dizziness, rapid heart rate, headaches, tremors, confusion and unconsciousness. Eating or drinking foods containing high levels of benzene can cause vomiting, irritation of the stomach, dizziness, sleepiness, convulsions and death. Since benzene is a constituent of auto exhaust and fuel evaporation, there is a need to monitor it. The US Occupational Safety and Health Administration (OSHA) has set a permissible exposure limit of (0.5 ppm of air) in the workplace during an 8-hour workday, 40-hour work week. The short-term exposure limit for airborne benzene is 5 ppm for 15 minutes. [59]

3.1.2 Toluene

Toluene, like benzene, is also a volatile aromatic hydrocarbon compound with a 21.86 Torr vapour pressure at 20 ºC. Toluene is roughly 25 times more reactive than benzene due to the methyl group, particularly for electrophilic aromatic substitution reactions. It is a common

solvent and is used as a chemical intermediate for explosives (TNT). It is also used as a carbon source for making multi-wall carbon nanotubes and is a component of gasoline.

High concentrations of toluene cause severe irritation that has the ability to destroy tissue. It causes coughing, headaches, vomiting and lung irritation. The major dangers of toluene can be explained mostly by its metabolism. As toluene has very low water solubility, it cannot exit the body via the normal routes (urine, faeces, or sweat). [60]

3.1.3 Xylene

Xylene is also known as dimethyl benzene, having three isomers. It is a volatile aromatic hydrocarbon compound with vapour pressure of: o-xylene, 4.89 Torr, m-xylene, 6.15 Torr; and p-xylene, 6.51 Torr at 20 ºC. It has widespread use as a solvent and as a component in the manufacturing process of polymers, fuels, plasticizers and as a cleaning agent for steel and silicon wafers.

High concentrations of xylene have an effect on the brain and central nervous system. High levels of xylene can cause irritation of the skin, eyes, nose and throat; problems with lungs; memory difficulties; stomach discomfort and possibly changes in the liver and kidneys. At very high levels it can cause unconsciousness and even death.

3.1.4 Ethyl benzene

Ethylbenzene is a volatile aromatic hydrocarbon with a vapour pressure of 7.08 Torr at 20 ºC. Ethyl benzene is used mainly in the petrochemical industry as an intermediate compound for the production of styrene. Styrene in turn is used for making polystyrene and plastic material. Ethyl benzene is also present in small amounts in crude oil.

Exposure to ethyl benzene for a short time results in respiratory effects, such as throat irritation and chest constriction, irritation of the eyes and neurological effects such as

dizziness. Chronic (long-term) exposure to ethyl benzene by inhalation has shown conflicting results regarding its effects on the blood. [61]

3.1.5 Early monitoring result of BTEX compounds

These compounds were monitored by Environment Canterbury agency (ECan) in Christchurch, New Zealand, in 2005. The monitoring was done by a passive sampling method followed by solvent desorption and GC-MS analysis. The results are shown in Figures 5.1 and 5.2 for the annual and the seasonal analysis of the BTEX compounds in different sites around Christchurch.[62] The ECan result showed high concentration of the relevant compounds in road sites, especially in the winter season. Benzene particularly, was found near to the guideline value (10 μg) and exceeded that in the winter season at road sites.

Figure 5.1 Monitoring results of the BTEX compounds in Christchurch as recorded in the 2005 ECan report. The dashed line in Figure A represents the current guideline value and the lower dashed line represents the 2010 guideline value.

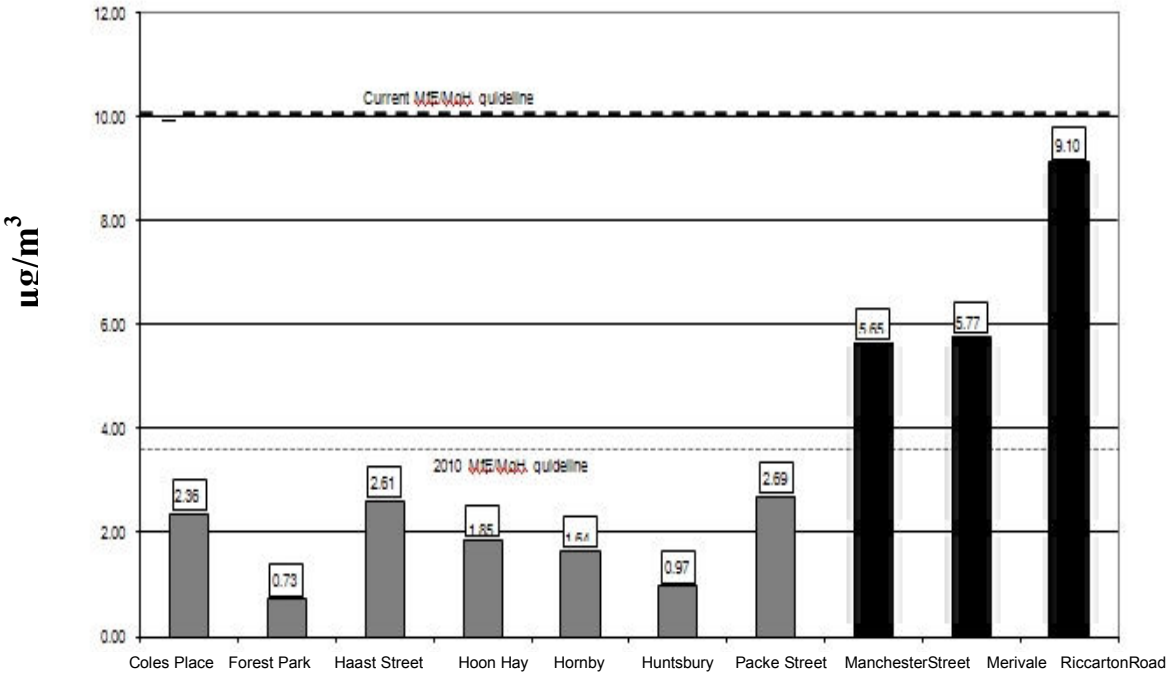

Figure 5.1.1 Annual average benzene concentrations

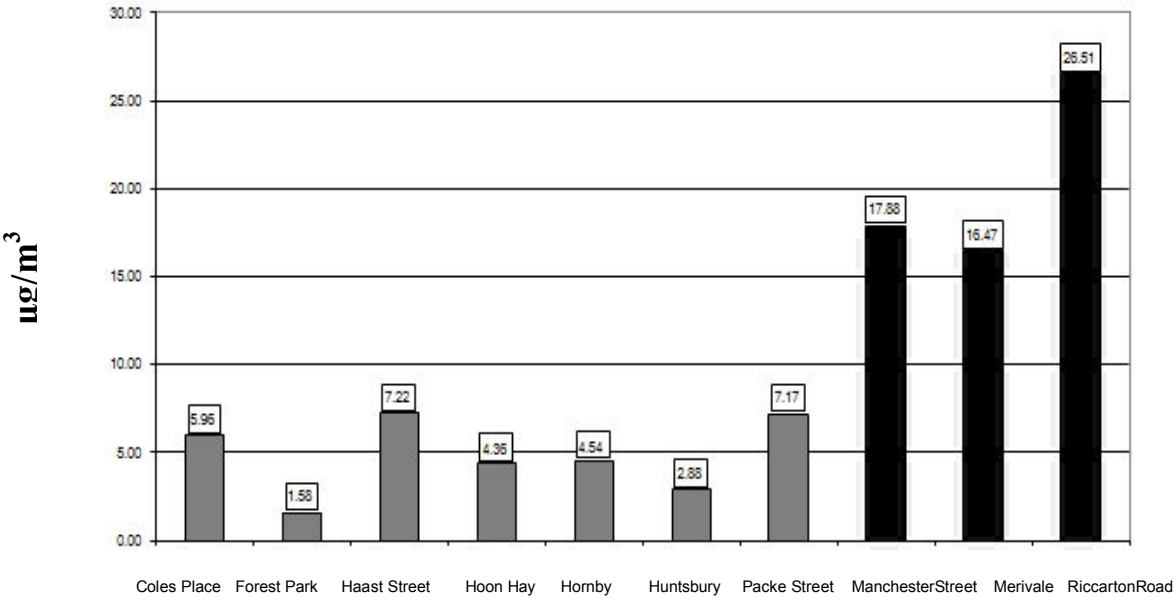

Figure 5.1.2 Annual average toluene concentrations

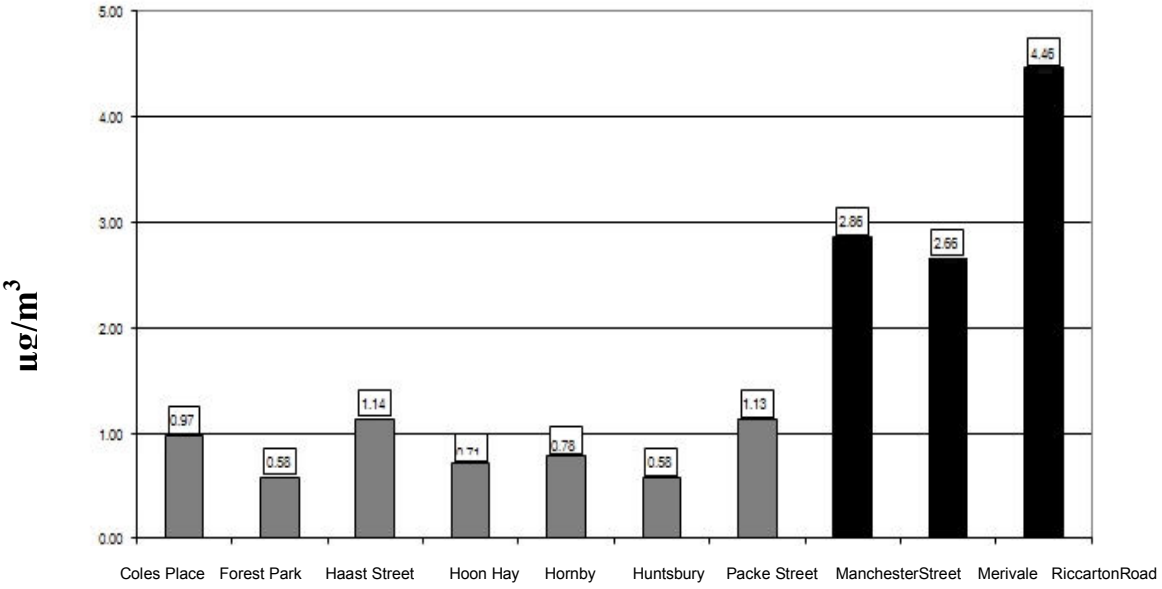

Figure 5.1.3 Annual average ethylbenzene concentrations

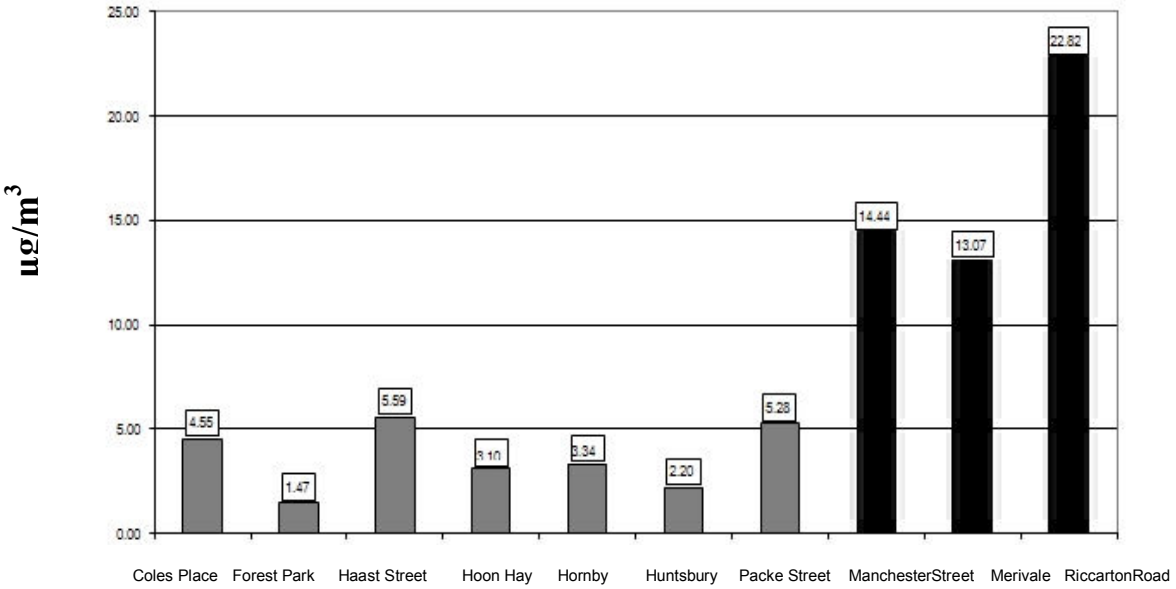

Figure 5.1.4 Annual average xylene concentrations

Figure 5.2 Seasonal analysis results of the BTEX compounds in Christchurch as recorded in the 2005 ECan report

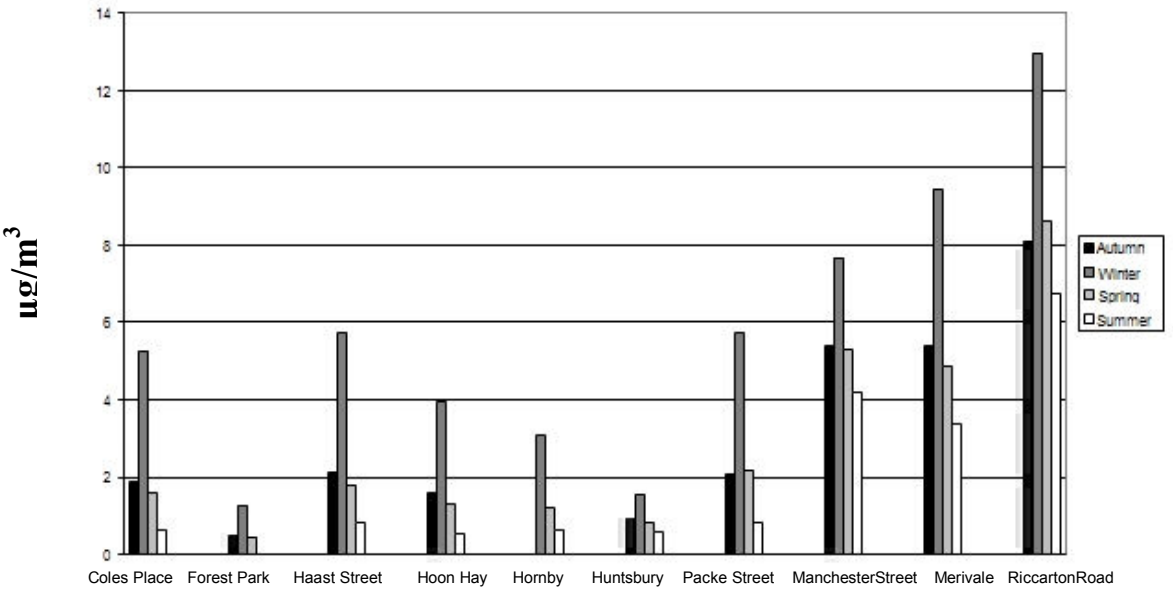

Figure 5.2.1 Seasonal (three-month) average concentrations of benzene

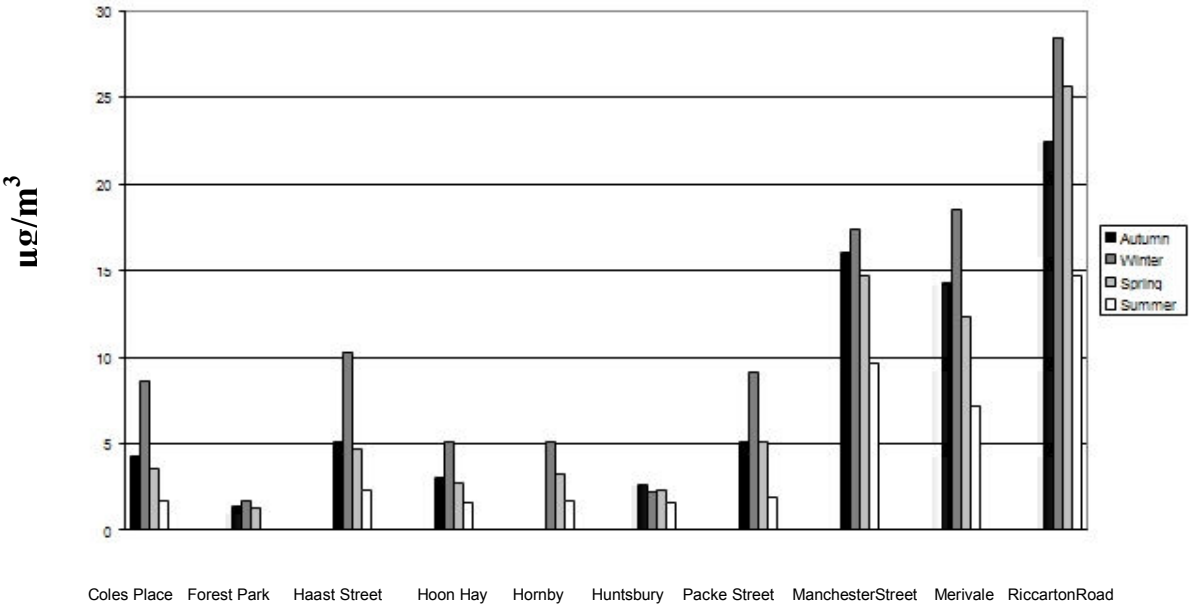

Figure 5.2.2 Seasonal (three-month) average concentrations of xylene

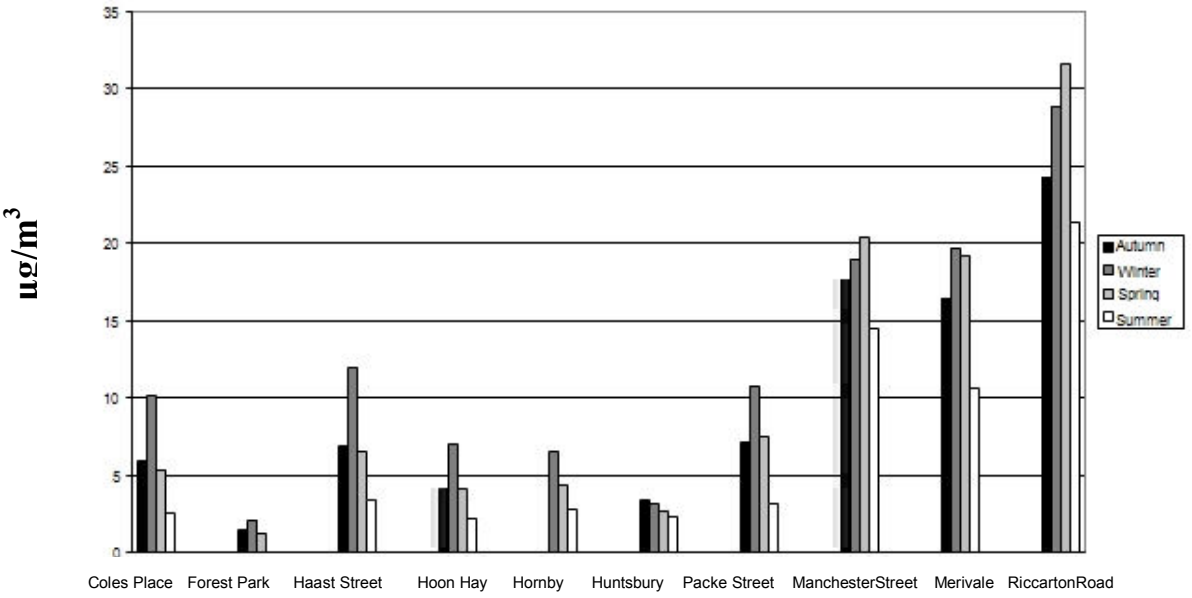

Figure 5.2.3 Seasonal (three-month) average concentrations of toluene

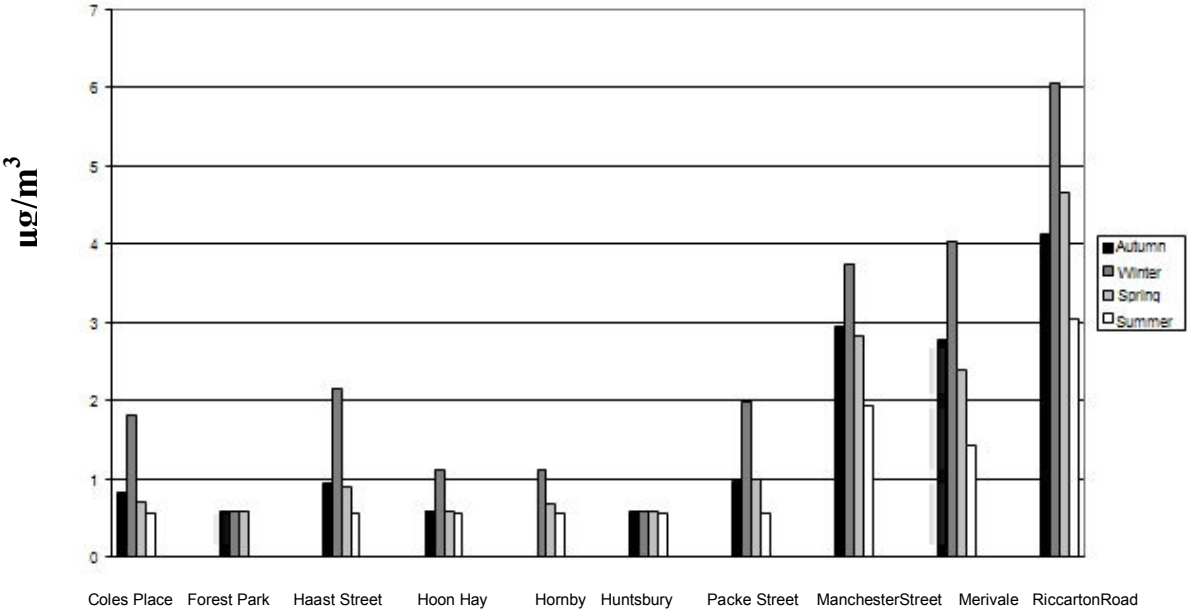

Figure 5.2.4 Seasonal (three-month) average concentrations of ethylbenzene

3.2 Other VOCs

3.2.1 Mesitylene

Mesitylene, or 1,3,5-trimethyl benzene (C_9H_{12}), is an aromatic hydrocarbon of boiling point 174.6 °C and very low freezing point of -43.8 °C. It has a vapour pressure of 1.86 Torr at 20°C. Mesitylene is commonly used as a solvent in research and industry. 1,3,5-trimethylbenzene is also a major urban volatile organic compound (VOC) which results from combustion. It plays a significant role in aerosol and tropospheric ozone formation as well as other reactions in atmospheric chemistry. Exposure to trimethyl benzene can occur through inhalation, ingestion and eye or skin contact. Workers exposed to a solvent containing 80 % trimethyl benzenes complained of nervousness, tension, anxiety and asthmatic bronchitis. In addition, the peripheral blood showed a tendency to hypochromic anemia and prolonged coagubility of blood.[62] The National Institute for Occupational Safety and Health (NIOSH) has established a recommended exposure limit for trimethyl benzene of 25 ppm (125 mg/m^3) for up to a 10-hour workday and a 40-hour work week [NIOSH 1992].

3.2.2 1,3-butadiene

1, 3-butadiene is a volatile organic compound, and it is a colourless gas of boiling point -4°C. It has a vapour pressure of 245 kPa (1837 Torr) at 20°C. It has a characteristic aromatic odour and is produced mainly by the dehydrogenation of n-butenes or by thermal cracking of light oil or naphtha. 1,3-butadiene is an important industrial chemical used as a monomer in the production of synthetic rubber. It is a starting material for many organic syntheses. It is of low toxicity at low concentrations. However, at high concentrations, irritation of the eyes, nose, mouth and respiratory tract occurs. Several studies show butadiene exposure increases risk in cardiovascular diseases and cancer. For example, 1,3-butadiene is characterized as

carcinogenic to humans by inhalation Under EPA's 1999 Guidelines for Carcinogen Risk Assessment (U.S. EPA, 1999). [63]

3.2.3 Vinyl chloride

Vinyl chloride (VC) is a colourless and flammable gas of boiling point -13.9°C and 2530 Torr vapour pressure at 20°C. It has a slightly sweet odour. The primary sources are in the chemical industry and include the manufacture of (polyvinyl chloride, ethylene dichloride, methyl chloroform, 1,1,1 trichloroethane, caprolactam, vinyl acetate and vinylidene chloride) and the plastics industry. VC is produced industrially by two main reactions: the hydro chlorination of acetylene and the thermal cracking of 1,2-dichloroethane. About 95% of the world production of VC is used for the production of polyvinyl chloride (PVC). [64] The atmospheric concentration of VC in ambient air is low, being less than 3μg/m^3. [64] Until 1974, vinyl chloride was used in aerosol spray propellant. Vinyl chloride is a known human carcinogen that causes a rare cancer of the liver. Allowed exposure limit in the workplace is 5 ppm (13 mg/m^3). [65] Under the National Model Regulations for the Control of Workplace Hazardous Substances, vinyl chloride requires health surveillance. Vinyl chloride is listed by the NOHSC as a substance under review for carcinogenicity. [65] It is classified by the NOHSC as a Category 1 carcinogen.

Table 5.2 exhibits the physical characteristics of the compounds of interest.

Table 5.2 Physical characteristics of the compounds of interest

Name	Formula	Chemical Structure	Molecular weight
Benzene	C_6H_6		78.1118
Toluene	$C_6H_5CH_3$		92.1384
Ethyl benzene	C_8H_{10}		106.1650
o-xylene	C_8H_{10} ($C_6H_4 + (CH_3)_2$)	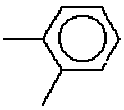	106.1650
m-xylene	C_8H_{10} ($C_6H_4 + (CH_3)_2$)	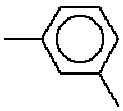	106.1650
p-xylene	C_8H_{10} ($C_6H_4 + (CH_3)_2$)	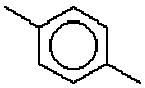	106.1650
Mesitylene	C_9H_{12}	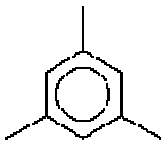	120.1916
1,3-butadiene	C_4H_6		54.0904
Vinyl chloride	C_2H_3Cl		62.4979

4. Air pollutants monitoring methods

Several methods and techniques have been used to measure toxic compounds in air. These may be classed as either active or passive methods.

Active methods can be used both for real time and non real time analysis. In real time analysis, technologies such as SIFT-MS, ATOFMs (Aerosol Time-of-Flight Mass Spectrometry), BAM (Beta Attenuation Monitors) can be used. In non real time, GC-MS and SIFT-MS techniques can be used. Passive monitoring on the other hand can be used only for non real time methods using, for example, diffusion samplers. [56] In active sampling methods, the pollutants may be collected from different sites for subsequent analysis in the laboratory. In contrast, in passive sampling methods, the pollutants are collected over a period of time and subsequently analyzed.

Recently, the determination of VOCs in the atmosphere has been accomplished using different passive methods. VOCs may be collected by canister sampling and on sorbent sampling tubes. In the sampling tube option, VOCs can be sampled by pumping air at a known rate through the substrate or by a diffusive sampling technique with many choices of sorbent. The sorbent is selected with regard to the compounds of interest. Subsequently, analytes adsorbed onto sorbents can be desorped by two popular desorption techniques: 1) using a solvent extraction technique and 2) using a thermal desorption technique. One example of SIFT-MS applied to canister sampling was that of Spanel and co-workers. [66] They used a stainless steel pipe attached to a 2 L evacuated stainless steel cylinder to collect a sample for studying engine exhaust gases. They included BTEX compounds in their analysis along with other compounds.

5. Objective of this research

The main objective of this research was to explore the SIFT-MS instrument potential to provide a reliable and rapid technique that could be used for routine air quality analysis tasks, particularly for BTEX compounds. The first part of this exercise was to demonstrate the ability of SIFT-MS to cope with the passive methodology. A known amount of these compounds was adsorbed and that was followed by online thermal desorption to the SIFT-MS instrument. The second part was to employ the use of passive sampling methodologies for sampling air pollutants as is currently done by ECan (with the exception of a solvent extraction) to monitor hazardous compounds including benzene, toluene, ethyl benzene, xylene, mesitylene, 1,3-butadiene and vinyl chloride with a specific sorbent (Tenax TA).

6. Diffusion sampling

6.1 Overview

A diffusive sampler is a device that is capable of taking samples of gas or vapour pollutants from the atmosphere, at a rate controlled by a physical process, such as diffusion through a static air layer. This takes place by permeation through a membrane or diffusion cap, without the active movement of the air through the sampler. The analyte is then adsorbed on the specific sorbent substrate. [67] Measuring the VOCs by using a diffusive sampler has been used frequently. It is one of the most convenient and widely employed ways to monitor VOCs in ambient air. Figure 5.3 shows examples of passive Tenax TA sorbent tubes that were used in this research. This method was originally developed for workplace monitoring of organic vapour and ambient air quality. [68] Nowadays, determination of VOCs is typically performed with passive badges, air canister sampling and sorbent tubes. For instance, the environment Canterbury agency (ECan), in New Zealand, uses this technique

for measuring the concentration of these compounds using a solvent extraction technique. Furthermore, the environmental measuring group, in Sheffield, for example, used it for monitoring aromatic hydrocarbons in different sites.

Figure 5.3 Passive sampling tubes, stainless steel and glass Tenax sorbent tubes.

Diffusive sampling offers the following advantages: it is simple and convenient to use and re-use, not expensive, well characterized, appropriate for a range of analytes, user-friendly and can be operated by an inexperienced person.

They also have some disadvantages in that it is important to ensure adequate air movement. They are not suitable for particulates and sampling rates (uptake rates) are not always available. Further, the use of the sampling tube technique is usually limited to compounds that are retained strongly by the sorbent.

Air sampling in this research is done using passive sampling tubes. These tubes have been evaluated for their potential for ambient air monitoring for BTEX compounds [68] and have shown good accuracy and reproducibility. The passive sampling method using sampling tubes, will be used for the compounds mentioned in section (3) coupled with SIFT-MS analysis. These compounds have also been measured using passive sampling and GC-MS.

6.2 Passive sampling tubes and Sorbents

6.2.1 Passive sampling tubes

There are two types of tube samplers; a radial diffusive sampler and an axial diffusive sampler. The radial diffusive sampler has a cylindrical diffusive surface with a short diffusive path (Figure 5.4.a). It has an effective sampling rate, typically 100 times that of common axial tubes due to the high diffusive surface area (Figure 5.4.b). Therefore, it can be used for airborne VOCs analysis for a short exposure time of 1-6 hours. [69]

In contrast, the axial diffusive sampler is a more popular choice than the radial diffusive sampler. In the axial diffusive samplers (Perkin-Elmer) used in this work, sorbent tubes are constructed of stainless steel, 6.4 mm OD, 5.0 mm ID and 89 mm long. The tubes are packed with preconditioned sorbent, and the sorbent is retained within the desorber heated zone. The critical air gap is defined by the distance between the internal stainless steel gauze, retaining the sorbent and the end of the tube. This critical air gap is 14 -14.6 mm for the Perkin-Elmer tubes. [70] The characteristics of the axial tube are given in Figure 5.4.c.

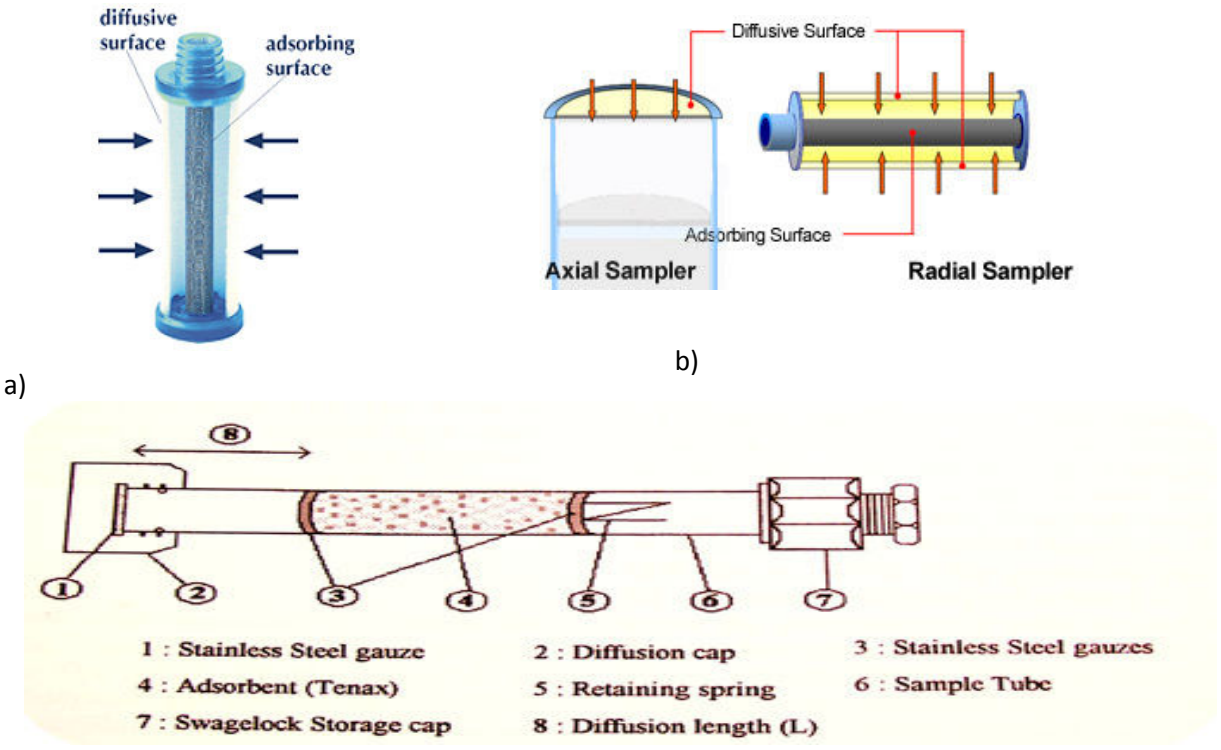

Figure 5.4 a) Radial diffusive sampler design. [71] b) Diffusive surface comparison between axial and radial samplers. c) Schematic illustration of the Perkin-Elmer axial passive sampling tube.[72]

6.2.2 Sorbents

A sorbent is a material used to adsorb either liquids or gases. Different sorbent substrates may be used in the tubes such as Tenax TA, Tenax GR, Charcoal, Porapak and Spherocarb. Tenax TA was selected as the sorbent to be used in this research. Tenax is a porous polymer based on 2.6-diphenylene oxide. It was widely adopted during the 1970s as a more reliable sorbent than charcoal for ppb levels (Barkley et al. 1980, Krost et al. 1982) [73] [74]. It has low background contamination, where the minimum concentration that can be detected is restricted to the blank concentration level of the substrate. Moreover, it is stable at temperatures up to 250 ºC, allowing thermal desorption instead of solvent desorption, and it can also be used many times. Tenax is found to be appropriate for aliphatic hydrocarbons from C6-C10 and aromatic compounds from benzene to cumene with good long-term stability [75] which is essential to this application. [76] The applications of passive sorbent tubes to monitoring known concentration of the BTEX compounds, gives confidence to the method proposed. Both the EPA and NIOSH specify the use of Tenax in their standard methods. [77] Tenax TA is especially useful for the purging and trapping of volatiles from high moisture content samples, including the analysis of volatile organic compounds in water, due to its low affinity for water and its low breakthrough volume for water [77] as shown in Table 5.3. Breakthrough volume is defined as the volume of carrier gas that will purge an analyte through one gram of adsorbent resin in an adsorption tube at specific temperature. Table 5.3 specifies the breakthrough volume data in litres per gram of resin and the volume of gas required to elute the organic compound off one gram of resin at the indicated temperature. The blue highlighted areas indicate an acceptable breakthrough value for the trapping of the specified organic compound at that temperature, with a volume greater than 10 litres per gram of resin. The red highlighted areas indicate a good temperature to assure

complete desorption of the organic compound off the adsorbent resin, during the thermal desorption process with breakthrough volume less than 0.01 litres per gram of resin. [79]

Table 5.3 Tenax TA breakthrough volume for the compounds of interest**.**

Temperature	0	20	40	60	80	100	120	140	160	180	200	220
Water	0.130	0.065	0.035	0.018	0.010	0.006	0.004	0.002	0.001			

Temperature	0	20	40	60	80	100	120	140	160	180	200	220	240	260	280	300
Benzene	410	70.0	18.0	8.10	0.86	0.268	0.099	0.040	0.018	0.009	0.004	0.002	0.001			
Toluene	8,100	400	62.0	12.5	2.70	0.806	0.250	0.086	0.035	0.015	0.007	0.003	0.002	0.001		
Ethylbenzene	12,500	1,400	200	33.0	7.30	2.00	0.611	0.186	0.065	0.027	0.011	0.005	0.003	0.001		
p-Xylene	13,500	1,550	230	42.0	8.50	2.30	0.630	0.198	0.067	0.028	0.011	0.005	0.003	0.001		
m-Xylene	13,500	1,550	230	42.0	8.50	2.30	0.634	0.195	0.069	0.028	0.011	0.005	0.003	0.001		
o-Xylene	14,500	1,650	250	45.0	9.00	2.50	0.719	0.229	0.080	0.033	0.014	0.006	0.003	0.002	0.001	
1,3,5-Trimethylbenzene	50,000	5,000	600	100	20.0	5.00	1.30	0.402	0.129	0.048	0.019	0.008	0.004	0.002	0.001	
Vinylchloride	1.70	0.550	0.180	0.063	0.025	0.012	0.006	0.004	0.002	0.001						

Tenax, however, shows some drawbacks that include artifact formation of several chemicals. These artifacts correspond to peaks that appear as benzaldehyde and phenol for example, when using GC-MS. [78] Moreover, Tenax has an inability to retain very volatile organic chemicals such as vinyl chloride and methylene chloride.

More volatile molecules must be sampled on stronger sorbent substrates such as Porapak or charcoal. Multi sorbent systems also can be used. Tenax and charcoal, for example, can be used together, where Tenax collected the bulk of VOCs and the activated charcoal collected those analytes having greater volatility that had broken through the Tenax. [78]

6.3 Using passive sampling for ambient air monitoring

Passive sampling is a rapidly expanding technique in environmental monitoring. It has been adapted for ambient air monitoring by Choo-Yin and Layton-Matthews (1987). [79] In ambient air monitoring the sampling device is exposed to air for a certain time period. The

analytes migrate into the sampler by diffusion and are collected on the sorbent. It has a relatively low sampling rate. For environmental applications, it may be necessary to expose the sampler for several days, to collect sufficient material for accurate analysis. In conventional environmental monitoring technology, it is common to sample many liters or even cubic metres of air in order to have sufficient sensitivity. Sampling with an electrically driven pump is impractical for more than a day or so without a dedicated power supply.

The adsorbed analytes are then desorped from the sorbent by heat in a thermal desorption (TD) apparatus and after desorption are transferred by inert carrier gas into an analysis instrument such as GC-MS and SIFT-MS. This method is valid for analytes in the concentration range between 0.2 to 100 $\mu g/m^3$ for samples of 2.5L of air. [76] Also, it is valid in an atmosphere containing up to 95% humidity. [76] The sampling rate or alternatively, the uptake rate should be determined by prior exposure in a standard atmosphere. An air concentration of an analyte can therefore be deduced from the measured mass uptake.

6.4 Uptake rate

An uptake rate is a quantity which is determined under standard conditions. It is used to convert the results of mass uptake obtained during the sampling into a concentration. It can be defined as:

$$\text{Uptake rate} = \frac{mass\ uptake}{(\text{pollutant concentration}) \times (\text{exposure time})}$$

The uptake rate is measured conveniently in ng $(ppm)^{-1}$ $(min)^{-1}$, and it is equivalent to ml $(min)^{-1}$, where the volume term refers to the volume of air, from which the mass of pollutant has been extracted by the sampler. [67] The uptake rate of a diffusive sampler is ideally, a constant. This rate depends mainly on the geometry, dimensions of the sampler and the individual pollutant vapour, which has a particular diffusion coefficient in air. However, it

may vary slightly with changes in pollutant concentration, exposure time, atmospheric temperature, pressure and humidity. [67] The concentration of an analyte in air can therefore be deduced from a measured mass uptake, if the time of exposure is known.

If diffusive rate data is not available and if there is no time to measure or calculate an uptake rate, then a diffusive uptake rate may be calculated from diffusion coefficients according to the equation: [80]

$U = A \times D / l$

U= uptake rate in ml/min

A= cross-sectional area of the diffusion path, or equivalent sorption surface, (cm^2)

D= diffusion coefficient of analyte ($cm^2.min^{-1}$)

l= length of static air layer in sampler (cm)

Uptake rates in ml/min and ng. ppm^{-1}. min^{-1} are related by

U`= U*M*293*P/ 24.5* T* 101 [81]

Where:

U`= theoretical diffusive uptake rate in $ng.ppm^{-1}$ min^{-1}

M= molecular mass of analyte ($g.mol^{-1}$)

P= pressure of the sampled atmosphere during sampling, (kPa)

T= temperature of the atmosphere sampled (K)

The experimentally determined uptake rates are different from the theoretical value, since no adsorbent can act as a perfect sink. Therefore, uptake rates should be determined experimentally.

6.5 Analyte concentration

In passive sampling methods, the concentration of the analyte in the sampled air can be calculated in $\mu g/m^3$ by the following equation:

C= F-B/ U* t U= uptake rate in ml/min

or in ppm

C= F-B/ U* t U= uptake rate in ng $ppm^{-1}min^{-1}$

Where F= mass of the analyte present in the actual sample, B= mass of analyte present in the blank, U= uptake rate, t= time of exposure in minutes, C= concentration in $\mu g/m^3$ or ppm depending on the version of U used.

If conditions of pressure and temperature are used that differ from the standard of 101.3 kPa and 298K during collection of the sample, C can be calculated by this equation:

C_{corr}= C. (101/P)*(T/298)

Where P is the actual pressure in kPa and T is the actual temperature in K.

7. Thermal desorber (TD)

Figure 5.5 Thermal desorber ATD 400

A thermal desorber is essentially a straightforward gas extraction process. It is a technique that is used to extract volatiles from a non-volatile matrix, by heating the sample in a stream of inert gas. The volatiles are then swept to the instrument that is used for analysis such as a GC-MS or SIFT-MS. It offers great versatility in contrast to the conventional solvent extraction method, in that it provides improvement in detection limits, a reusable sample tube, no chromatographic interference from solvent or solvent artifacts and a lower cost per analysis. It has the ultimate advantage of avoiding the uses of solvent extraction, which makes the technique more sensitive and environmentally friendly.

The thermal desorber model used here is the ATD 400 (Figure 5.5). In the process of operating the TD, an automatic sequence of operations takes place. Each sample tube is taken from the carousel; it is uncapped and then sealed in the carrier gas stream. Then the TD performs a leak test on the sample tube and the cold trap before the thermal desorption process starts. This sequence ensures that the tube has been sealed correctly and there is no leak in the system. A carrier gas (helium) is also used to extract the

volatiles from the headspace of the heated sample tube and the heated trap. After the sample tube has been leak tested and purged of air, it is heated for a period. The volatiles released from the sample are swept by the stream of inert gas to the cold trap, where they are reconcentrated. At the end of this period, the cold trap is heated rapidly to release the volatiles to the analysis instrument line when they are carried by the helium carrier gas to the SIFT-MS. Lighter and poorly adsorbed compounds are eluted first and pass to the SIFT-MS instrument quickly. More strongly adsorbed compounds are released more slowly and are eluted later.

8. Reactions of SIFT-MS reagent ions with the compounds of interest

After transferring the sample from the TD carried by the carrier gas to the SIFT-MS, the reagents ions (H_3O^+, NO^+, O_2^+) react with the relevant compounds. These relevant compounds react via proton transfer reaction; charge transfer; NO^+ association and dissociative electron-transfer reactions, as illustrated in the equations below. The number in brackets illustrates the product ratio and the collision rate coefficients.

Benzene

$C_6H_6 + H_3O^+ \longrightarrow C_6H_6.H^+ (1) + H_2O$ k= 1.9 (1.9)

$C_6H_6 + O_2^+ \longrightarrow C_6H_6^+(1) + O_2$ k= 1.6(1.6)

$C_6H_6 + NO^+ \longrightarrow C_6H_6^+ (0.85) + NO$ k=1.5(2.6)

$\longrightarrow C_6H_6.NO^+ (0.15)$

Ethyl benzene

$C_8H_{10} + H_3O^+ \longrightarrow C_8H_{10}.H^+ (1) + H_2O$ k= 2.4 (2.4)

$C_8H_{10} + O_2^+ \longrightarrow C_8H_{10}^+ (0.7) + O_2$ k= 2 (1.9)

$\longrightarrow C_7H_7^+ (0.3)$ + products

$C_8H_{10} + NO^+ \longrightarrow C_8H_{10}^+ (1) + NO$ k= 2 (2)

Toluene

$C_7H_8 + H_3O^+ \longrightarrow C_7H_8.H^+ (1) + H_2O$ k= 2.2 (2.2)

$C_7H_8 + O_2^+ \longrightarrow C_7H_8^+ (1) + O_2$ k= 1.8 (1.8)

$C_7H_8 + NO^+ \longrightarrow C_7H_8^+ (1) + NO$ k= 1.7 (1.8)

Xylene

$C_8H_{10} + H_3O^+ \longrightarrow C_8H_{10}.H^+ (1) + H_2O$ k= 2.3 (2.3)

$C_8H_{10} + O_2^+ \longrightarrow C_8H_{10}^+ (0.8) + O_2$ k=1.9 (1.9)

$\longrightarrow C_7H_7^+ (0.2)$ + products

$C_8H_{10} + NO^+ \longrightarrow C_8H_{10}^+ (1) + NO$ k=1.9 (1.9)

Mesitylene

$C_9H_{12} + H_3O^+ \longrightarrow C_9H_{12}.H^+ (1) + H_2O$ k= 2.3(2.3)

$C_9H_{12} + O_2^+ \longrightarrow C_9H_{12}^+ (0.95) + O_2$ k=1.9(1.9)

$\longrightarrow C_8H_9^+ (0.05)$ + products

$C_9H_{12} + NO^+ \longrightarrow C_9H_{12}^+ (1) + NO$ k=1.9(1.9)

1,3-Butadiene

$C_4H_6 + H_3O^+ \longrightarrow C_4H_6.H^+ (1) + H_2O$ k= 1.4

$C_4H_6 + O_2^+ \longrightarrow C_4H_6^+ (0.7) + O_2$ k=1.2

$\longrightarrow C_3H_3^+ (0.3)$ + products

$C_4H_6 + NO^+ \longrightarrow C_4H_6^+ (1) + NO$ k=1.2

Vinyl chloride

$CH_2CHCl + H_3O^+ \longrightarrow C_2H_3(Cl^{35}).H^+ (0.75) + H_2O$ k= 2

$\longrightarrow C_2H_3(Cl^{37}).H^+ (0.25) + H_2O$

$CH_2CHCl + O_2^+ \longrightarrow C_2H_3(Cl^{35})^+ (0.75) + O_2$ k=1.7

$\longrightarrow C_2H_3(Cl^{37})^+ (0.25) + O_2$

$CH_2CHCl + NO^+ \longrightarrow C_2H_3(Cl^{35}).NO^+ (0.75) + NO$ k= 0.0093

$\longrightarrow C_2H_3(Cl^{37}).NO^+ (0.25) + NO$

The analysis results of this study were based on the average count rate value of the reactions of the reagent ions that are indicated next.

Benzene:	NO^+ and O_2^+	, Xylene :	$H_3O^+$and NO^+	, Vinyl chloride:	O_2^+
Toluene:	H_3O^+,$NO^+$and O_2^+	, Mesitylene:	H_3O^+ and NO^+		
Ethylbenzene:	H_3O^+ and NO^+	, 1,3-butadiene:	NO^+		

9. Gas chromatography – Mass spectrometry (GC-MS)

In this part of the study, TD was coupled to a GC-MS (GC-17A, QP 5000 mass spectrometry), where the thermally desorbed organic components were analyzed. The correlation of results between the GC-MS and SIFT-MS provided validity assurance. As previously described, the VOCs are thermally desorbed in the TD and transferred to a GC-MS. The GC instrument then separates the components of a mixture over a period of time. Only compounds that are volatile or can be made volatile can be analysed by the GC-MS. This involves a sample being vaporised after injection onto the head of the chromatographic column. The sample is transported through the column by the flow of inert gas: helium in this case. The column itself contains a stationary phase, which is adsorbed onto the surface of an inert solid. Two types of column can be used in the GC: capillary and packed columns. A capillary column is a column that has walls coated by a thin layer of a non-volatile substance. A packed column on the other hand, has a thin layer of compound, coated onto an inert solid that is added into the column. These columns allow volatiles to be restricted selectively by the stationary phase. A slow increase in the column temperature then allows gradual release of the volatile, through the column to the mass spectrometer (MS). The MS measures the mass-to-charge ratios (m/z) of the gas phase ions that are produced by electron-impact ionisation (IE) (typically > 0 eV) of the analyte molecules, unlike SIFT-MS that uses much softer ionization.

The GC-MS results can be presented as a chromatogram, showing the abundance and the retention time, which is the time each compound remains on the GC column. The retention time is a valuable aid to the identification of individual compounds and is recorded for all analytes in a sample. This chromatogram can then be searched by using mass spectral interpretation techniques of the MS software library. Data matching with the library for retention time and m/z ratio, allows identification of the analyet.

10. Experimental procedure

10.1 Preparing the TD-SIFT-MS instruments for the study

First, the kinetic parameters for each of the relevant compounds were calibrated for the SIFT-MS instrument using standard gas solutions. Calibration gives a more accurate response for each analyte. Mesitylene and ethyl benzene were calibrated using permeation tubes with the unhumidified permeation oven. The remaining analytes, were calibrated using a standard gas mixture containing them, produced from Scotty special gases.

Second, the TD was installed and connected to the SIFT-MS. It was coupled to the SIFT-MS and the carrier gas, through the TD, was adjusted to a suitable flow rate that was approximately equal to the sample flow rate in the SIFT-MS of about 150 ml/min. The transfer line temperature was set to 170 ^{o}C, which was compatible with the sorbent tubes desorption temperature as stated in the manufacturer's procedure document. A second TD was coupled to the GC-MS and was used in parallel to the TD-SIFT-MS for cross validation between techniques.

All the sorbent tubes were conditioned before use as described next. Moreover, a quantitative assessment of TD-SIFT-MS using an adsorbed gaseous standard on to the sorbent tube was explored. Further, a preliminary passive tube experiment, where the tube was left for a month at the Syft company's backyard, was performed to ensure useful data could be obtained. In addition, workplace monitoring was performed in parallel with real time monitoring, for

added assurance of the quantitative validity of the results using passive sampling and TD-SIFT-MS.

10.1.1 Sorbent tubes conditioning

Prior to use, the sorbent tubes were conditioned following the manufacturer's procedure for 30 minutes at 220°C. Then, two tubes were chosen arbitrarily and analyzed to ensure the blank levels were acceptable for the intended application. The blank level is acceptable, as mentioned in the Health and Safety Executive Occupational Medicine and Hygiene Laboratory, MDHS72, 1993, if it is not greater than 100 ng (0.1µg).[82] It was difficult to reduce the concentration below the minimum level, by repetitive conditioning and desorption. Figure 5.6 elucidates the mass of the relevant compounds before and after conditioning. It illustrates the blank level value of these compounds, which were at acceptable levels, lower than 100 ng.

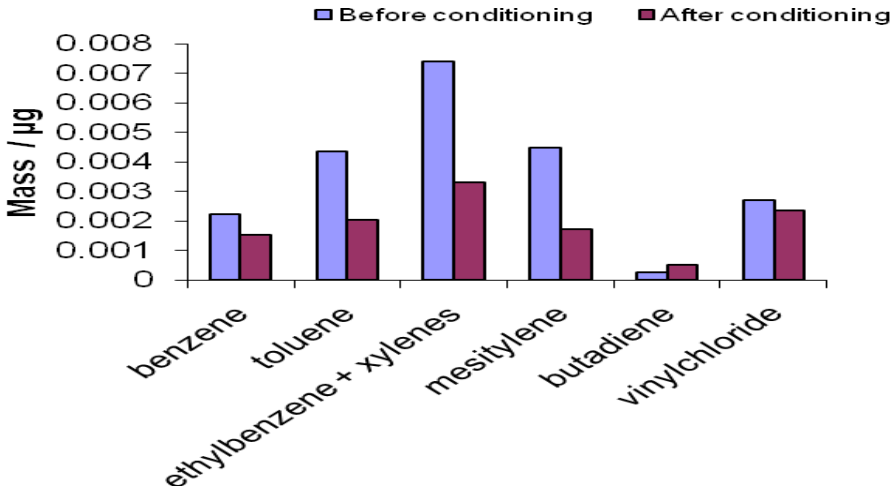

Figure 5.6 The residue of the compounds of interest in the tube before and after the conditioning process.

10.1.2 Quantitative assessment of TD-SIFT-MS

The TD-SIFT-MS system was quantitatively assessed by using sorbent tubes spiked with known amounts of the compounds of interest: benzene, toluene, ethyl benzene and xylene and then analyzed by SIFT-MS. Three sorbent Tenax TA tubes were used in this measurement. The spiking was performed using a small battery-powered pump with a flow of 100 ± 5 ml/min. These tubes were analysed at the end of the spiking period, using the TD-SIFT-MS. Moreover, a second breakthrough tube was used and was analysed at the end for more indication about the gas breakthrough volume and the deposition potential. The breakthrough tube showed evidence of some breakthrough of the gas to the second tube, in the range of about 15% maximum breakthrough with a 100 ml/min pump flow rate and about 7% breakthrough with a 50 ml/min flow rate. However, in air monitoring applications the diffusive uptake rate, which is equal to the flow rate, is very much lower.

10.1.2.1 Analysis

After spiking, the sorbent tubes were placed in a compatible TD apparatus. The tubes were then heated to displace the adsorbed compounds, which were transferred to the SIFT-MS by means of a helium carrier gas. Figures 5.7 and 5.8 display the outcome profile result as it appeared in the SIFT-MS instrument screen for a spiked sample tube and for a conditioned tube respectively.

The calculation of the mass of each analyte adsorbed was done by calculating the area under the curve (adsorption area) for each analyte as shown next.

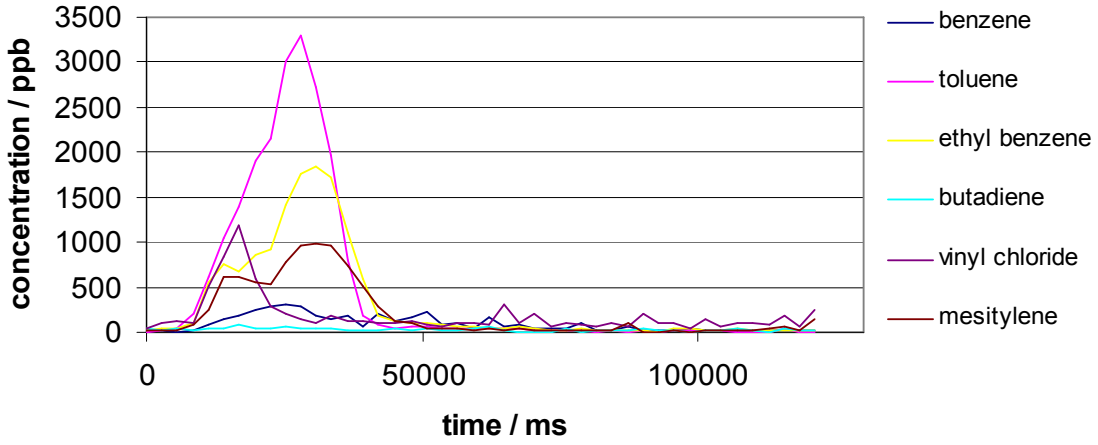

Figure 5.7 TD-SIFT-MS desorption spectrum for a sampled spiked Tenax TA sorbent tube.

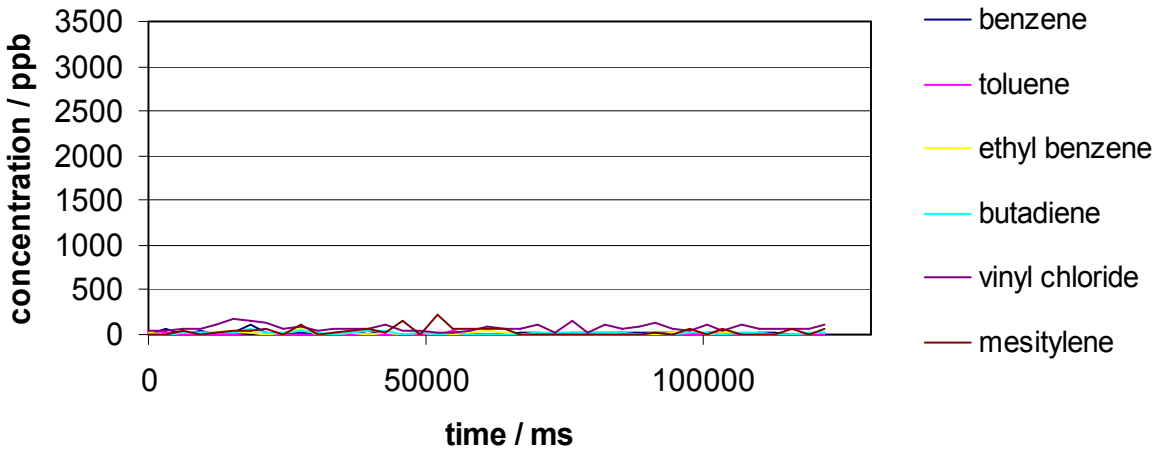

Figure 5.8 SIFT-MS desorption spectrum for conditioned Tenax TA sorbent tube.

10.1.1.1 Calculation of concentration

10.1.1.1.1 Calculation of sample concentration from desorption profile

First, the concentration of analyte represented by a product ion count in the flow tube is given by: [83]

$$[\mathrm{A}] = \frac{1}{t}\,\frac{\sum_{1}^{n} I_{si}\, d_i}{\sum_{1}^{n} k_i\, I_{pi}\, d_i}$$

Where: I_{pi} = reagent ion counts (counts per second, cps),

I_{si} = product counts over all channels,

d_i = diffusion factor,

t = l/v_i = reaction time l= the reaction length, v_i= the ion velocity,

v_g = the carrier gas velocity in m s^{-1}

$$v_g = \frac{4}{\pi d^2\ [\mathrm{m}^2]}\,\frac{\text{gas flow rate [Torr } \mathbf{m^3}\ \mathrm{s}^{-1}] \times T_{gas}\ [\mathrm{K}]}{P_{flow\ tube}\ [\mathrm{Torr}] \times 273\ [\mathrm{K}]}$$

[A] = analyte concentration in molecules cm^{-3}

At this point, [A] is a real time measurement of the concentration. It can be used to calculate concentrations in ppb for:

1. A gas sample introduced directly into the SIFT inlet (the standard procedure).
2. A sample that has been desorbed from a sorbent tube, using the procedure described next.

The calculation of mass of analyte released from the sorbent tube to the flow tube was made as follows:

Analyte molecules A were released from the sorbent tube over time t_d (desorption time in seconds) of the measurement. In this calculation, we used the mean concentration [A] for the duration of the desorption SIFT-MS measurement sequence.

In time t_d, the volume of gas that passed through the flow tube was

$$V_g\ [\mathrm{m}^3] = 0.25\pi\, d^2\, t_d\, v_g.$$

Hence, the number of moles of analyte was given by,

$$n_A = [\mathrm{A}]_{\mathrm{mean}} \times V_g \times 10^6 \quad \text{molecules (the } 10^6 \text{ factor converts m}^3 \text{ to cm}^3\text{)}$$

$$= \frac{[\mathrm{A}]_{\mathrm{mean}} \times V_g \times 10^6}{6.022\times10^{23}} \quad \text{moles}$$

The mass of analyte detected was hence:

$$m_A = n_A\, M_r(A)$$

$M_r(A)$ is the molar mass of the analyte.

10.1.1.1.2 Calculation of mass of analyte deposited on the sorbent tube

The deposited mass on the sorbent tube was calculated from the total number of moles using the following equation:

$n_{gas} = \frac{1.013*10^5 * V_s}{8.314 * T_s}$ the total number of moles of gas passed through the tube

where V_s is the volume of the gas passed through the tube [m^3]

Subsequently, the total number of moles of analyte passed through the tube

$n_{analyte} = C_{analyte} \times n_{gas}$

The mass of analyte deposited was

$m_{analyte} = n_{analyte} \times M_{analyte}$ where M is the analyte molecular weight

10.1.1.2 Result

The mass concentration of analyte measured on the sampling tube was found as described in the previous calculations. The recovery of analyte after desorption was obtained from these spiked tubes. The spiked tubes showed different recovery amounts ranging from 126- 89 % with a total maximum uncertainty of ± 27% of the deposited mass as shown in Figure 5.9. This data indicated the validity of the SIFT-MS technique for use in combination with passive sampling in quantitative analysis. Furthermore, the limit of detection (LOD), which was determined for the relevant compounds in terms of mass (µg) and based on 6 analyses, is displayed in Table 5.4.

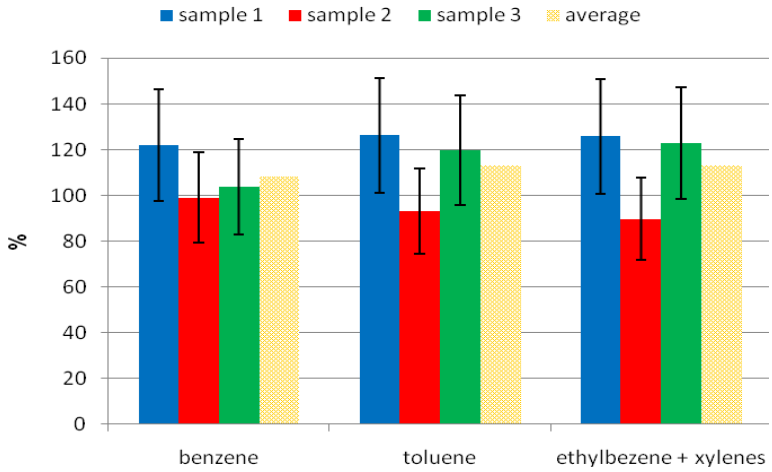

Figure 5.9 Recovery of relevant analytes and their average with experiment uncertainty of ± 27%

Table 5.4 Measured LODs for passive conditioned sorbent in a stainless steel tube: (Conditioned tube-TD-SIFT-MS)

LOD (µg)	Benzene	Toluene	Ethyl benzene	Mesitylene	Butadiene	Vinyl chloride
	0.0054	0.0084	0.0052	0.0034	0.001	0.0048

10.1.2 Air sampling assurance test

Air sampling experiments were performed for three different periods: 11 days, 25 days , and 33 days, by passive sampling at the Syft Technology company's backyard. The purpose of these experiments was to gain an insight into the methodology required and to ensure that useful data could be obtained using this technique. The result was satisfactory in that measurable amounts of analyte were deposited in a month period as illustrated in Figure 5.10. In addition, it was observed that the sorbent tubes were not able to adsorb any vinyl chloride or 1,3 butadiene, as was certified in the literature, due to their high vapour pressure and their very low breakthrough value (Table 5.3). This result provided more confidence in the use of this method of passive sampling, for monitoring air quality in Christchurch, particularly for BTEX compounds.

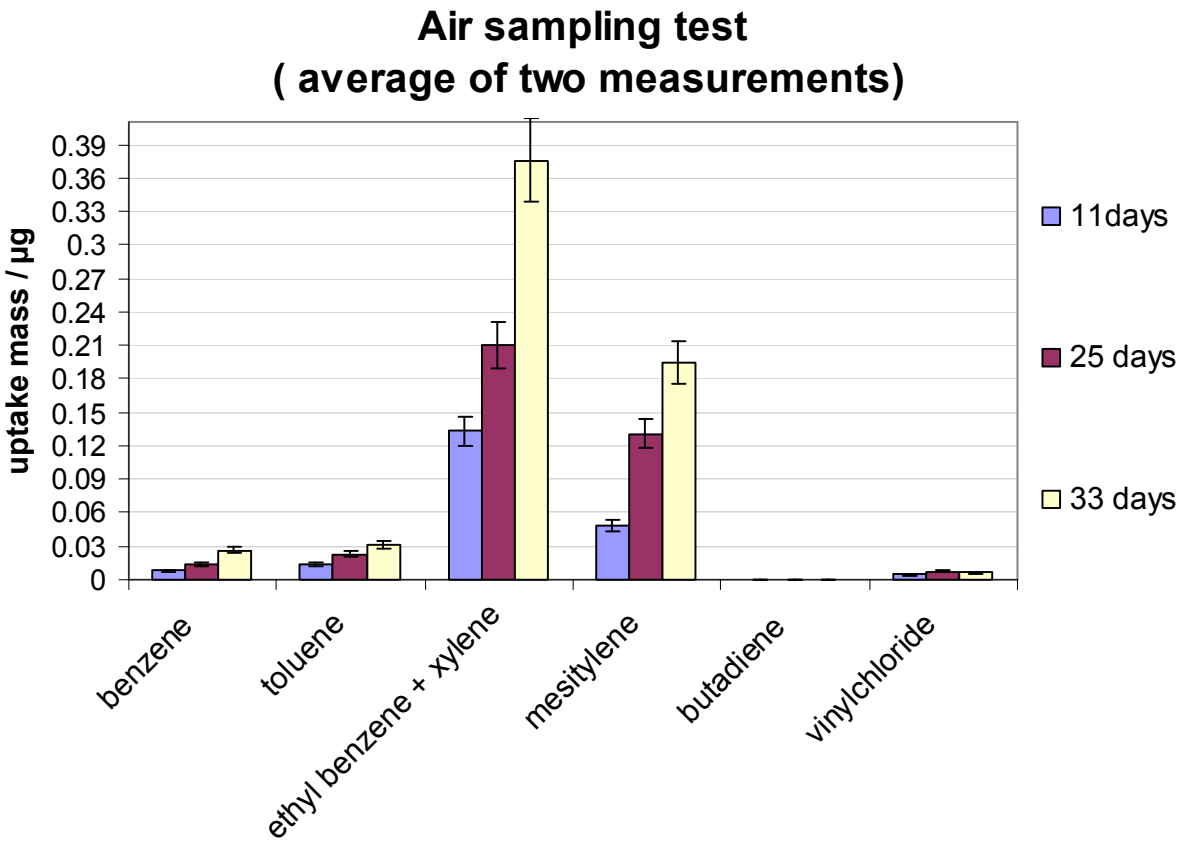

Figure 5.10 Air monitoring test at Syft Company's backyard storage for period of 11, 25 and 33 days.

10.1.3 Workplace monitoring test

Workplace sampling is typically done with a sampling time between 30 minutes to 8 hours. It has been recognized as an efficient technique for personal exposure assessment in occupational hygiene. Ambient air sampling time is, on the other hand, prolonged: typically 1-4 weeks are needed.

A workplace-monitoring test was performed using a pump sampling technique in the SIFT-MS instruments laboratory. A real time and passive time analyses were carried out in parallel to each other. Different glass sorbent tubes were used in this experiment: they were as follows: a) Tenax TA single bed sorbent b) Anasorb GCB1 and Anasorb CMS bed sorbents. c) Tenax and Carbopack bed sorbents. Each sorbent tube was placed next to the SIFT-MS inlet as shown in Figure 5.11 for the best representation of the real time sample, after being conditioned for 15 min at 220 °C. The pump was used to withdraw a sample from the lab air into the sorbent tube with 25 ml/min flow rate. In this experiment, the pump flow rate was equivalent to the uptake rate.

The sample was collected by the sorbent tube for 60 min. Likewise, the SIFT-MS instrument was programmed to take a sample from the lab air every 10 min over the same period as the passive sample was obtained.

The main objective of this experiment was to show the validity of quantitation using passive sampling, in comparison to the real time analysis. Toluene in particular, was the most attractive monitoring analyte due to its elevated concentration in the lab air, that was significantly above the LOD limit. Figure 5.12 shows the result of the real time and passive time analysis of the lab air within 60 min with different sorbent beds. The results obtained from passive sampling were acceptably close to real time analysis, particularly with the

Tenax TA single sorbent. Nevertheless, the passive sampling method was not able to adsorb the analytes vinyl chloride and 1,3 butadiene which were apparent in the real time sampling test experiment. What was unexpected was that the passive sampling also failed to absorb benzene, while other BTEX compounds were adsorbed efficiently, especially with the Tenax sorbent as shown in Figure 5.12. The absence of benzene in this passive sampling experiment may be attributed to the relatively high measured concentration of benzene in the tube as compared to the concentration in the lab and also to the low breakthrough volume of benzene as shown in Table 3 previously. The passive sampling total uncertainty was about ±27% whereas the real time SIFT-MS uncertainty is believed to be within ±10%.

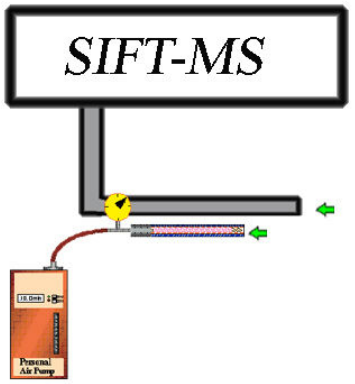

Figure 5.11 Sketch diagram displays the passive sampling location next to the SIFT-MS.

To conclude, this experiment indicates the validity of using passive sampling quantitatively for monitoring BTEX compounds, particularly with Tenax TA sorbent for long period monitoring. Good agreement was found between pumped samples adsorbed onto sorbent tubes and the real time sampling. These results give more assurance and confidence in the measurements that were done using this passive sampling methodology. These results underscore the reliability of passive sampling, coupled to SIFT-MS for monitoring the air quality in Christchurch, particularly for BTEX compounds.

a)

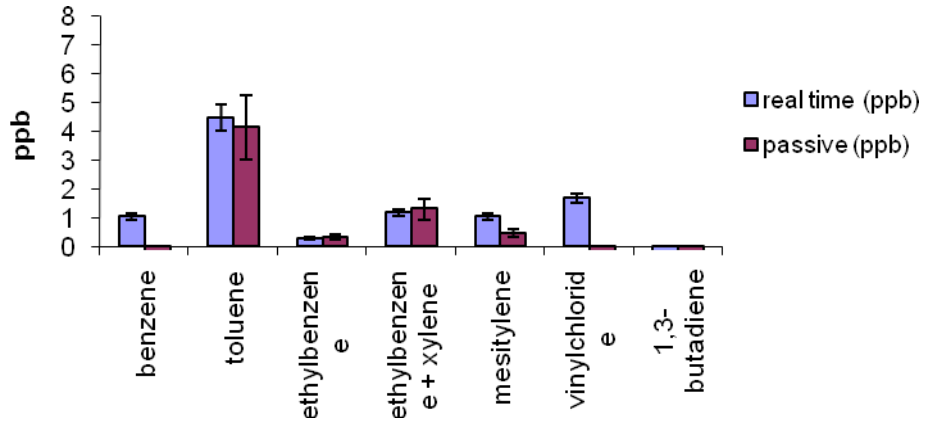

b)

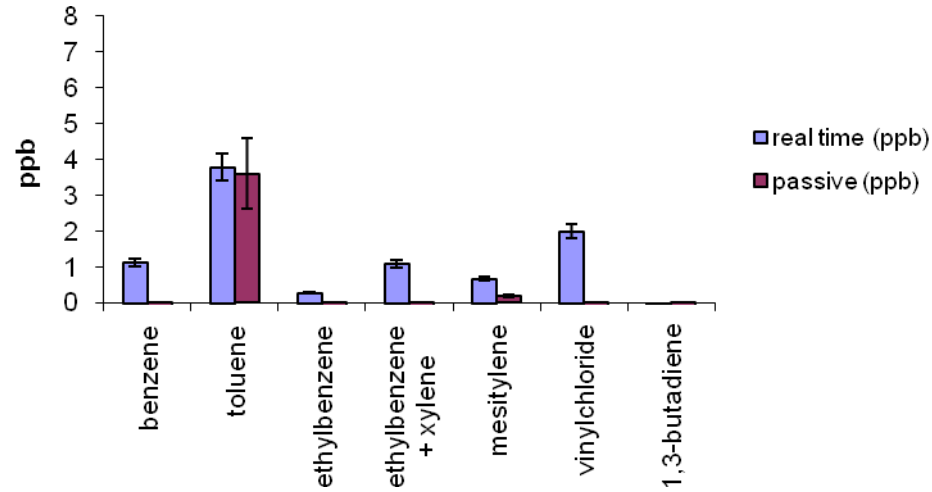

c)

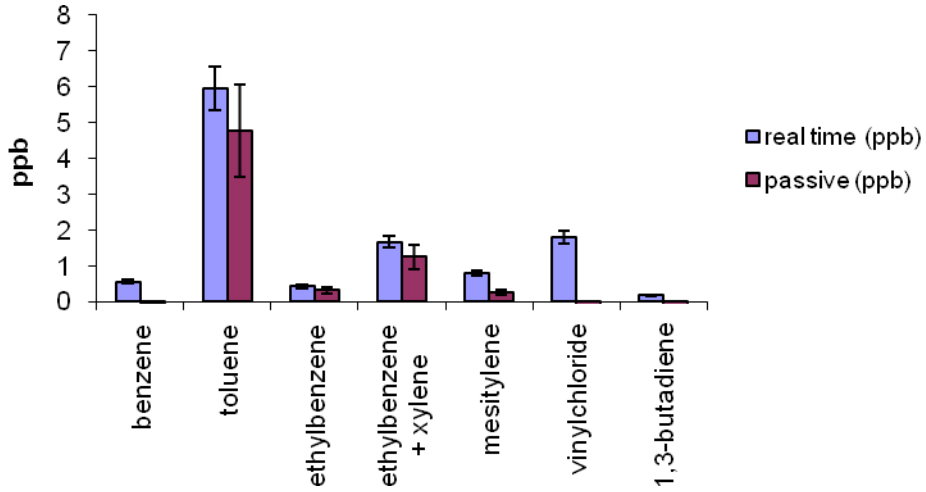

Figure 5.12 Workplace monitoring by real time SIFT-MS and passive tube with a) Tenax TA single bed sorbent b) Anasorb GCB1 and Anasorb CMS bed sorbents. c) Tenax and Carbopack bed sorbents.

10.2 Christchurch air monitoring.

10.2.1 Collection of the samples

Twenty Tenax TA sorbent tubes were deployed in three sites: Coles Place, a Woolston site and Riccarton Road. Figure 5.13 shows the locations of the chosen sites on the Christchurch map. These sample site environments can be described briefly as (a) a residential suburb area relatively close to the town and near to roadways, (b) an industrial area and (c) a busy roadway, respectively.

The twenty sorbent tubes were deployed as follows: six tubes in each site (three tubes for GC-MS analysis and three tubes for SIFT-MS analysis). The remaining two tubes were deployed as blanks (capped tubes) at two of the sites and subjected to the same handling procedure as the sample tubes.

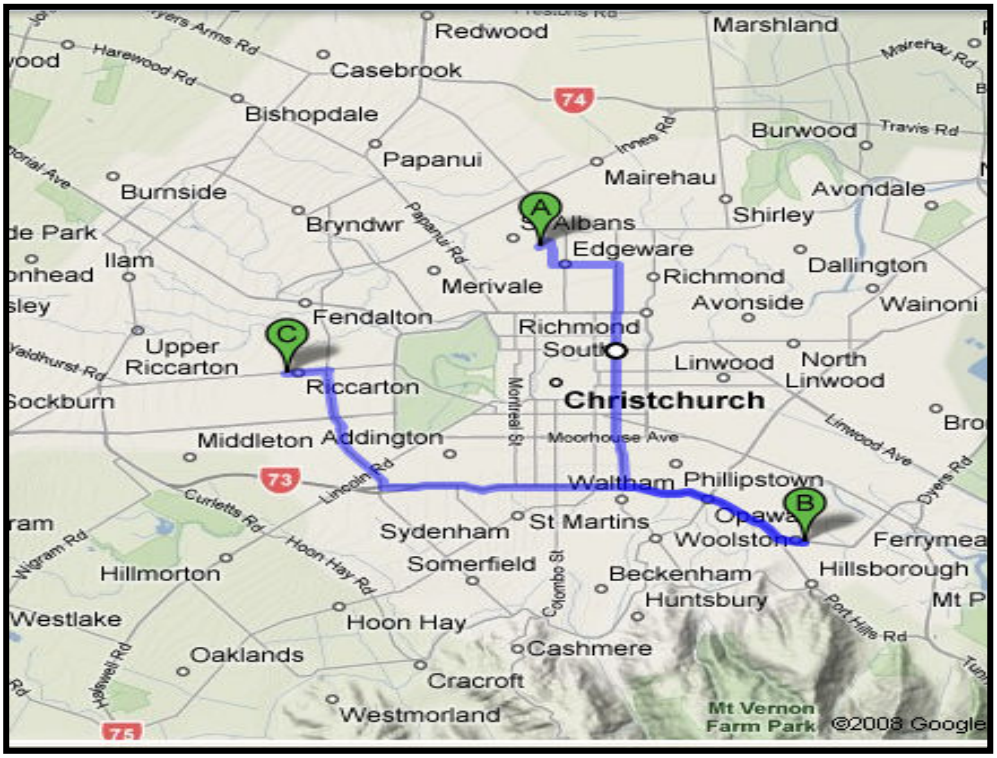

Figure 5.13 The three chosen sites: A) Coles Pl B) Woolston C) Riccarton.

The air samples were collected over a period of one month and from the sites that are used by the ECan agency. The end-caps of the tubes were removed from the sample tubes and replaced with diffusion caps. A problem can be encountered at high air velocities if a draught shield is not used; therefore, all tubes were shielded by a plastic container, which gave protection from water and strong draughts (Figure 5.14). Furthermore, the caps were tightened properly to ensure they were appropriately seated before they were hung at a height of approximately 3.3 m (Figure 5.14). A tight fit of the diffusion cap to the tube is important, in terms of maintaining the air gap between the sorbent and end cap (diffusion path length). At the end of the exposure time (one month), the diffusion caps were removed and replaced by metal storage caps. The tubes were then collected and were analyzed in the Syft laboratory using both the TD-SIFT-MS and TD-GC-MS techniques. The tubes were redeployed within 36 hours after the analysis. The weather conditions during the sampling process are recorded in Table 5.5.

Figure 5.14. Photos illustrate the sampling procedures that were taken in this work.

Table 5.5 The average weather conditions recorded during the sampling process. RH% is the Relative Humidity.

Site / Month	Riccarton			Coles Pl			Woolston		
	T (°C)	Wind Speed m/s	RH %	T (°C)	Wind Speed m/s	RH %	T (°C)	Wind Speed m/s	RH %
JUL	8.1	0.6	78.7	7.0	2.6	83.1	7.8	2.8	80.2
AUG	7.6	0.53	77.4	6.5	2.2	82	7.4	2.4	78.3
SEP	11.7	0.64	67.8	10.6	2.7	74.2	11.1	2.6	71.3

10.2.2 Results and discussion

The accuracy of the BTEX compounds analysis results depends upon using the correct diffusive uptake rate for Tenax TA, to calculate the airborne components' concentrations. Previous research revealed slight differences in the values of the uptake rates of the relevant compounds over a four-week (environmental analysis) period. [84][77] Therefore, in this study the mean uptake rate was used in our calculation (see Table 5.6). The uptake rate values, especially the experimental values for some of the compounds of interest (e.g. ethyl benzene), were difficult to find for Tenax TA sorbent. However, ethyl benzene and xylene have similar breakthrough volumes with a 13% difference between the lower and the higher breakthrough value at 0°C. [77] Therefore, xylene and ethyl benzene were assigned with the

same uptake rate, due to their similar breakthrough volumes as indicated in Table 5.3 previously.

Table 5.6 Literature uptake rate values and their average for the compounds of interest over a four-week period.

Compounds	Uptake rate (ng.(ppm.min)$^{-1}$)				Average
	1	Ref.	2	Ref.	
Benzene	0.86	84	0.93 (SD .02)	67	0.895
Toluene	1.2	84	1.41(SD .01)	67	1.305
Xylene	1.91	84	1.86(SD .04)	67	1.885
Ethyl benzene	1.91	84*	1.86(SD .04)	67*	1.885
Trimethylbenzene	2.65	84			2.65

* The xylene uptake rate was used for ethylbenzene (see text for explanation)

The sorbent tubes were collected and analyzed in the Syft laboratory using both the TD-SIFT-MS and TD-GC-MS techniques. The SIFT-MS results in general, were lower than the GC-MS results, but still indicate a satisfactory result that was in agreement with the GC-MS, except for the total ethylbenzene+xylenes as shown in Figure 5.15. The results showed good agreement in benzene and toluene concentrations with differences in concentration ranging between 5% to 18% for the GC-MS and SIFT-MS analyses. The total ethyl benzene+xylenes however showed a clear difference in concentrations between the two techniques ranging between 14% to 36%. Xylene isomers and ethyl benzene could not be distinguished by the SIFT-MS technique. Ethyl benzene and xylenes have very similar ion chemistries with the common SIFT-MS reagent ions except for the O_2^+ reagent ion. The O_2^+ reagent ion analysis result showed slightly more scatter than the H_3O^+ and NO^+ reagent ion. Xylene reacts with O_2^+ to give the same products as ethyl benzene but with a different product ratio. However, the different product ratios observed using O_2^+ did not enable definitive identification.

Therefore, *the total concentration* of the xylenes and ethyl benzene was measured and reported. The ethyl benzene value presented in the SIFT-MS result gave approximate agreement with the GC-MS result by assuming an equal quantity of xylene isomers and ethyl benzene presented in the air.

The results of these studies showed, not surprisingly, that higher concentrations were present in the industrial (Woolston) and heavy traffic areas (Riccarton), except for benzene. Benzene showed higher concentrations at Riccarton and Coles Pl sites, which were close to roadways. The result also indicated that the closer the tubes were placed to roadways, the higher were the concentrations of benzene observed. The industrial site, which was not close to a major roadway, had a lower benzene concentration. Measurements of the total of ethylbenzene+xylenes indicated higher concentrations existed at the heavy traffic and industrial sites (Riccarton and Woolston respectively) with a slightly higher concentration at the heavy traffic site of Riccarton. Moreover, toluene was high at the heavy traffic site (Riccarton) and higher at the industrial site (Woolston). The August results showed slightly lower concentrations compared to July, except for the total ethylbenzene+ xylenes. A notable change in the concentration of the total ethyl bezene+xylenes was observed in air monitoring during August at the Riccarton site. This change was noted and observed by all the three monitoring techniques: TD-SIFT-MS, TD-GC-MS and the ECan (Figure 5.15-Aug).

In September, which was the start of the spring season, a problem was experienced with the TD instrument that was connected to the SIFT-MS. The concentrations observed using the TD-SIFT-MS reduced by 45 to 50% compared with the July results (winter season). This reduction was found to originate from a problem in the TD. An apparent dilution was occurring either as a result of a leak or a blocked capillary. This dilution problem was confirmed by further experiment. A known amount of BTEX compounds were loaded in a tube and then analyzed by the TD-SIFT-MS. This experiment showed concentrations half of

those deposited in the tube (Table 5.7). The observed results for the TD-SIFT-MS for September were then scaled by a factor of 2.

Table 5.7 Experimental measurements that confirmed the encountered dilution problem with TD instrument.

Compound	Deposited mass (μg)	Measured mass (μg)	Breakthrough tube measured mass (μg)
Benzene	0.067	0.038	0.001
Toluene	0.056	0.029	0.001
Ethyl benzene+ xylenes	0.108	0.057	0.003

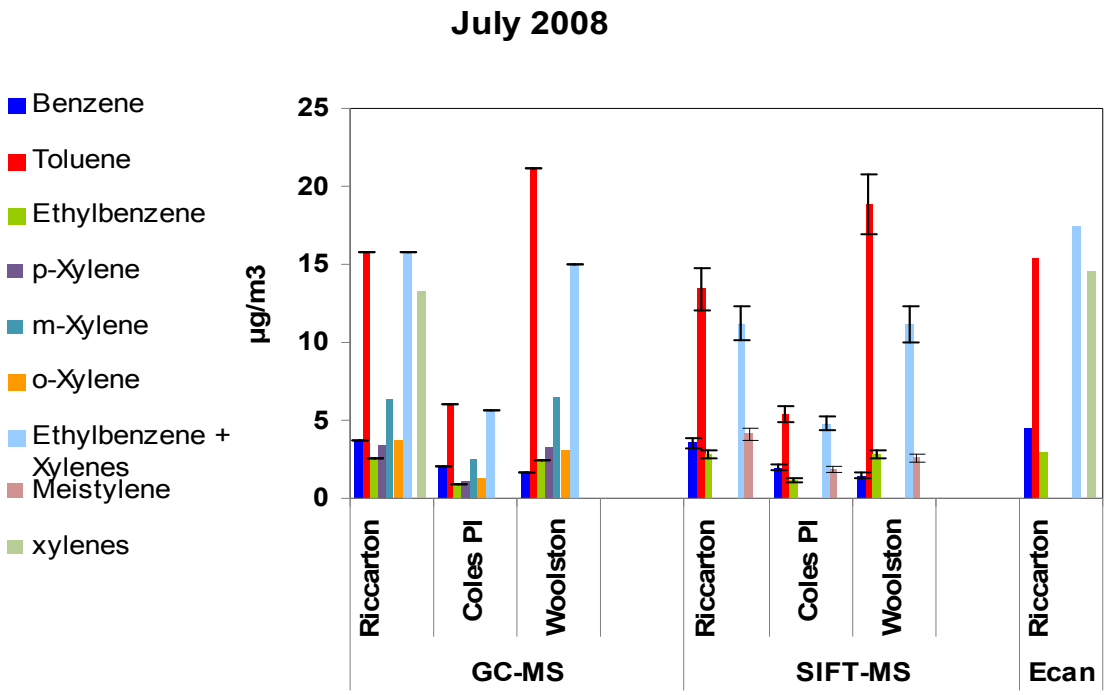

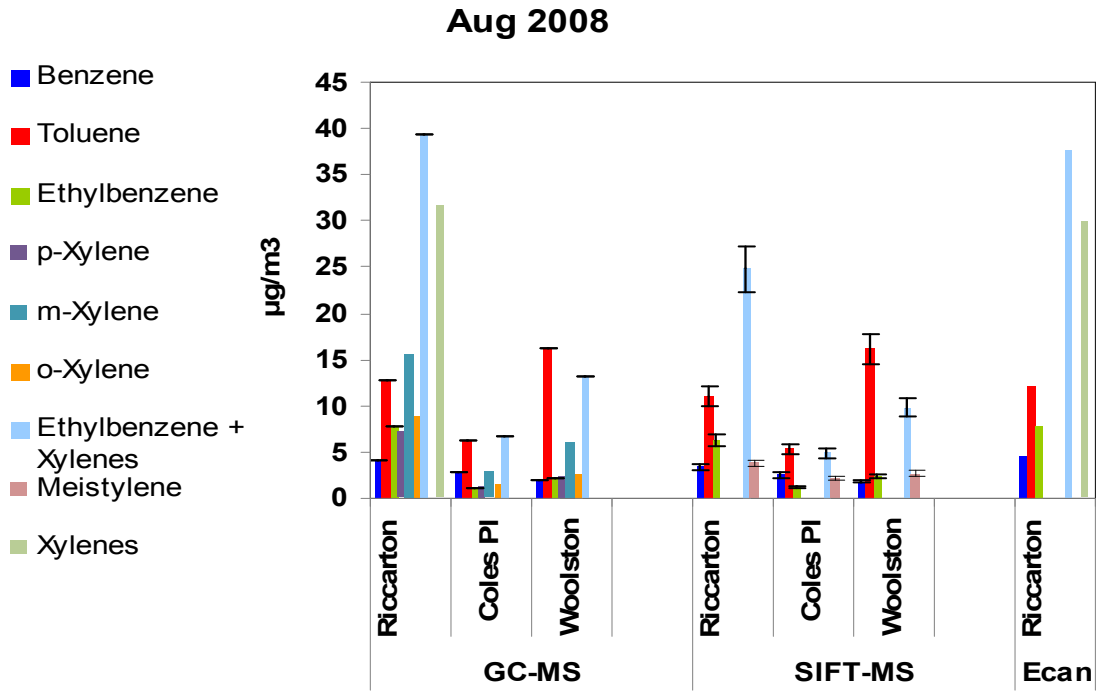

Figure 5.15 A comparison of the analyses results of TD-GS-MS, TD-SIFT-MS and ECan agency for JUL and AUG in 2008.

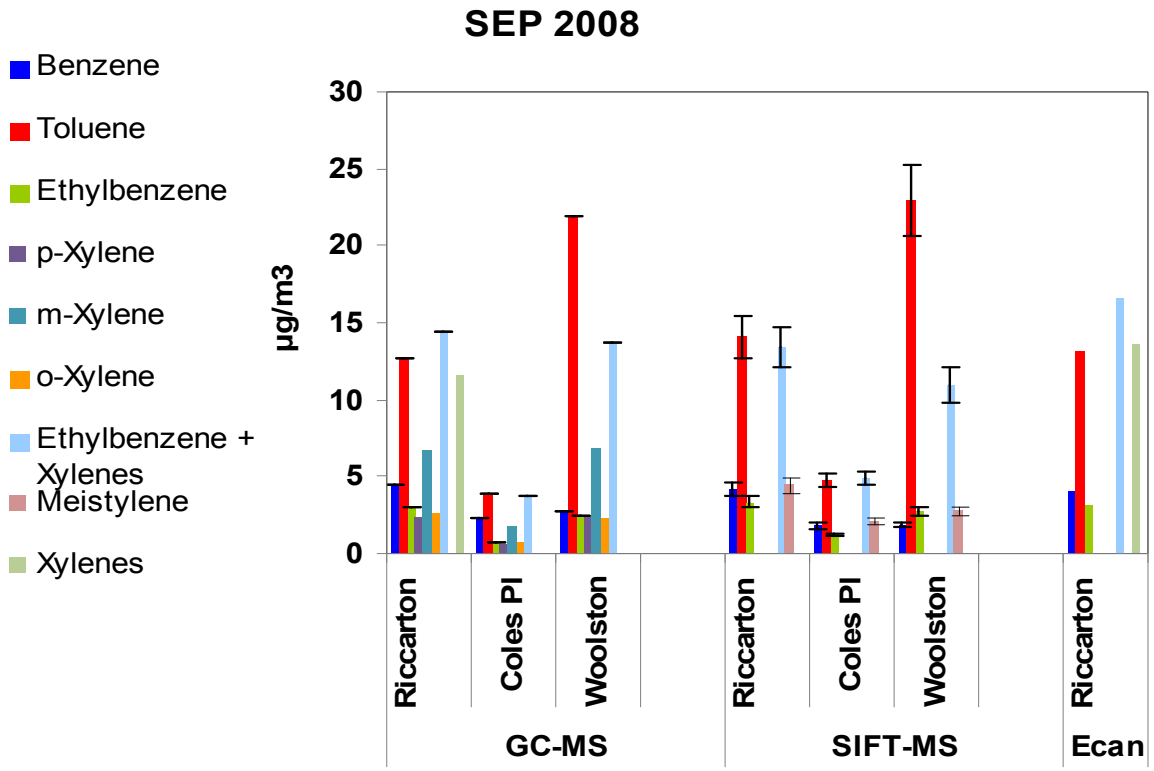

Figure 5.16 A comparison of the analyses results of TD-GS-MS, TD-SIFT-MS and ECan agency for SEP in 2008.

11. Conclusion

The work presented in this chapter shows the potential of SIFT-MS to merge with TD. The combined TD-SIFT-MS instrument can be readily applied to air analysis applications, using passive sampling. This conclusion was validated by comparing the results of the analysis of BTEX compounds in Christchurch air with those obtained and analyzed by the ECan agency and a further supplementary GC-MS analysis. These comparable satisfactory results using TD-SIFT-MS technique indicates that this technique offers more advantages than the conventional analysis method that requires analyte calibrations and the use of the solvent desorption method. However, further study is still required for elucidation of some isobaric analytes as demonstrated by TD-GC-MS.

Chapter 6

Conclusion and suggestions for future work

1. Conclusion

Ion-molecule reactions have introduced various and novel applications in analytical chemistry, primarily in the analytical field. Using soft ionisation, from the chemical ionization reaction of multiple reagent ions, has helped solve complex structural mass spectrum problems that are found in the selected ion flow tube mass spectrometry (SIFT-MS) technique. The use of SIFT-MS requires a knowledge of several dynamic parameters before an analyte concentration can be determined, as well as the essential kinetic parameters, as explained in chapters 1 and 2. Among these parameters are the carrier gas flow rate; the ion velocity; the sample flow rate; the relative diffusion rates of the reagent ion and product ions and the flow dynamics of the gas inside the flow tube. Therefore, it is necessary to know or measure these parameters (some of which are instrument dependent) before optimum results can be achieved. Further, knowledge about the validity of the sample container such as Tedlar bags, for a particular analysis task, is also beneficial for an accurate analysis.

In this project the SIFT-MS technique reveals its potential for applications related to petroleum and air quality. The SIFT-MS shows the potential to quantify confidently some sulfur compounds in natural gas with good linear responses. The advantage that SIFT-MS offers is a quick response time to measure these compounds in natural gas, for reasons of workers' safety and maintenance of drilling and refinery plant infrastructure. The petroleum project also involved an examination of the capability of SIFT-MS as a chemical tracer analyser in the complex mixture of natural gas. This research presents the SIFT-MS's ability to trace brombenzene and cholorobenzene to a relatively low concentration ppbv. The ability demonstrated by the SIFT-MS creates

a very useful technique in the investigation of oil-rig characteristics that requires reliable, fast and real-time analysis. Moreover, further investigations examined the applicability of SIFT-MS to establish some tentative fingerprints or a qualitative profile for hydrocarbon mixtures. In this fingerprint study, the special characteristic of the NO^+ reagent ion was exploited, enabling distinctive product ions that can be utilised for qualitative analysis.

SIFT-MS also displays its versatility in accommodating passive sampling methodology, which is currently used as a widespread method for air quality monitoring. This method does not require the use of chemical solvents, analyte calibrations and a long analysis time, as are customary with the conventional GC-MS. In this study, it was clear that the potential for use of the combined TD-SIFT-MS in air monitoring is high. Confirmation of the potential of TD-SIFT-MS was provided by monitoring the BTEX range of compounds in the air of Christchurch city in conjunction with ECan agency.

2. Suggestions for Future work

There are several suggestions that are important for future work. First, and as noted in the sulfur compounds experiment (chapter 3), the initial methods could not distinguish between DMS and ethylmercaptan. Therefore, another reagent ion is suggested, such as $CH_3OCH_2^+$ that could be used to discriminate between them as was published elsewhere. [52] [53] Further experimental investigations of the capability of this reagent ion for analytes containing sulfur are also required. Early work has indicated an ability to distinguish between some isomeric hydrocarbons. [53]

Furthermore, exploring more common chemical tracers that are currently used, such as cyclic perfluorocarbons would be useful. In addition, a study of the use of other reagent ions, such as negative reagent ions, which may be less reactive with hydrocarbons for halocompound tracing applications, would also be useful.

Third, a quantitative study of the use of the H_3O^+ reagent ion for the analysis of large linear hydrocarbons C10-C14 with the use of a Nafion dryer is also suggested. This study would be a complementary work to the quantitation analysis of C1-C9 linear hydrocarbons that was studied earlier in 2007. [11] Quantitative analyses of these hydrocarbons will be necessary for air monitoring and might be accompanied with the use of passive methodology and Tenax sorbent. The H_3O^+ will prevent the fragmentations problem that appears with the NO^+, which may lead to an error in any quantitative analysis as noted in chapter 5. It would also be necessary to implement a kinetic study for some cyclohydrocarbons that seem to be important, such as cyclopentane and cyclohexane.

Finally, expanding the target compounds in air analysis with the use of multi sorbents is recommended for a longer environmental study. Experimentally determining the uptake rate value for some of the unavailable common pollutants in air, such as ethylbenzene, is also required. Furthermore, some improvement in permeation tube calibration and sensitivity will achieve better results. This, in fact, would have a significant effect on environment applications, particularly for air quality monitoring, where concentrations of VOCs are extremely low. Therefore, more sensitivity of the SIFT-MS instrument and better analyte calibration could promote passive air analysis results.

References

[1] J.S. Brodbelt, *Analytical Applications of Ion-Molecule Reactions.* Mass spectrometry reviews, **16**, 91-110, 1997

[2] E.E. Ferguson, F.C. Fehsenfeld and A.L. Schmeltekopf in Advances in Atomic and Molecular Physics, Academic Press, New York, **5**: 1-56, 1969.

[3] D. Smith and N.G. Adams, *The Selected Ion Flow Tube (SIFT): Studies of Ion-Neutral Reactions*. Advances in Atomic and Molecular Physics, **24**:1-49, 1987

[4] N.G. Adams and D. Smith, *The Selected Ion Flow Tube (SIFT); A Technique for Studying Ion-Neutral Reactions*, International Journal of Mass Spectrometry and Ion Physics **21**, 349-359 (1976).

[5] A.L. Schmeltekopf and H.P. Broida.J.Chem.Phys., **39**:1261-1268, 1963.

[6] N.G. Adams and D. Smith, Int. J. Mass Spectrum. Ion Phys., **21**: 349-359, 1976.

[7] P. Spanel and D. Smith, *Selected Ion Flow Tube Mass Spectrometry (SIFT-MS) for On-line Trace Gas Analysis*. Mass spectrometry reviews, **24**:661-700, 2005

[8] P.E. Millerrr and M.B. Denton, *The Quadrupole Mass Filter: Basic Operating Concepts*, Journal of chemical education, **63**(7): 617-622, 1986.

[9] *Channeltron Electron Multiplier Handbook for Mass Spectrometry Applications*, Burle channeltron Book.

[10] J. Gray, *Electron Multipliers for 2000 and Beyond: Discrete-dynode Technology Comes of Age*, Application note, 2000.

[11] G.J. Francis, *SIFT-MS: Development of Instrumentation and Applications*, PhD thesis, University of Canterbury, New Zealand, 2007.

[12] M. McMaster and C. McMaster, *GC-MS A practical User's Guide Bbook*, 1st ed, New York, Wiley, 1998, pp 42

[13] D.A. Fairley, *Selected Ion Flow Tube Drift Tube (SIFDT) Studies of Reactive Ion-Neutral Encounters*, PhD thesis, University of Canterbury, New Zealand, 1998

[14] P. Spanel P and D. Smith, *SIFT Studies of the Reactions of H_3O^+, NO^+ and O_2^+ with Several Aliphatic and Aromatic Hydrocarbons*. Int. J. Mass Spectrom **181**: 1-10, 1998e

[15] P. Spanel and D. Smith, *SIFT Studies of the Reactions of H_3O^+, NO^+ and O_2^+ with some Organosulphur Molecules.* Int. J. Mass Spectrom, **176**: 167-176, 1998d

[16] T. Su and W.J. Chesnavich, J. Chem. Phys., **76**(10):5183-5185, 1982.

[17] M.L. Katherine, *Identification and Analysis of MVOCs Produced by Fungi Growing on Building*, MSC thesis, University of Canterbury, New Zealand, 2005.

[18] M. McMaster and C. McMaster, *GC-MS A practical User's Guide Book*, 1st ed, New York, Wiley, 1998, pp 51

[19] White paper, Measuring the Instrument Calibration Function via the Constant Cumulative Count Method, Syft technical notes, 2006.

[20] *J. Pawliszyn,* Sampling and Sample Preparation for Field and Laboratory*, 1st ed, Elsevier Science, 2002, pp 464.*

[21] S. Tumbiolo, L. VIncent, J.F. Gal and P.C. Maria, *Thermogravimetric Calibration of Permeation Tubes Used for the Preparation of Gas Standards for Air pollution Analysis*, Royal Society of Chemistry, **130**: 1369-1374, 2005.

[22] D.K. Bohme, *Ion-Molecule Interaction*, Plenum Press, New York, 1975, pp 489-504.

[23] H. Maarse, *Volatile Compounds in Foods and Beverages*, 1st ed, CRC, 1991, pp 94-96

[24] Nielsen, *Quantification of Volatile Sulfur Compounds in Complex Gaseous Matrices by Solid-Phase Micro Extraction*, J. Chromatogr. A **963**: 57-64, 2002.

[25] M.M.L. Steeghs, S.M. Cristescu and F.J.M. Harren, The Suitability of Tedlar Bags for Breath Sampling in Medical Diagnostic Research, Physiol. Meas. **28**: 73-84, 2007

[26] L. Skrtic, *Hydrogen Sufide, Oil and Gas, and People's Health*, Master thesis, Energy and Resources Group, University of California, Berkeley, 2006

[27] *Oil and Gas at Your Door? A Landowner's Guide to Oil and Gas Development.* OGAP, P.I-2, 2005.

[28] West Virginia University's Alternative Fuel Vehicle Training Program, *Propane Review*, (http://www.wps.com/LPG/WVU-review.html) (accessed Aug 31,2008)

[29] Using Gas Geochemistry to Assess Mercury Risk, http://www.gaschem.com/mercur.html (accessed Aug 31,2008)

[30] Southern Gas Services Limited, Riccarton, Christchurch, New Zealand.

[31] Environmental Protection Agency, *The Petroleum Industry*, AP 42, Fifth Edition, Volume 1, Chapter 5, available at (http://www.epa.gov/ttn/chief/ap42/ch05/final/c05s03.pdf).

[32] E.A. Holleman and E. Wiberg, *Inorganic Chemistry*, 34th ed, San Diego: Academic Press; Berlin; New York: De Gruyter, 1995.

[33] K.J. Donham et al., *Acute Toxic Exposure to Gases from Liquid Manure*. Journal of occupational medicine, **24**: 142-145, 1982.

[34] Environmental Protection Agency, *Report to Congress on Hydrogen Sulphide Air Emissions Associated with the Extraction of Oil and Natural Gas*.EPA-453/R-93-045, P.III-4, October 1993.

[35] World Health Organization, *Hydrogen Sulfide*, Geneva, Environmental Health Criteria, No.19, 1981.

[36] E.A. Holleman and E. Wiberg, *Inorganic Chemistry*, 34th ed, San Diego: Academic Press; Berlin; New York: De Gruyter, 1995, pp 519.

[37] A. M. Chapman, *Characterizing Salmonella Fecal Shedding among Racehorses in Louisiana*, Master thesis, Department of Veterinary Clinical Sciences, Louisiana State University, 2006.

[38] Health Bulletin No. 26, *Clean Air – Hydrogen Sulphide Project (H_2S), 2007*

[39] The Science of Smell Part 1: *Odor Perception and Physiological Response*, Iowa State University,UniversityExtension,(http://www.extension.iastate.edu/Publications/PM1963A.pdf), (accessed Aug 31,2008)

[40] H. N. Savolainen expertgruppen f6r gransvardesdokumentation. 40. Dihydrogensulfide [Nordic expert group for TLV evaluation. 40. Hydrogen sulfide]. Arbeta och hdlsa, **31**:1-27, 1982.

[41] *L.F. Drbal, P.G. Boston, K.L. Westra and Black & Veatch*, Power Plant Engineering*, Springer; 1st ed, 1996, pp 110.*

[42] P.J. Marcus, Chem. Phys., 1991, 88, 1697

[43] M. Quinlan, *Evaluation of Selected Emerging Sulfur Recovery Technologies*, GRI Gas Tips, 3(1) L 26-35, 1996. In K.E. McIntush, D.A. Darymple, and C.O. Rueter, *New Process Fills Technology Gap in Removing H_2S from Gas*, world oil, July, 2001.

[44] Environmental Protection Agency, *Report to Congress on Hydrogen Sulfide Emission*, P.III-35

[45] API Recommended Practice(RP) 54, Recommended Practice for Occupational Safety for Oil and Gas Well Drilling and Servicing Operations and API RP 49m Safe Drilling of Wells Containing Hydrogen Sulfide.

[46] D. Smith, N.G. Adams and Miler, *A Laboratory Study of The Reactions of N^+, N_2+ , N_3^+, N_4^+, O^+ , O_2^+ and NO^+ Ions with Several Molecules at 300 K*, J. Chem. Phys., **69**(1):308-318, 1978

[47] T.L. Williams, N.G. Adams and L.M. Babcock, *Selected Ion Flow Tube Studies of $H_3O^+(H_2O)_{0,1}$ Reactions with Sulfide and Thiols*, University of Georgia, department of chemistry, Athens , GA 30602, USA, International Journal of Mass Spectrometry and Ion Process, **127**: 149-159, 1998

[48] J.H. Futrell, *Gaseous Ion Chemistry and Mass Spectrometry*, New York: Wiley, 1986.

[49] White paper, V. Langford, *Syft Analytics Limited Standard Operating Procedure*, Syft notes.

[50] A. Pysanenko, P. Spanel and D. Smith, *A Study of Sulphur- Containing Compounds in Mouth- and Nose-Exhaled Breath and in the Oral Cavity Using Selected Ion Flow Tube Mass Spectrometry*, IOP publishing, 2008.

[51] M.J. McEwan and et al., *Reaction of $CH_3OCH_2^+$ with Hydrocarbons and O, N, and S Compounds: Applications for Chemical Ionization in Selected Ion Flow Tube Studies*, American Society for Mass Spectrometry, **13**: 1028-1033, 2002.

[52] T. Keough, Dimethyl Ether as a Reagent Gas for Organic Functional Group Determination by Chemical Ionization Mass Spectrometry, Anal.Chem., **45**: 2540-2547,1982.

[53] R.N. Horne, K.A. Breitenbach, M. P. Fossum, *Retention of Chemical Tracers in Geothermal Reservoirs*, Stanford Geothermal Program, Stanford University, California, 1982.

[54] P.F. Wilson, C.G. Freeman, M.J. McEwan, *Reaction of Small Hydrocarbons with H_3O^+, O_2^+ and NO^+ Ions*, International Journal of Mass Spectrometry, **299**: 143-149, 2003.

[55] R.A. Spronken-Smith, A.P. Sturman, E.V. Wilton, *The Air Pollution Problem in Christchurch, New Zealand—Progress and Prospects*, Clean Air and Environmental quality, **36**: 23 – 28, 2001.

[56] W. Chalermot, *Measuring VOCs in Christchruch Ambient Air: Using SIFT-MS Technique*, Master thesis, University of Canterbury, New Zealand, 2003.

[57] M. McCauley, *Concentration of Benzene, Toluene, Ethyl benzene and Xylene in Ambient Air*, Christchurch, Environmental Canterbury, report NO. R05/21, ISBN 1-86937-575-0, 2005.

[58] World Health Organization, *Air Quality Guidelines for Europe*, 2ed ed, WHO regional publication, European series, No. 91, 2000.

[59] R. P. Ryan, C.E. Terry and S.S. Leffingwell, *The Toxic Exposure & Medical Monitoring* Index, CRC press, 5th edition, volume II, pp. 1312, 1999-2000

[60] Wikipedia the free encyclopedia, *Toluene*, available at (http://en.wikipedia.org/wiki/Toluene), (visited at 13/9/2008)

[61] U.S. Environmental Protection Agency , *Ethyl benzene*, Air Toxics Web Site (http://www.epa.gov/ttn/atw/hlthef/ethylben.html) , (visited at 13/9/2008)

[62] Occupational Safety & Health Administration, *Trimethyl benzene*, available at http://www.osha.gov/SLTC/healthguidelines/trimethylbenzene/recognition.html, (visited at 13/9/2008)

[63] U.S Environmental Protection Agency , Integrated Risk Information System, *1,3-Butadiene* (CASRN 106-99-0), available at (http://www.epa.gov/iris/subst/0139.htm), (visited at 13/9/2008)

[64] International Programme on Chemical Safety (IPCS), *Vinyl Chloride*, Health and Safety Guide No. 109, World Health Organization and and United Nations Environment, 1999, (http://www.inchem.org/documents/hsg/hsg/hsg109.htm), (visited at 13/9/2008)

[65] Environment Australia, *Air Toxics and Indoor Air Quality in Australia* , ISBN 0-642547394, 2001, available at (http://www.environment.gov.au/atmosphere/airquality/publications/sok/vinyl.html), (visited at 13/9/2008)

[66] D. Smith, P. Spanel, D. Babill, J. Cocker and B. Rajan, *Online Analysis of Diesel Engine Exhaust Gases by Selected Ion Flow Tube Mass Spectrometry*, Rapid communications in mass spectrometry, **18**: 2830-2838, 2004.

[67] Method for determination of Hazardous Substances (MDHS 27), *Protocol for Assessing the Performance of a Diffusive Sampler*, Health and Safety Executive, ISBN 0-7176-0635-X, 1994.

[68] Brown et al., *The Use of Diffusive Sampling for Monitoring of Benzene, Toluene, and Xylene in Ambient Air*. Pure Appl. Chem., **71**(10): 1993-2008, 1999.

[69] Principles of Diffusive Monitoring, *Thermal Desorption* Technical Support, Note 8, Markes International Limited, UK, 2002, (http://www.markes.com).

[70] Method for determination of Hazardous Substances (MDHS), (*63/2) 1, 3 Butadiene in Air*, Health and Safety Executive, ISBN 0-7176-2898-1, 2005. Available at: (www.hse.gov.uk/pubns/mdhs/pdfs/mdhs63-2.pdf).

[71] A. Roche et al., *Performance of A Thermally Desorbable Type-tube Diffusive Sampler for Very Low Air Concentrations Monitoring*, Atmospheric Environment **33**: 1905-1912, 1999.

[72] *Radiello Diffusive Sampling System*, Sigma-Aldrich, (http://www.sigmaaldrich.com/Area_of_Interest/Analytical__Chromatography/

Sample_Preparation/Radiello/What_is_Radiello.html)

[73] K.J. Krost, E.D. Pellizzari, S.G. Walburn, et al., *Collection and Analysis of Hazardous Organic Emissions*. Anal Chem **54**:810-817, 1982.

[74] J. Barkley, J. Bunch, J.T. Bursey, et al., *Gas chromatography Mass Spectrometry Computer Analysis of Volatile Halogenated Hydrocarbons in Man and his Environment- a Multimedia Environmental Study*. Biomed Mass Spectrum **7**: 139-147, 1980.

[75] Method for determination of Hazardous Substances (MDHS), *80 Volatile Organic Compounds in air*, Health and Safety Executive, ISBN 0-7176-0913-8, 1995

[76] Method for determination of Hazardous Substances (MDHS 72),*Volatile Organic Compounds in Air*, Health and Safety Executive, ISBN 0-11-885692-8, 1993

[77] Scientific Instrument Services, Inc., *Tenax® TA Adsorbent Resin Physical Properties*, available at (http://www.sisweb.com/index/referenc/tenaxtam.htm).

[78] J. D. Spengler, J. M. Samet, J. F. McCarthy, *Indoor Air Quality Handbook*, McGraw-Hill Professional, pp. 33.3, ISBN 0-07-445549-4, 2001

[79] R.H. Brown, *The Use of Diffusive Samplers for Monitoring of Ambient Air*, Pure & Appl. Chem., **65**(8): 1859-1874, 1993

[80] ISO 6143:2000, *Gas Analysis-Requirements for Certificates for Calibration Gases and Gas Mixtures*, 2000.

[81] Council Directive 99/30/EC relating to limit values for sulphur dioxide, nitrogen dioxide and oxides of nitrogen, particulate matter and lead in ambient air, Official Journal of the European Communities, EN Series, L163/41, 1999.

[82] Method for the Determination of Hazardous Substances (MDHS), 33/2 *Sorbent Tube Standards*, Health and Safety Executive, ISBN 0-776-3372, 1997, Available at: (www.hse.gov.uk/pubns/mdhs/pdfs/mdhs33-2.pdf).

[83] White paper, *Calculation of sample concentration from desorption profile*, Syft notes.

[84] *Diffusive Uptake Rates-PerkinElmer*, The Diffusive Monitor, Health and Safety Executive Committee on Analytical , Working Group 5, issue 12, 2001